

# Bayesian variable and hazard structure selection in the General Hazard model

Yulong Chen

Department of Statistical Science, University College London  
and

Jim Griffin

Department of Statistical Science, University College London  
and

Francisco Javier Rubio

Department of Statistical Science, University College London

February 4, 2026

## Abstract

The proportional hazards (PH) and accelerated failure time (AFT) models are the most widely used hazard structures for analysing time-to-event data. When the goal is to identify variables associated with event times, variable selection is typically performed within a single hazard structure, imposing strong assumptions on how covariates affect the hazard function. To allow simultaneous selection of relevant variables and the hazard structure itself, we develop a Bayesian variable selection approach within the general hazard (GH) model, which includes the PH, AFT, and other structures as special cases. We propose two types of  $g$ -priors for the regression coefficients that enable tractable computation and show that both lead to consistent model selection. We also introduce a hierarchical prior on the model space that accounts for multiplicity and penalises model complexity. To efficiently explore the GH model space, we extend the Add–Delete–Swap algorithm to jointly sample variable inclusion indicators and hazard structures. Simulation studies show accurate recovery of both the true hazard structure and active variables across different sample sizes and censoring levels. Two real-data applications are presented to illustrate the use of the proposed methodology and to compare it with existing variable selection methods.

**Keywords:** Bayesian variable selection; Survival analysis; Censoring; Hazard structure; Model misspecification.

# 1 Introduction

Survival regression models are central to the analysis of time-to-event data across scientific areas such as medicine, biology, engineering, and related fields. These models are typically specified by linking the hazard function to a set of covariates  $\mathbf{x} \in \mathbb{R}^p$ , where the specific manner in which covariates enter the hazard function determines the *hazard structure*. Popular formulations include the proportional hazards (PH; [Cox 1972](#)), accelerated failure time (AFT; [Cox & Oakes 2018](#)), and accelerated hazards (AH; [Chen & Jewell 2001](#)) models, as well as more general hazard structures (GH; [Etezadi-Amoli & Ciampi 1987](#), [Chen & Jewell 2001](#)) specifications that encompass these as special cases. These structures differ in whether covariates act multiplicatively on the hazard, on the time scale, or on both. The literature offers two main perspectives on how to approach the problem of selecting the variables that best explain the times-to-event and the hazard structure that most appropriately represents the data-generating process. One stream focuses on selecting the hazard structure under the assumption that all relevant covariates are included. In the Bayesian setting, [Zhang et al. \(2018\)](#) studied model selection across six parametric survival models (including PH, AFT, and proportional odds), and [Zhou & Hanson \(2018\)](#) extended this idea to a semiparametric framework. A limitation is that these methods enforce the same role for each covariate across structures. The second stream of the literature starts from a fixed hazard structure and develops Bayesian variable-selection methods for sparse settings. Recent work includes spike-and-slab priors for AFT models ([Sha et al. 2006](#)), generalised  $g$ -priors that incorporate censoring for PH and AFT models ([Castellanos et al. 2021](#), [García-Donato et al. 2023](#)), and non-local priors for PH and AFT models ([Nikooienejad et al. 2020](#), [Rossell & Rubio 2023](#)). While these methods address covariate sparsity, they rely on a pre-specified hazard structure, which, if misspecified, can affect both variable selection and inference ([Rossell & Rubio 2023](#)). The limitations of these two approaches motivates joint selection of variables and the hazard structure. The GH family provides an appealing framework for this task as effects are easily

interpretable and popular models (PH, AFT, AH) arise as special cases through specifying whether covariates influence the hazard scale, the time scale, or both. In this line, the GH model was used for variable selection in the frequentist setting by [Tong et al. \(2013\)](#), who proposed penalised likelihood methods for variable selection within the GH class.

In this paper, we develop the first Bayesian treatment of variable and hazard selection within the general hazard model. This is challenging since the model priors on the two sets of model coefficients and the model space must be carefully designed to accommodate the differing roles that covariates may play, to reflect the partitioning of the model space into distinct hazard structures, and to adjust for multiplicity in both variable and hazard structure selection. Our approach enables identification of the variables that predict survival and whether those variables act on the hazard and time scales, as well as offering principled model uncertainty quantification and providing theoretical guarantees for model selection consistency. Our main contributions are as follows. We introduce two  $g$ -prior formulations for the regression coefficients, a likelihood-curvature-matching prior and a product  $g$ -prior, that align with the GH model's two-component structure and yield consistent model selection under suitable regularity conditions. We propose a prior on the model space that generalises the Beta–Binomial model-multiplicity correction ([Scott & Berger 2010](#)) to situations where covariates may appear in multiple roles (hazard level and/or time scale), a key feature of GH models. We develop computational tools that enable efficient exploration of the model space via a tailored Markov chain Monte Carlo (MCMC) strategy that accommodates moves both within and across hazard structures. We also implement fast approximations to the marginal likelihood, which is required for computing posterior model probabilities and for evaluating MCMC moves, using Laplace and integrated Laplace approximations.

The remainder of the paper is organised as follows. Section 2 introduces the key notation and the GH model, and formalises the model selection problem within this class of models. Section 3 outlines prior specifications for structure and variable selection. Section 4 introduces the

approximation and MCMC methods used to compute posterior model probabilities. Section 5 presents theoretical results on the model selection consistency of the proposed approach. Section 6 evaluates its performance through a series of simulation studies, including comparisons with alternative methods. Section 7 illustrates the use of the proposed methodology using two real-data applications. Finally, Section 8 concludes with a discussion and possible extensions of this work.

## 2 Model and Variable Selection for the GH Structure

In this section, we introduce our notation, describe the GH model structure, and formalise the problem of simultaneous model and variable selection within this class of models.

### Hazard-based regression models

Let  $\{o_1, \dots, o_n\}$  be a sample of times-to-event, and  $\{c_1, \dots, c_n\}$  be right-censoring times. Suppose that we observe  $\mathbf{t} = \{t_1, \dots, t_n\}$ , where  $t_i = \min\{o_i, c_i\}$ ,  $i = 1, \dots, n$ . Let  $\delta_i = I(o_i < c_i)$  be the corresponding right-censoring indicators ( $\delta_i = 1$  observed,  $\delta_i = 0$  right-censored); and  $\mathbf{z}_i \in \mathbb{R}^d$  be the vector of available covariates associated to the  $i$ th individual. Throughout, we assume that the times-to-event are independent of the censoring times conditional on the covariates (non-informative censoring). We adopt the GH structure to model the time-to-event outcomes of interest. The GH model is defined through the hazard function:

$$h(t \mid \boldsymbol{\alpha}, \boldsymbol{\beta}, \boldsymbol{\xi}) = h_0 \left( t \exp \left\{ \tilde{\mathbf{x}}_i^\top \boldsymbol{\alpha} \right\} \mid \boldsymbol{\xi} \right) \exp \left\{ \mathbf{x}_i^\top \boldsymbol{\beta} \right\}, \quad (1)$$

where  $h_0(\cdot \mid \boldsymbol{\xi})$  is a parametric baseline hazard function, with parameter  $\boldsymbol{\xi} \in \mathbb{R}^r$ ,  $\mathbf{x}_i \in \mathbb{R}^p$  are the covariates included as hazard-level effects, and  $\tilde{\mathbf{x}}_i \in \mathbb{R}^q$  are the covariates included as time-level effects, with  $\mathbf{x}_i \subseteq \mathbf{z}_i$  and  $\tilde{\mathbf{x}}_i \subseteq \mathbf{z}_i$ . Then, the cumulative hazard function can be written as:

$$H(t \mid \boldsymbol{\alpha}, \boldsymbol{\beta}, \boldsymbol{\xi}) = H_0 \left( t \exp \left\{ \tilde{\mathbf{x}}_i^\top \boldsymbol{\alpha} \right\} \mid \boldsymbol{\xi} \right) \exp \left\{ \mathbf{x}_i^\top \boldsymbol{\beta} - \tilde{\mathbf{x}}_i^\top \boldsymbol{\alpha} \right\},$$

thus avoiding the need for numerical integration whenever  $H_0(\cdot \mid \boldsymbol{\xi})$  is available in closed-form. Such models have been used in several practical applications (Rubio et al. 2019), as they provide a simple way to incorporate time-level effects (through the coefficients  $\boldsymbol{\alpha}$ ) and hazard-level effects (through the coefficients  $\boldsymbol{\beta}$ ) while retaining tractable estimation. The GH family includes the proportional hazards (PH) model ( $\boldsymbol{\alpha} = 0$ ), the accelerated failure time (AFT) model ( $\boldsymbol{\alpha} = \boldsymbol{\beta}$  and  $\mathbf{x}_i = \tilde{\mathbf{x}}_i$ ), and the accelerated hazards (AH) model ( $\boldsymbol{\beta} = 0$ ) as special cases (see Rubio et al. 2019 for a more detailed discussion of this hazard structure). The GH model (1) is identifiable if and only if the baseline hazard is not Weibull (Chen & Jewell 2001), since in the Weibull case the PH, AFT, and AH models coincide, corresponding to a situation in which a simpler model structure suffices. We focus on the case where the baseline hazard  $h_0$  belongs to the log-location-scale family. That is, the corresponding probability density function (pdf) can be expressed as:

$$f_0(t \mid \boldsymbol{\xi}) = f_0(t \mid \mu, \sigma) = \frac{1}{\sigma t} f\left(\frac{\log(t) - \mu}{\sigma}\right), \quad (2)$$

where  $\mu \in \mathbb{R}$  is a location parameter,  $\sigma > 0$  is a scale parameter, and  $f$  is a fully specified pdf with support on  $\mathbb{R}$  that is symmetric about 0. The corresponding hazard function is defined in the usual way  $h_0(t \mid \mu, \sigma) = \frac{f_0(t \mid \mu, \sigma)}{1 - F_0(t \mid \mu, \sigma)}$ . This family includes distributions commonly used in survival analysis, such as the log-normal, log-logistic, and log-Laplace (Vallejos & Steel 2015). Members of this family can accommodate a variety of hazard shapes, including unimodal (log-normal) and monotone increasing or decreasing (log-logistic) forms. This interpretability of the parameters also facilitates prior elicitation. Within the GH structure (1) with baseline given by (2), the parameter  $\mu$  acts as a log-location parameter on the same scale as the linear predictor  $\tilde{\mathbf{x}}_i^\top \boldsymbol{\alpha}$  and can be interpreted as an intercept.

We consider the reparametrisation  $\exp(\nu) = 1/\sigma$ ,  $\theta_0 = \mu/\sigma$ ,  $\boldsymbol{\theta} = -\boldsymbol{\alpha}/\sigma$ , and  $\boldsymbol{\eta} = -\boldsymbol{\beta}$ , which transforms all parameters to the real line and absorbs the original scale into the coefficient  $\boldsymbol{\theta}$ . After

some algebra, the log-likelihood function can then be expressed as follows:

$$\begin{aligned}\ell_n(\Psi) &= n_o\nu - \sum_{i=1}^n \delta_i \log(t_i) + \sum_{i=1}^n \delta_i \left( \tilde{\mathbf{x}}_i^\top \boldsymbol{\theta} e^{-\nu} - \mathbf{x}_i^\top \boldsymbol{\eta} \right) + \sum_{i=1}^n \delta_i \log f \left( e^\nu \log(t_i) - \tilde{\mathbf{x}}_i^\top \boldsymbol{\theta} - \theta_0 \right) \\ &+ \sum_{i=1}^n \log F \left( -e^\nu \log(t_i) + \tilde{\mathbf{x}}_i^\top \boldsymbol{\theta} + \theta_0 \right) \left[ \exp \left( \tilde{\mathbf{x}}_i^\top \boldsymbol{\theta} e^{-\nu} - \mathbf{x}_i^\top \boldsymbol{\eta} \right) - \delta_i \right],\end{aligned}\quad (3)$$

where  $\Psi = (\nu, \theta_0, \boldsymbol{\theta}^\top, \boldsymbol{\eta}^\top)^\top$ . Thus, the likelihood function for the GH structure is as tractable as that of standard parametric AFT and PH models. The gradient and Hessian of the log-likelihood function are provided in the Supplementary Material.

## 2.1 Hazard structure and variable selection

We now formulate the model selection problem, which defines the proposed methodology for performing Bayesian variable and hazard-structure selection within the GH family. Suppose we begin with the full vector of available covariates,  $\mathbf{x}_i = \tilde{\mathbf{x}}_i = \mathbf{z}_i$ , of dimension  $p$ . Since our goal is to perform simultaneous variable and hazard structure selection, we formalise this task by introducing the following notations for individual variables and hazard structure:

$$\gamma_j = \begin{cases} 0, & \text{if } \theta_j = 0, \eta_j = 0, \quad (\text{No effect}) \\ 1, & \text{if } \theta_j \neq 0, \eta_j = 0, \quad (\text{Time-level effect}) \\ 2, & \text{if } \theta_j = 0, \eta_j \neq 0, \quad (\text{Hazard-level effect}) \\ 3, & \text{if } \theta_j \neq 0, \eta_j \neq 0 \text{ and } e^{-\nu}\theta_j \neq \eta_j, \quad (\text{Both effects at different level}) \\ 4, & \text{if } \theta_j \neq 0, \eta_j \neq 0 \text{ and } e^{-\nu}\theta_j = \eta_j, \quad (\text{Both effects at same level}) \end{cases},$$

corresponding to no effect, a hazard-level effect only, a time-level effect only, and both effects with different/same magnitudes of each covariate  $j = 1, \dots, p$ . That is,  $\boldsymbol{\gamma} = (\gamma_1, \dots, \gamma_p)^\top$  determines what covariates enter the model and their role in the model.

The different hazard structures can then be characterised in terms of  $\boldsymbol{\gamma}$ : let  $\emptyset$  denote the null model and  $\text{Hz}(\boldsymbol{\gamma})$  denotes the hazard structure of  $\boldsymbol{\gamma}$ . These four types of hazard structure are

characterised as

$$\text{Hz}(\gamma) = \begin{cases} \emptyset, & \text{if } \gamma = 0, \\ \text{AH, if } \gamma \neq 0 \text{ and } \forall j \in \{1, \dots, p\}, \gamma_j \in \{0, 1\}, \\ \text{PH, if } \gamma \neq 0 \text{ and } \forall j \in \{1, \dots, p\}, \gamma_j \in \{0, 2\}, \\ \text{GH, if } \gamma \neq 0 \text{ and } \forall j \in \{1, \dots, p\}, \gamma_j \in \{0, 1, 2, 3\} \text{ and } \text{Hz}(\gamma) \neq \text{AH or PH}, \\ \text{AFT, if } \gamma \neq 0 \text{ and } \forall j \in \{1, \dots, p\}, \gamma_j \in \{0, 4\}. \end{cases}$$

In other words, for the rest of this paper, we will use GH to denote any GH model defined in (1) that is not one of AH, PH, and AFT for convenience. This formulation leads to  $4^p - 1$  PH, AH, and GH models and  $2^p - 1$  AFT models, which, including the null model, come down to  $4^p + 2^p - 1$  total models to consider. One implication of this formulation is that we do not consider variables to have both effects at the exact same level for GH models to reduce the number of trivial or redundant model configurations.

Let  $\Psi_\gamma = (\nu, \theta_0, \boldsymbol{\theta}_\gamma^\top, \boldsymbol{\eta}_\gamma^\top)^\top$  denote the parameters associated to the model  $\gamma$ , and  $\mathbf{X}_{o,\gamma}$  and  $\mathbf{X}_{c,\gamma}$  denote the submatrices of the design matrices for observed times  $\mathbf{X}_o$  and censored times  $\mathbf{X}_c$ , respectively. The main quantities of interest are the posterior model probabilities, which are given by

$$\pi(\gamma | \mathbf{t}) = \frac{p(\mathbf{t} | \gamma) \pi(\gamma)}{\sum_{\gamma'} p(\mathbf{t} | \gamma') \pi(\gamma')} = \left( 1 + \sum_{\gamma' \neq \gamma} B_{\gamma', \gamma} \frac{\pi(\gamma')}{\pi(\gamma)} \right)^{-1},$$

where  $\pi(\gamma)$  is the model prior probability,  $B_{\gamma', \gamma} = p(\mathbf{t} | \gamma')/p(\mathbf{t} | \gamma)$  is the Bayes factor between  $(\gamma', \gamma)$ , and  $p(\mathbf{t} | \gamma) = \int \exp(\ell(\Psi_\gamma)) \pi(\Psi_\gamma | \gamma) d\Psi_\gamma$  is the integrated likelihood  $\exp(\ell(\Psi_\gamma))$  with respect to a prior density  $\pi(\Psi_\gamma | \gamma)$ . Note that the parameters  $\boldsymbol{\theta}_\gamma$  and  $\boldsymbol{\eta}_\gamma$  are specific to each model, while  $(\nu, \theta_0)$  are common to all models. Next, we discuss the choices for these two parts and the prior on the model space  $\pi(\gamma)$ , along with the computational tools used to calculate the model posterior probability  $\pi(\gamma | \mathbf{t})$ .

### 3 Priors

We assign the following vague prior distributions to the common parameters  $(\nu, \theta_0)$ :

$$\pi(\nu) = \frac{\beta_\nu^{\alpha_\nu} e^{\alpha_\nu \nu} e^{-\beta_\nu e^\nu}}{\Gamma(\alpha_\nu)}, \quad \pi(\theta_0) = N(0, K), \quad (4)$$

where  $\alpha_\nu$  and  $\beta_\nu$  are hyper-parameters with small values and  $K$  is a large constant. The prior on  $\nu$  corresponds to a  $Gamma(\alpha_\nu, \beta_\nu)$  prior on  $1/\sigma$ , which is, with small values of  $\alpha_\nu$  and  $\beta_\nu$ , a common vague prior for the precision of noise in the literature. The parameter  $\theta_0$  is the scaled intercept, and we assign it a vague normal prior with zero mean and large variance. The default values we choose are  $\alpha_\nu = \beta_\nu = 0.01$  and  $K = 10^6$ . Using improper priors on common parameters is also a popular choice when employing the  $g$ -prior in various contexts (Castellanos et al. 2021, Li & Clyde 2018). For the GH model, this would require establishing that the joint posterior distribution under improper priors is proper, which is beyond the scope of this work.

#### 3.1 Likelihood curvature matching prior for model-specific coefficients

The prior on model-specific coefficients,  $\pi(\theta_\gamma, \eta_\gamma)$ , plays a crucial role in Bayesian variable selection as it determines the asymptotic behaviour of the Bayes factor and model selection consistency rates. In the context of Bayesian survival analysis, there are two common types of priors on model coefficients: the  $g$ -prior (Castellanos et al. 2021, Zhang et al. 2018, García-Donato et al. 2023) and non-local priors (Rossell & Rubio 2023, Nikooienejad et al. 2020). The calibration of hyperparameters in non-local priors is essential, as they directly control the threshold beyond which an effect is detectable. However, such calibration could be difficult (although not impossible) under the GH model, as this requires simultaneously calibrating the time level and the hazard level, and the same values of the coefficients in time and hazard levels do not usually imply an equal influence on the survival function. On the other hand, the  $g$ -prior (Zellner 1986), having the form  $N(\mathbf{0}, g\mathcal{J}^{-1})$ , incorporates the expected Fisher information matrix  $\mathcal{J}$  into the prior covariance matrix, which intuitively reflects the curvature of the log-likelihood. The single hyperparameter  $g$

can be interpreted as the prior sample size, which can be calibrated based on, for example, the unit information principle (Li & Clyde 2018). Castellanos et al. (2021) and García-Donato et al. (2023) applied this  $g$ -prior construction, respectively, to AFT and PH models, demonstrating that in the survival context it can automatically adjust the contribution of each observation to the prior covariance according to its censoring status. We extend the  $g$ -prior construction to the model coefficients  $[\boldsymbol{\theta}_\gamma, \boldsymbol{\eta}_\gamma]$  of the GH model, following the reasoning outlined above. Since the  $g$ -prior is defined using the expected Fisher information matrix, we first analyse the structure of this matrix in the following result.

**Proposition 1** *The  $[\boldsymbol{\theta}_\gamma, \boldsymbol{\eta}_\gamma]$  block of the expected Fisher information could be decomposed into*

$$\begin{aligned} \mathcal{I}_{\boldsymbol{\theta}_\gamma, \boldsymbol{\eta}_\gamma}(\boldsymbol{\Psi}_\gamma) &= \sum_{k=1}^n \mathbb{E} \left[ -\nabla_{\boldsymbol{\theta}_\gamma, \boldsymbol{\eta}_\gamma}^2 \ell(\boldsymbol{\Psi}_\gamma) \mid \boldsymbol{\Psi}_\gamma, \delta_k = 0 \right]_k \cdot p(\delta_k = 0 \mid \boldsymbol{\Psi}_\gamma) \\ &\quad + \sum_{k=1}^n \mathbb{E} \left[ -\nabla_{\boldsymbol{\theta}_\gamma, \boldsymbol{\eta}_\gamma}^2 \ell(\boldsymbol{\Psi}_\gamma) \mid \boldsymbol{\Psi}_\gamma, \delta_k = 1 \right]_k \cdot p(\delta_k = 1 \mid \boldsymbol{\Psi}_\gamma), \end{aligned}$$

where  $\nabla_{\boldsymbol{\theta}_\gamma, \boldsymbol{\eta}_\gamma}^2 \ell(\boldsymbol{\Psi}_\gamma)$  is the Hessian matrix of  $\ell(\boldsymbol{\Psi}_\gamma)$  with respect to  $[\boldsymbol{\theta}_\gamma, \boldsymbol{\eta}_\gamma]$ , and  $v_k = \exp(e^{-\nu} \tilde{\mathbf{x}}_{\gamma, k}^\top \boldsymbol{\theta}_\gamma - \mathbf{x}_{\gamma, k}^\top \boldsymbol{\eta}_\gamma)$ . Then,  $\mathbb{E} \left[ -\nabla_{\boldsymbol{\theta}_\gamma, \boldsymbol{\eta}_\gamma}^2 \ell(\boldsymbol{\Psi}_\gamma) \mid \boldsymbol{\Psi}_\gamma, \delta_k \right]$  has the form  $\begin{pmatrix} \tilde{\mathbf{X}}_\gamma^\top \mathbf{M}_{\boldsymbol{\theta}_\gamma}^{\delta_k} \tilde{\mathbf{X}}_\gamma & \tilde{\mathbf{X}}_\gamma^\top \mathbf{M}_{\boldsymbol{\theta}_\gamma \boldsymbol{\eta}_\gamma}^{\delta_k} \mathbf{X}_\gamma \\ \mathbf{X}_\gamma^\top \mathbf{M}_{\boldsymbol{\theta}_\gamma \boldsymbol{\eta}_\gamma}^{\delta_k} \tilde{\mathbf{X}}_\gamma & \mathbf{X}_\gamma^\top \mathbf{M}_{\boldsymbol{\eta}_\gamma}^{\delta_k} \mathbf{X}_\gamma \end{pmatrix}$ , where  $\mathbf{M}^{\delta_k}$  are  $n \times n$  diagonal matrices (with no closed-form expressions).

The derivation and explicit expressions are provided in the Supplementary Material, including the particular case where  $f$  is standard normal. These expressions show that many components of the information matrix depend on integrals of the baseline hazard and its derivative with respect to the lifetime distribution. These integrals have closed-form solutions for PH models and, assuming the censoring times are known, also for AFT models. However, for the AH and GH models, closed-form solutions are not available. Moreover, the expected Fisher information depends on the value of the regression coefficients, which are unknown, resulting in a non-standard distribution. In summary, there are two challenges that prevent us from directly using the expected Fisher information matrix in the prior covariance: (i) it does not have a closed-form expression, and (ii) it depends on the unknown regression coefficients themselves.

The first challenge on tractability of the expression of the expected Fisher information matrix could be solved by using the sample average of the observed Fisher information matrix as an estimate of the expected Fisher information, which reflects the curvature of the finite-sample likelihood function. For the second challenge, there are two common solutions: either evaluate the parameters at 0 (Castellanos et al. 2021) or at the model-specific maximum likelihood estimate (MLE) (Wang & George 2007). The former choice is based on the argument that the only information available on the model-specific parameters comes from the null model, which assigns positive probabilities of them being 0 (Castellanos et al. 2021). The latter choice, our preferred choice, is better at capturing the large sample covariance structures of the model coefficients and the local geometry under the current model (Li & Clyde 2018). This feature is particularly important in our setting, as not only the structure of the coefficients within each of time and hazard level could be captured, but also that between them. Combining the solutions above towards the two challenges, we consider the following likelihood-curvature-matching (LCM)  $g$ -prior:

$$(\boldsymbol{\theta}_\gamma, \boldsymbol{\eta}_\gamma)^\top \mid g_E \sim N(\mathbf{0}, n g_E \mathcal{J}_{\boldsymbol{\theta}_\gamma, \boldsymbol{\eta}_\gamma}(\widehat{\boldsymbol{\Psi}}_\gamma)^{-1}), \quad (5)$$

where  $\mathcal{J}_{\boldsymbol{\theta}_\gamma, \boldsymbol{\eta}_\gamma}(\widehat{\boldsymbol{\Psi}}_\gamma)$  is the  $\boldsymbol{\theta}_\gamma$  and  $\boldsymbol{\eta}_\gamma$  block of the observed Fisher information matrix with all parameters evaluated at the MLE  $\widehat{\boldsymbol{\Psi}}_\gamma$ , and  $g_E > 0$  is a hyperparameter. The single hyperparameter  $g_E$  plays the same role as in the standard  $g$ -prior, and we set its default value to  $g_E = 1$  based on the unit information principle. The prior form in (5) was first investigated by Wang & George (2007) in the context of generalised linear models (GLMs). Our proposal further extends this prior specification to the survival modelling framework by incorporating it within the GH model.

A natural extension of (5) consists of placing a prior on the hyperparameter  $g_E$ . Although many options exist (Liang et al. 2008), we select a single specification for illustration, as benchmarking these priors is not the central objective of this paper and, as we show in Section 4, the computational methods and costs are comparable across different choices. While our main analysis considers fixed  $g_E$ , we also examine the robust prior of Bayarri et al. (2012) due to its appealing theoretical

properties. The robust prior has the following form (Castellanos et al. 2021):

$$\pi(g_E) = \frac{1}{2} \sqrt{\frac{1+n}{n(d_\gamma + 1)}} \left( g_E + \frac{1}{n} \right)^{-3/2}, \quad g_E > \frac{1+n}{n(d_\gamma + 1)} - \frac{1}{n}, \quad (6)$$

where  $d_\gamma$  is the model size and  $n$  is the sample size.

### 3.2 Product prior for model-specific coefficients

Although the prior in (5) offers practical benefits, its reliance on the observed survival times and censoring indicators might be less appealing to some users. Consequently, we now seek an alternative specification of the  $g$ -prior for the GH model. Note first that the expected Fisher information matrix for  $\theta_\gamma$  and  $\eta_\gamma$ , shown in Table S1 of Supplementary Material, could be written in the form of  $\tilde{\mathbf{X}}_\gamma^\top \mathbf{M}_{\theta_\gamma} \tilde{\mathbf{X}}_\gamma$  and  $\mathbf{X}_\gamma^\top \mathbf{M}_{\eta_\gamma} \mathbf{X}_\gamma$ , where  $\mathbf{M}_{\theta_\gamma}$  and  $\mathbf{M}_{\eta_\gamma}$  are diagonal matrices. Motivated by this structure, we propose a simpler and intuitive Product  $g$ -prior specification for AH, PH, AFT and GH models, and their corresponding coefficients:

$$\pi_P(\boldsymbol{\theta}_\gamma, \boldsymbol{\eta}_\gamma \mid g_{C_t}, g_{C_h}) = N\left(\boldsymbol{\theta}_\gamma; \mathbf{0}, g_{C_t} n \left(\tilde{\mathbf{X}}_\gamma^\top \tilde{\mathbf{X}}_\gamma\right)^{-1}\right) \cdot N\left(\boldsymbol{\eta}_\gamma; \mathbf{0}, g_{C_h} n \left(\mathbf{X}_\gamma^\top \mathbf{X}_\gamma\right)^{-1}\right), \quad (7)$$

where  $g_{C_t} > 0$  and  $g_{C_h} > 0$  are hyperparameters. For AFT models, the prior becomes  $N\left(\boldsymbol{\theta}_\gamma; \mathbf{0}, g_{C_t} n \left(\tilde{\mathbf{X}}_\gamma^\top \tilde{\mathbf{X}}_\gamma\right)^{-1}\right)$ , as  $e^{-\nu} \boldsymbol{\theta}_\gamma = \boldsymbol{\eta}_\gamma$ . In other words, the formulation in (7) assumes that all samples contribute equally to the prior covariance. Consequently, we expect the prior covariance for  $\boldsymbol{\theta}_\gamma$  to deviate slightly from the inverse of the expected Fisher information matrix in the AH, AFT, and  $\boldsymbol{\theta}_\gamma$  component of the GH models, while it remains aligned with the expected information for the PH model and the  $\boldsymbol{\eta}_\gamma$  component of the GH model, though it may be sensitive to the calibration of  $g_{C_t}$  and  $g_{C_h}$  depending on the quality of the approximation. The default value we set is  $g_{C_t} = g_{C_h} = 1$  for the sake of comparison with (5). However, since the censoring contribution is, to some extent, absorbed into  $g_{C_t}$  and  $g_{C_h}$ , a more thoughtful choice that reasonably accounts for this information could be considered.

### 3.3 Prior on the model space

For the prior on the model space,  $\pi(\boldsymbol{\gamma})$ , we aim to specify a non-informative prior that assigns equal weight across model sizes and hazard structures. A naive uniform prior,  $\pi(\boldsymbol{\gamma}) = (4^p + 2^p - 1)^{-1}$ , is not appropriate because, for example, the number of GH models far exceeds that of PH, AH, and AFT models, thereby allocating most of the prior mass to GH models. To correct for this kind of imbalance, we adopt a multiplicity-adjusted formulation that extends the widely used Beta–Binomial prior (Scott & Berger 2010).

We identify three sources of multiplicity that we would like to control in our setting: (i) variation in the number of variables included, (ii) variation in the hazard structure, and (iii) variation in the number of effects. We distinguish here between the number of variables and the number of effects: there are  $p$  variables in total, and each variable can contribute 0, 1, or 2 effects. A variable having 0 effects corresponds to not being included in the model; 1 effect corresponds to having a time level OR hazard level effect, or both effects at the same scale; 2 effects corresponds to having both effects at difference scale. This three-layered multiplicity naturally suggests a hierarchical prior structure, which sequentially accounts for these sources. Define  $\boldsymbol{\Lambda}$  as a binary vector of length  $p$  with  $\boldsymbol{\Lambda}_j = 1$  indicating variable  $j$  is included. Let  $p_i$  denote the number of variables with  $\gamma_j = i$  for  $i \in 1, 2, 3, 4$ , so that the number of included variables is  $|\boldsymbol{\Lambda}| = \sum_{i=1}^4 p_i$ , and  $p_0 = p - |\boldsymbol{\Lambda}|$  counts the not-included variables. Denote  $\omega = |\boldsymbol{\Lambda}| + p_3$  as the number of effects. Following the multiplicity argument, we have that  $\pi(\boldsymbol{\gamma}) = \pi(\boldsymbol{\Lambda}, \text{Hz}(\boldsymbol{\gamma}), \omega)$ , and we consider the following factorisation:

$$\pi(\boldsymbol{\gamma}) = \pi(\boldsymbol{\Lambda}, \text{Hz}(\boldsymbol{\gamma}), \omega) = \pi(\omega \mid \text{Hz}(\boldsymbol{\gamma}), \boldsymbol{\Lambda}) \pi(\text{Hz}(\boldsymbol{\gamma}) \mid \boldsymbol{\Lambda}) \pi(\boldsymbol{\Lambda}). \quad (8)$$

For  $\pi(\boldsymbol{\Lambda})$ , we consider only the number of included variables (not their individual effects) and adopt the Beta–Binomial prior of Scott & Berger (2010). Marginalising a prior Beta( $a_{\boldsymbol{\Lambda}}, b_{\boldsymbol{\Lambda}}$ ) on the inclusion probability yields the Beta–Binomial prior  $\pi(\boldsymbol{\Lambda}) \propto B(a_{\boldsymbol{\Lambda}} + |\boldsymbol{\Lambda}|, b_{\boldsymbol{\Lambda}} + p_0)$ , where  $B(\cdot, \cdot)$  is the Beta function. The hyperparameters  $a_{\boldsymbol{\Lambda}}$  and  $b_{\boldsymbol{\Lambda}}$  control prior sparsity: for fix value of

$a_\Lambda$ , a larger  $b_\Lambda$  favours fewer included variables. A simple and intuitive approach to calibrate them is by setting  $a_\Lambda = 1$  and interpreting  $b_\Lambda$  as the prior odds between  $p_0$  and  $|\Lambda|$ . The default choice we recommend is setting  $a_\Lambda = b_\Lambda = 1$ , which corresponds to a Beta(1, 1) (uniform) prior on the inclusion probability and hence a non-preferential prior for the number of included variables. Apart from the Beta-Binomial prior, there are plenty of choices for  $\pi(\Lambda)$ : for example, for larger  $p$  settings, the priors considered by [Ley & Steel \(2009\)](#) might be of interest.

Next, we consider the conditional  $\pi(\text{Hz}(\gamma) \mid \Lambda)$ . Given  $|\Lambda|$ , there are  $(3^{|\Lambda|} + 1) \binom{p}{|\Lambda|}$  possible models in total. Among these, there are  $\binom{p}{|\Lambda|}$  possible PH, AH, and AFT models, respectively. The number of GH models is therefore  $(3^{|\Lambda|} - 2) \binom{p}{|\Lambda|}$ , where  $2 \binom{p}{|\Lambda|}$  is the number of AH and PH models. Consequently, the ratio of the number of PH, AH, or AFT models to the number of GH models is  $1/(3^{|\Lambda|} - 2)$ . To correct for this multiplicity imbalance, we consider the following structure:

$$\pi(\text{Hz}(\gamma) \mid \Lambda) \propto \begin{cases} h_{AH}, & \text{Hz}(\gamma) = \text{AH} \\ h_{PH}, & \text{Hz}(\gamma) = \text{PH} \\ h_{AFT}, & \text{Hz}(\gamma) = \text{AFT} \\ h_{GH} \cdot (3^{|\Lambda|} - 2)^{-1}, & \text{Hz}(\gamma) = \text{GH}, \end{cases} \quad (9)$$

where  $h_{GH}, h_{AH}, h_{PH}, h_{AFT} > 0$  are hyperparameters. These four hyperparameters, or more precisely the ratios between them, encode the prior beliefs on the four hazard structures. The default choice is setting all to 1, leading to a non-preferential prior on hazard structures.

Lastly,  $\pi(\omega \mid \text{Hz}(\gamma), \Lambda)$  aims to control the number of effects. However, since a variable can have more than one effect only in GH models, this term would only affect the prior probability of GH models. Note that we require  $|\Lambda| > 1$ , as for  $|\Lambda| = 1$  the only valid GH model has a single active variable with  $\gamma = 3$  and no correction is needed. Given  $|\Lambda| > 1$  and  $\text{Hz}(\gamma) = \text{GH}$ , the possible number of effects,  $\omega$ , takes values between  $|\Lambda|$  to  $2|\Lambda|$ . In general, the number of GH models that

has  $|\Lambda|, |\Lambda| + 1, \dots, 2|\Lambda|$  effects is

$$\{ \# \text{ GH Models with } \omega \text{ effects} \mid |\Lambda| > 1 \} = \binom{p}{|\Lambda|} \binom{|\Lambda|}{\omega - |\Lambda|} 2^{2 \cdot |\Lambda| - \omega} - \mathbf{1}_{\omega=|\Lambda|} \cdot 2 \cdot \binom{p}{|\Lambda|}.$$

In other words,  $(\omega - |\Lambda|) \sim \text{Bin}(|\Lambda|, 1/3)$  with a correction term when  $\omega = |\Lambda|$ . Without adjusting for this source of multiplicity, the posterior probability of GH models would concentrate around models with  $p + |\Lambda|/3$  effects. To address this, we apply inverse probability weighting and yield

$$\pi(\omega \mid \text{Hz}(\gamma), \Lambda) \propto \begin{cases} 1, & \text{Hz}(\gamma) = \text{AH/PH/AFT} \\ \left( \frac{\left[ P_{Bin}((\omega - |\Lambda|) \mid |\Lambda|, q) \cdot (1 - 2^{(1-|\Lambda|) \cdot \mathbf{1}_{\omega=|\Lambda|} + \mathbf{1}_{\omega \neq |\Lambda|}} \right]^{-1}}{\sum_{i=0}^{|\Lambda|} \left[ P_{Bin}(i \mid |\Lambda|, q) \cdot (1 - 2^{(1-|\Lambda|) \cdot \mathbf{1}_{i=0} + \mathbf{1}_{i \neq 0}}) \right]^{-1}} \right)^{\mathbf{1}_{|\Lambda| > 1}}, & \text{Hz}(\gamma) = \text{GH}, \end{cases} \quad (10)$$

where  $P_{Bin}(x \mid a, b)$  is the probability mass function of the Binomial distribution with parameter  $n = a$  and  $p = b$  evaluated at  $x$ . The hyper-parameter  $q \in [0, 1]$  controls the number of effects in GH models: the closer it is to 1, the more heavily we penalise the number of effects. The default choice is 1/3, which only corrects for multiplicity arising from the number of effects. Having these three components, we could derive the full expression of  $\pi(\gamma)$  based on (8). This proposal builds on the widely used Beta-Binomial prior for the model space and provides full multiplicity control over the number of variables, effects, and model types. Moreover, it constitutes a fully Bayesian prior with a set of interpretable hyperparameters, allowing convenient multi-level adjustment of sparsity relative to the given non-preferential baselines.

## 4 Computations

### 4.1 Marginal Likelihood Approximations

We begin by describing the computations required to implement the Bayesian variable selection strategy under the LCM prior for model-specific parameters in (5). [Wang & George \(2007\)](#)

proposed an alternative to the Laplace approximation (LA), namely the integrated Laplace approximation (ILA), to approximate the marginal likelihood under this class of priors. Briefly, the key idea of ILA is that, instead of expanding the log-posterior at the maximum a posteriori (MAP) estimate, as is typical in the standard LA (Rossell & Rubio 2023), ILA expands the log-likelihood function at the MLE and evaluates the marginal likelihood integral using this approximated likelihood. The integral admits a closed-form if the prior on the model parameters is defined as a multivariate normal. The resulting procedure is much faster than the usual LA, as we need to conduct only one optimisation scheme to calculate the MLE for each model, instead of two optimisation steps required by the LA, one to obtain the MLE required in the specification of the LCM prior and one to obtain the MAP.

A direct application of ILA does not yield a closed-form expression for the marginal likelihood, since  $\pi(\nu)$  follows a log-Gamma distribution, whereas ILA requires all prior densities to be Gaussian or uniform. To address this, we approximate  $\pi(\nu)$  with a normal distribution. In particular, for the choice  $Gamma(0.01, 0.01)$ , which is the vague prior we suggested for  $\tau$  in the previous section, a normal prior with mean 9.34 and standard deviation 41.15 provides an accurate approximation, with  $< 1\%$  difference in probability density for  $\sigma > 0.01$ .

Let  $\mathcal{J}_{aa}$  denote the block of the observed Fisher information matrix of the parameter  $a$ , and  $\mathcal{J}_{a,b}$  denotes the crossing block of parameters  $a, b$ . With the approximation for  $\pi(\nu)$ , the marginal likelihood  $p(\mathbf{t} | \boldsymbol{\gamma})$  has the following closed-form under the ILA:

$$\hat{p}(\mathbf{t} | \boldsymbol{\gamma}) = \exp[\ell(\widehat{\boldsymbol{\Psi}}_{\boldsymbol{\gamma}})](1 + ng_E)^{-d_{\boldsymbol{\gamma}}/2} |\mathbf{P}_{\boldsymbol{\gamma}}|^{-\frac{1}{2}} \exp \left\{ \frac{1}{2} \mathbf{h}_{\boldsymbol{\gamma}}^{\top} \mathbf{P}_{\boldsymbol{\gamma}}^{-1} \mathbf{h}_{\boldsymbol{\gamma}} + C_{\boldsymbol{\gamma}} \right\}, \quad (11)$$

where  $d_{\boldsymbol{\gamma}} = p_{\boldsymbol{\gamma}} + q_{\boldsymbol{\gamma}}$ ,  $\mathbf{h}_{\boldsymbol{\gamma}}$  is a vector of length 2,  $\mathbf{P}_{\boldsymbol{\gamma}}$  is a  $2 \times 2$  symmetric matrix, and  $C_{\boldsymbol{\gamma}}$  is a scalar. Each of these terms is composed of entries from the observed Fisher information matrix evaluated at the MLE  $\widehat{\boldsymbol{\Psi}}_{\boldsymbol{\gamma}}$ . The full expression for those terms and the detailed derivation are provided in Section 3 of the Supplementary Material. The MLE can be computed numerically using gradient descent or any general-purpose optimisation method. We employ the `nlminb` function in R,

which works well in our simulations and real-data applications.

If the robust prior on  $g_E$  in (6) is used, we could simply perform a one-dimensional integration:

$$\hat{p}(\mathbf{t} | \boldsymbol{\gamma}) = \int_0^\infty \hat{p}(\mathbf{t} | \boldsymbol{\gamma}, g_E) \pi(g_E) dg_E.$$

Evaluating this integral through numerical integration is computationally inexpensive because we do not need to re-evaluate the MLE and the observed information matrix at each iteration of the integration. Moreover, this method is applicable for all types of properly defined priors on  $g_E$ . In our implementation, we use the `integrate` function within the `stats` package of base R to perform this numerical integration.

For the Product prior (7), we adopt the Laplace Approximation (LA) to obtain the approximated marginal likelihood:

$$\tilde{p}(\mathbf{t} | \boldsymbol{\gamma}) = \exp\{\ell(\tilde{\boldsymbol{\Psi}}_\gamma) + \log \pi_P(\tilde{\boldsymbol{\Psi}}_\gamma)\} (2\pi)^{d_\gamma/2} \left| H(\tilde{\boldsymbol{\Psi}}_\gamma) + \nabla^2 \log \pi_P(\tilde{\boldsymbol{\Psi}}_\gamma) \right|^{-1/2}, \quad (12)$$

where  $\tilde{\boldsymbol{\Psi}}_\gamma = \arg \max_{\boldsymbol{\Psi}_\gamma} \{\ell(\boldsymbol{\Psi}_\gamma) + \log \pi_P(\boldsymbol{\Psi}_\gamma)\}$  is the maximum a posteriori (MAP) under the Product prior and  $\pi_P(\boldsymbol{\Psi}_\gamma) = \pi_P(\boldsymbol{\theta}_\gamma, \boldsymbol{\eta}_\gamma | g_{C_t}, g_{M_t}) \pi(\nu) \pi(\theta_0)$ . We use the `nlminb` function to obtain the MAP in our implementation.

## 4.2 Model Space Exploration

Given the marginal likelihood (or an approximation thereof, under either prior structure) and the prior on model probabilities, we can now obtain samples from the model posterior. For low-dimensional scenarios, it is possible to compute the posterior probabilities for all models. However, since the number of models is  $4^p + 2^p - 1$ , this becomes infeasible even for relatively small values of  $p$ . This implies the need for using Markov chain Monte Carlo methods to explore high-probability regions of the model space. To sample from the posterior of the models,  $\pi(\boldsymbol{\gamma} | \mathbf{t})$ , we consider the Add-Delete-Swap (ADS) algorithm (Madigan et al. 1995, Tadesse & Vannucci 2021) due to its extendable design. The original ADS algorithm has three possible moves: the

Add move (**A**) and Delete move (**D**) picks one variable at random, and include or exclude it from the current model; the Swap move (**S**) draws a pair of variables: one from the current model and one not in the current model and swaps them. Direct application of the ADS algorithm on  $\gamma$  would be problematic in two ways: (i) it is not compatible with the setup of  $\text{Hz}(\gamma)$  in Section 2, as an AFT model is almost impossible to reach from a GH/AH/PH model with these three moves; (ii) as hinted in Section 3.3, the ratio between GH models than the other three types of models grows exponentially with the number of included variables. For example, if the true model is a PH model with a few active variables, then the sampler may take a large number of iterations to converge and could easily get stuck in local modes. Therefore, it is necessary to extend the ADS sampler to accommodate the need to move between the four types of hazard structures by introducing corresponding moves.

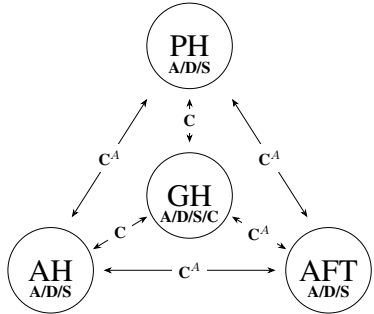


Figure 1: Illustration of the extended ADS sampler. The bold letters represent different moves.

Move	Usage	Detail
With-in hazard	<b>A</b> All	Add one variable to the current model
	<b>D</b> All	Remove one variable from the current model
	<b>S</b> All	Swap the value of $\gamma$ between two variables with different $\gamma$
Between hazard	<b>C</b> GH	Change $\gamma$ of an included variable to a different value in $\{1, 2, 3\}$
	AH, PH, GH	
<b>C</b> <sup>A</sup>	All	When all included variables have the same values of $\gamma \in \{1, 2, 3, 4\}$ , change all to another; for GH changes only allowed between/from AFT

Table 1: Detailed description of each of the moves in the left figure. Note that **C** is used for both within and between structure sampling.

Figure 1 provides a general picture of the algorithm. In our setting, we keep the three moves from the original ADS algorithm for moving within the model space of every single structure. One modification we made to the **S** move is that, for GH models, we only swap one of the time-level or hazard-level effects (at random) for the chosen pair of variables, which prevents the jumps from being too large. For moving between the model structures, we design a pair of moves: Change

(C) and Change All (C<sup>A</sup>), as shown in 1. The C move randomly chooses a variable  $j$  from the current model and randomly changes  $\gamma_j$  to one of the other two values in  $\{1, 2, 3\}$ . Note that C move is not only used for between-hazard transition, but also for within-hazard sampling of GH models. The C<sup>A</sup> move, on the other hand, directly changes the hazard structure by changing all variables in the current model simultaneously. Note that the transition from GH to AFT requires all variables in the model to have both effects. Note that this proposal-generating step is the same regardless of the prior specification.

Having the new candidate model, we use the standard Metropolis-Hastings update to decide if the candidate model will be accepted. Let  $\gamma'$  denote the candidate model and  $q$  be the Hastings ratio, the acceptance probabilities under the two proposed priors are given by:

$$\text{acc}_{LCM} = \min \left\{ 1, \frac{\tilde{p}(\mathbf{t} \mid \gamma') p(\gamma')}{\tilde{p}(\mathbf{t} \mid \gamma) p(\gamma)} \cdot q \right\}, \quad \text{acc}_P = \min \left\{ 1, \frac{\tilde{p}(\mathbf{t} \mid \gamma') p(\gamma')}{\tilde{p}(\mathbf{t} \mid \gamma) p(\gamma)} \cdot q \right\}.$$

The detailed expression for  $q$  depends on the selected move in the extended ADS sampler. Details of the extended ADS sampler and methods of summarising the MCMC samples are provided in the Supplementary Material.

## 5 Asymptotic Theory

In this section, we characterise the asymptotic Bayes factor rates and model selection consistency for both prior types (LCM and product priors), using their corresponding approximations (ILA and LA). Throughout, we denote by  $\varphi_0(o_i, c_i, \mathbf{z}_i)$  the true generating mechanism, which may depend on additional unavailable covariates (that is,  $\tilde{\mathbf{x}}_i \subseteq \mathbf{z}_i$  and  $\mathbf{x}_i \subseteq \mathbf{z}_i$ ). Let us denote  $\mathbf{v} = (t_1, o_1, c_1, \delta_1)^\top$ , and define the functions

$$m(\Psi_\gamma, \mathbf{v}) = \delta_1 \log h(o_1 \mid \Psi_\gamma) - H(t_1 \mid \Psi_\gamma),$$

$$M(\Psi_\gamma) = E_{\varphi_0} [m(\Psi_\gamma)],$$

which represent the contribution of a single observation to the log-likelihood function, and the expected log-likelihood function, respectively. Define  $\Psi_\gamma^* = \text{argmax}_{\Gamma_\gamma} M(\Psi_\gamma)$ , the value that

maximises the expected log-likelihood. Let also  $\gamma^*$  be the indicator of the non-zero variables (most parsimonious model) that maximise  $M(\Psi)$ , that is,  $\Psi_{\gamma^*}^* = \text{argmax}_{\Gamma_\gamma} M(\Psi_{\gamma}^*)$ . Let us also denote by  $\mathbf{X}_\gamma$  and  $\tilde{\mathbf{X}}_\gamma$ , the design matrices associated with model  $\gamma$ , and  $\mathbf{X}_{\gamma,O}$  and  $\tilde{\mathbf{X}}_{\gamma,O}$ , the design matrices associated with model  $\gamma$  and the uncensored observations.

The conditions required for the proofs are listed in the Supplementary Material. We first provide a characterisation of the Bayes factor rates for the LCM prior obtained via the integrated Laplace approximation. We say that the model indicator vector  $\gamma$  contains  $\gamma^*$ , denoted by  $\gamma^* \subset \gamma$ , if every covariate that is active in the model  $\gamma^*$  is also active in the model  $\gamma$ . Formally, for all  $j = 1, \dots, p$ ,  $\gamma_j^* \neq 0 \Rightarrow \gamma_j \neq 0$  and  $\gamma_j \in \{\gamma_j^*, 3\}$ , while, for any  $k = 1, \dots, p$  such that  $\gamma_k^* = 0$ , we require  $\gamma_k \geq 0$ .

**Proposition 2** *Consider the GH model (1) with log-location-scale baseline hazard (2), together with the prior (4) on the common parameters and (5) on the model-specific parameters, where  $g_E$  is assumed to be non-decreasing in  $n$ . Let  $\hat{B}_{\gamma, \gamma^*}$  denote the Bayes factor obtained via an integrated Laplace approximation,  $\hat{B}_{\gamma, \gamma^*} = \frac{\hat{p}(\mathbf{t}|\gamma)}{\hat{p}(\mathbf{t}|\gamma^*)}$ , where  $\gamma^*$  is the model maximising  $M(\Psi_{\gamma^*})$ , and  $\gamma \neq \gamma^*$  is another hazard-based regression model of type (1). Assume that both models associated with  $\gamma^*$  and  $\gamma$  satisfy Conditions C1–C7 in Section 5 of the Supplementary Material. Then,*

1. *Overfitted models. If  $\gamma^* \subset \gamma$ , then*

$$\log(\hat{B}_{\gamma, \gamma^*}) = \frac{d_{\gamma^*} - d_\gamma}{2} \log(1 + ng_E) + \mathcal{O}_p(1),$$

2. *Non-overfitted models. If  $\gamma^* \not\subset \gamma$ , then*

$$\log(\hat{B}_{\gamma, \gamma^*}) = -n[M(\Psi_{\gamma^*}^*) - M(\Psi_\gamma^*)] + \frac{d_{\gamma^*} - d_\gamma}{2} \log(1 + ng_E) + \mathcal{O}_p(1).$$

Based on the results of Proposition 2, we can establish model selection consistency for the LCM prior, as described in the following corollary.

**Corollary 1** Assuming the prior probability assigned to  $\gamma^*$  is not 0, i.e.  $\pi(\gamma^*) \neq 0$ , and the Conditions C1-C7 hold, then  $\tilde{\pi}(\gamma^* | t, \delta) \xrightarrow{\text{Pr}} 1$ .

The following result provides a characterisation of the Bayes factor rates obtained with the Product prior (7), and approximated with the Laplace approximation.

**Proposition 3** Consider the GH model (1) with log-location-scale baseline hazard (2), together with the prior (4) on the common parameters and (7) on the model-specific parameters, where  $g_{C_t}$  and  $g_{C_h}$  are assumed to be non-decreasing in  $n$ . Let  $\tilde{B}_{\gamma, \gamma^*}$  denote the Bayes factor obtained via a Laplace approximation,  $\tilde{B}_{\gamma, \gamma^*} = \frac{\tilde{p}(t|\gamma)}{\tilde{p}(t|\gamma^*)}$ , where  $\gamma^*$  is the model maximising  $M(\Psi_\gamma)$ , and  $\gamma \neq \gamma^*$  is another hazard-based regression model of type (1). Assume that both models associated with  $\gamma^*$  and  $\gamma$  satisfy Conditions C1–C7 in Section 5 of the Supplementary Material. Then,

1. *Overfitted models.* If  $\gamma^* \subset \gamma$ , then

$$\log(\tilde{B}_{\gamma, \gamma^*}) = \frac{p_{\gamma^*} - p_\gamma}{2} \log(n g_{C_h}) + \frac{q_{\gamma^*} - q_\gamma}{2} \log(n g_{C_t}) + \mathcal{O}_p(1).$$

2. *Non-overfitted models.* If  $\gamma^* \not\subset \gamma$ , then

$$\log(\tilde{B}_{\gamma, \gamma^*}) = -n[M(\Psi_{\gamma^*}^*) - M(\Psi_\gamma^*)] + \frac{p_{\gamma^*} - p_\gamma}{2} \log(n g_{C_h}) + \frac{q_{\gamma^*} - q_\gamma}{2} \log(n g_{C_t}) + \mathcal{O}_p(1).$$

Finally, model selection consistency also holds for the Product prior, as stated in the following corollary.

**Corollary 2** Assuming the prior probability assigned to  $\gamma^*$  is not 0, i.e.  $\pi(\gamma^*) \neq 0$ , and the Conditions C1-C7 hold, then  $\tilde{\pi}(\gamma^* | t, \delta) \xrightarrow{\text{Pr}} 1$ .

For both priors, in overfitted models, the asymptotic Bayes factor rates do not depend on censoring or model misspecification, but only on the number of spurious variables at each level and the values of the hyperparameters. For non-overfitted models, the term  $M(\Psi_{\gamma^*}^*) - M(\Psi_\gamma^*)$  depends on censoring and potential model misspecification through the expected log-likelihood. Although the GH model encompasses a range of simpler models, when the true model structure is, for

example, a proportional odds or cure model, the value of this term depends on how the true generating model projects onto the GH family. Comparing Propositions 2 and 3, we see that when  $g_E = g_{C_t} = g_{C_h}$ , the Bayes factor rates are similar despite differences in the prior covariance matrices, with the LCM prior exhibiting a marginally better rate due to the additional “plus-one” term. In other words, the Bayes factor rates coincide when  $g_{C_t} = g_{C_h} = g_E - 1/n$ . Since a larger  $g$  implies stronger sparsity, the LCM prior, under the default hyperparameter setting, has slightly greater ability to rule out spurious variables than the Product prior.

Implicitly, the model selection consistency results in Corollaries 1 and 2 indicate that, asymptotically, the proposed methods recover the model that is closest to the true data-generating mechanism in terms of a generalised Kullback–Leibler divergence that accounts for the presence and type of censoring. When the model is correctly specified, one would therefore expect both the active variables and the underlying hazard structure to be identifiable asymptotically. Nevertheless, finite-sample performance may still be affected by the interplay among sample size, censoring rate, and length of follow-up.

## 6 Simulation Study

In this section, we evaluate the performance of the proposed methods for variable selection and hazard-structure selection using a simulation study. First, we assess robustness to misspecification of the baseline hazard and evaluate the extent to which the methods can recover the true underlying hazard structure. Second, we examine whether the posterior inclusion probabilities of the covariates change depending on whether hazard-structure selection is performed. This allows us to determine whether incorporating hazard-structure uncertainty affects the power to detect active or spurious variables.

Based on the objectives outlined above, we consider sample sizes of  $n = 250, 500, 1000$  and examine settings with  $p = 10, 50, 100$  covariates. To assess performance under different levels

of incomplete follow-up, we include censoring rates of 25% and 50%. We consider two types of underlying baseline hazard, Power Generalised Weibull (PGW, monotonically decreasing) and log-normal, and two common hazard structures, PH and AFT, and the more general GH as the true structures. In all scenarios, the design matrices  $\tilde{\mathbf{X}} = \mathbf{X}$  are generated from  $N(\mathbf{0}, \Sigma)$  with  $\Sigma_{i,j} = 0.7^{|i-j|}$ , and only four of the variables, positioned in  $(0.2p)^{\text{th}}$ ,  $(0.4p)^{\text{th}}$ ,  $(0.6p)^{\text{th}}$ , and  $(0.8p)^{\text{th}}$ , are active. Their coefficients are chosen such that we have a combination of large/small and positive/negative effects. In total, the simulation grid contains 90 scenarios, and we conduct  $N = 250$  Monte Carlo runs for each of the scenarios, where random samples are being generated at each of the runs. We use a log-normal baseline hazard for the model used in the selection process, and the same setting for MCMC across all runs. The details of the specifications are included in the Supplementary Material.

## 6.1 Interpretation of results

We examine variable-selection performance and hazard-structure selection performance separately. Figure 2 presents the sensitivity and specificity of variable selection under the two proposed priors across all simulation scenarios. For each of the 250 Monte Carlo replicates, the metrics are computed using the covariate with the highest posterior probability model, and the values shown in the figure represent the scenario-specific means. Corresponding standard errors and the running times of the chains are reported in the Supplementary Material. We begin by comparing the columns horizontally. First, misspecification of the baseline hazard has little impact on the true positive rates for PH models, but it degrades performance for AFT models. Since the PGW baseline hazard is monotonically decreasing, it becomes more difficult to distinguish between time-level effects, hazard-level effects, or their combination. That is, a monotonic baseline hazard implies that the role of the covariates is difficult to identify as the GH model is non-identifiable under Weibull baseline hazards (Chen & Jewell 2001), which are monotonic. Furthermore, smaller time effects require longer follow-up to become detectable, which explains why the true positive

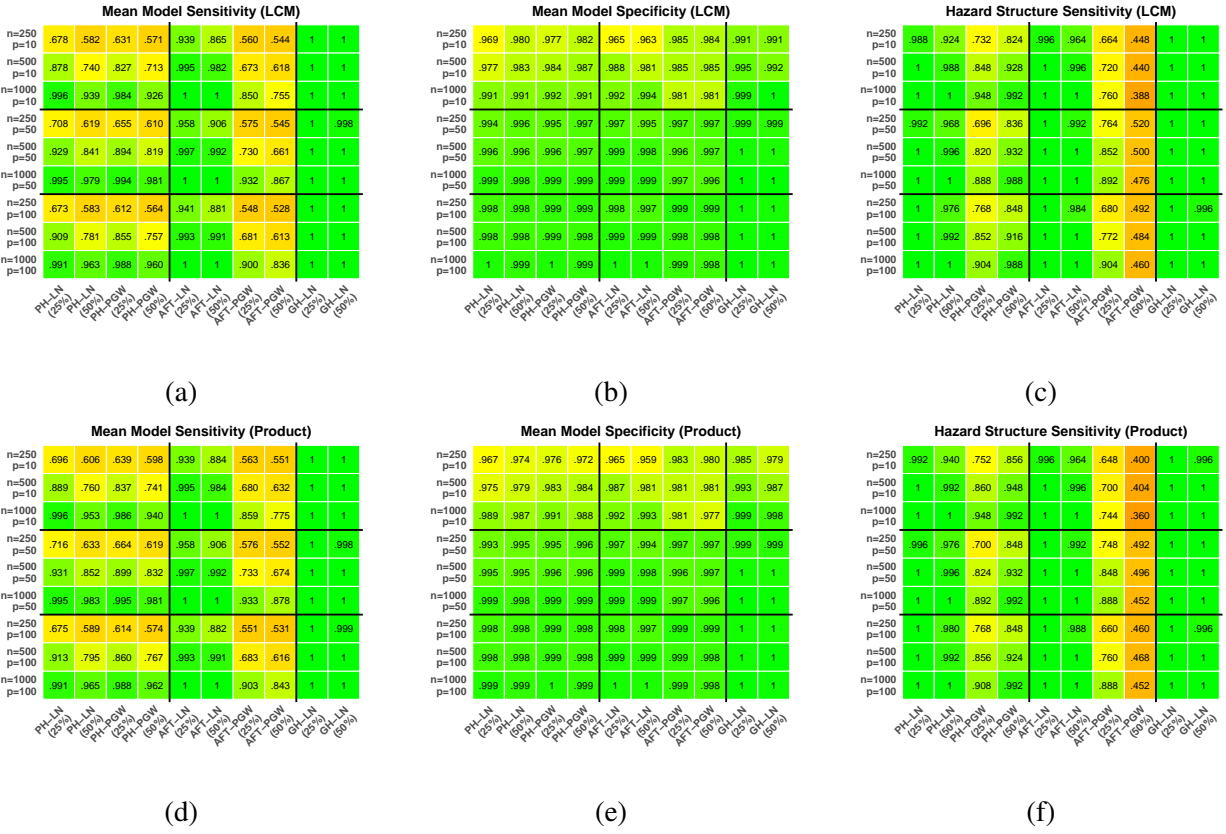


Figure 2: Mean sensitivity and specificity of variable selection (VS) and hazard selection (HS) across the 250 Monte Carlo simulations. (a)(b)(c) Mean VS sensitivity and specificity and HS accuracy under LCM prior; (d)(e)(f) Mean VS sensitivity and specificity and HS accuracy under Product prior.

rates for AFT and GH models slightly worsen under higher censoring. Notably, under correct baseline specification, the AFT model appears largely unaffected by the censoring rate, likely because an effect of 0.25 in an AFT specification has a stronger influence on the baseline hazard than the same magnitude of effect in a PH model, given that the covariate impacts both time and hazard scales. In contrast, the true negative rates remain consistently high across all scenarios, with most values exceeding 0.98.

Next, comparing across the rows, we observe slightly improved specificity in some settings when  $p$  increases. This is explained by the design of the covariate matrices, as the extra spurious

variables have decreasing correlation with the four active ones. In contrast, sample size has a much more substantial influence on variable-selection performance. With  $n = 250$ , only the two strongest-effect variables are consistently detectable across most scenarios. As the sample size increases, the smaller effects become detectable as well, although their recovery still depends on the censoring rate and on whether the baseline hazard is correctly specified. These findings are supported by the violin plots in Figure S1 of the Supplementary Material.

It is worth noting that the differences between the two priors are generally small. The Product prior exhibits slightly higher sensitivity but slightly lower specificity for the PH and AFT models. This pattern suggests that the LCM prior favours more parsimonious models when the true hazard structure corresponds to one of these simpler forms. It also indicates that the censoring information absorbed into the  $g$ 's under the Product prior has only a limited effect on variable-selection performance. In contrast, for GH models, the LCM prior achieves similarly high sensitivity but higher specificity than the Product prior across all scenarios. This is expected, since the LCM prior can capture dependencies between the time and hazard components, whereas the Product prior treats them independently. Finally, the standard errors of the sensitivity and specificity estimates are similar across all scenarios, indicating comparable stability between the two priors.

We now turn to the hazard-structure selection performance. Figure 2 presents the accuracy of selecting the correct hazard structure under both priors. For each Monte Carlo replicate, the posterior probability of each hazard structure is obtained by summing the estimated posterior probabilities of all models belonging to that structure. The hazard structure with the highest posterior probability is then selected for that replicate. In general, the accuracies of hazard selection are mostly above 0.7, with the exception of the AFT model with a misspecified baseline and 50% censoring rate. This demonstrates that the proposed prior on model space, which crucially influences the hazard selection, has generally good empirical performance. As for the single

exception, the reasoning is the same as mentioned earlier: under monotonic baseline and higher censoring rate, time-level effects are harder to detect, which makes it hard to identify the AFT structure from the PH structure (as both structures coincide when the baseline hazard is Weibull, thus monotonic). This is evidenced by the stacked barplots in Figure S1 of the Supplementary Material. Comparing (c) and (f) in Figure 2, we could see that the difference between the two priors is very small. This is because the prior on model coefficients has less impact on hazard selection than the prior on the model space, emphasising the importance of carefully selecting a prior on the model space.

Lastly, we also examine the effect of using a richer hazard structure on variable-selection performance, compared to restricting the analysis to the true hazard structure. The details are included in the Supplementary Material, and the main discovery is that hazard-structure selection usually does not affect the variable selection performance significantly. However, misspecification of the parametric GH model (for instance, in terms of the shape of the baseline hazard) and censoring (length of follow-up) can affect the selection of the hazard structure and the power to detect small effects in finite samples. The additional example presented in the Supplementary material, involving a case with a monotonic baseline hazard, shows that larger sample sizes and enough follow-up are required to identify the true hazard structure and active variables.

## 7 Real Data Applications

In this section, we present two real-data applications that illustrate the use and performance of the proposed methodology with LCM and Product priors. In the first application, we analyse the serum free light chain data set FLC, which represents a case where the data clearly favour the GH structure, indicating that the variables included in the selected model play distinct roles. The second application examines the metastasis-free survival data from the breast cancer data set NKI70. This example features a high censoring rate, high dimensionality, and a moderate sample

size, a combination that leads to greater uncertainty regarding both the hazard structure and the set of active variables.

## 7.1 Serum free light chain data set (FLC)

We analyse the FLC data set, which is publicly available in the `survival` R package. This data set has been used to study the prevalence of monoclonal gammopathy of undetermined significance (MGUS) in Olmsted County, Minnesota, based on approximately two-thirds of residents aged 50 years or older. [Dispenzieri et al. \(2012\)](#) assayed FLC levels in these samples and found that elevated levels were associated with increased mortality. The FLC data set contains a stratified random sample (by age and sex) comprising 1/2 of the originally studied subjects, with  $n = 7,874$  samples and 8 variables. Details on these variables are provided in the Supplementary Material. The longest follow-up time in the study is approximately 14 years. We consider the following 6 variables, matching the multivariate analysis in [Dispenzieri et al. \(2012\)](#): two binary variables (Sex and Mgus) and four numerical variables (Age, Kappa, Lambda, and Creatinine). Retaining only complete cases for these  $p = 6$  variables yields  $n = 6,521$  observations, of which 70% are censored. All numerical variables are then centred and scaled.

For each of the proposed priors (LCM and Product), we run the MCMC sampler for 50,000 iterations, with 10,000 burn-in steps and a thinning period set to 10. The baseline hazard is assumed to be log-normal, and the prior on the model space uses the default set of hyperparameters recommended in Section 3.3. Table 2 reports the 90% highest posterior probability credible sets ([Griffin 2025](#)) for the proposed prior structure. All selected models are GH models, with most variables exhibiting both time-level and hazard-level effects at different scales across the sets. The four variables that appear in these sets are mostly consistent with the multivariate analysis with the Cox PH model in [Dispenzieri et al. \(2012\)](#), where Age, Sex, and the sum of Kappa and Lambda have significant p-values.

Table 2: The 90% highest posterior probability model credible set for each prior structure for the FLC data set.  $haz$  in the superscript within the brackets stands for hazard-level effect only, and no superscript means the variable has both time-level and hazard-level effects but at a different level (i.e.  $\gamma_j = 3$ ). The superscript on the right bracket indicates the hazard type.

Model \ Posterior probability	LCM ( $g_E = 1$ )	Product ( $g_{C_t} = g_{C_h} = 1$ )	LCM (Robust $g$ )
{age, lambda, sex} <sup>GH</sup>	0.699	0.615	0.249
{age, kappa, lambda <sup>haz</sup> , sex} <sup>GH</sup>	0.166	0.220	0.218
{age, kappa, lambda, sex} <sup>GH</sup>	0.092	0.111	0.490

For the fixed- $g$  priors (LCM and Product), the models included in the sets are identical, with only slight differences in the distribution of model posterior probabilities. The MAP estimates of the regression coefficients,  $(\boldsymbol{\alpha}, \boldsymbol{\beta})$ , in the original parametrisation (1), for the top model under the fixed- $g$  LCM prior are:  $(-0.618, 0.967)$  for Age,  $(0.489, 0.357)$  for Lambda, and  $(-1.117, 0.203)$  for Sex. The estimates for the Product prior are similar. Therefore, an increase in Age, or being male compared to female, results in a proportional increase in hazard level, but also a later hazard peak and a slower decrease in hazard, under our log-normal baseline hazard assumption. The variable Lambda, on the other hand, has smaller and similar hazard-level and time-level effects. Note that the same value of a coefficient in the time and hazard levels does not imply the same influence on the baseline hazard, which usually depends on the study duration and the form of the baseline hazard. Examining the distribution of posterior probabilities, we observe that under both fixed- $g$  priors, the model posterior probability decreases as the model size increases from 6 to 8. Moreover, the conclusions obtained with the LCM prior coincide with those associated with the Product prior but with slightly stronger penalisation, as more posterior probability mass is concentrated in the smallest model. This observation is consistent with the results from the simulation study. It is noticeable that the hyper- $g$  LCM prior assigns the highest posterior probability to the largest

GH model, which ranked only third under the fixed- $g$  priors, with the additional variable Kappa. The MAP estimates of this full GH model under the hyper robust- $g$  LCM prior, in  $(\alpha, \beta)$  as in (1), are  $(-0.592, 0.964)$  for Age,  $(-0.511, 0.099)$  for Kappa,  $(0.318, 0.178)$  for Lambda, and  $(-1.123, 0.189)$  for Sex. The MAP estimates under the fixed- $g$  priors are very similar, reflecting the strong influence of the likelihood. An evident change is observed in the MAP estimate for Lambda when Kappa is included, likely due to the high correlation of 0.83 between the two variables. Compared to the fixed- $g$  priors, the hyper- $g$  prior tends to distribute posterior weight more evenly across the set of comparably high-probability models, rather than concentrating it on a single top model.

To better understand the effect of correlation, we create two new variables in place of Kappa and Lambda: their sum, “kap+lam”, and their ratio, “kap/lam”. The former represents the overall FLC level, while the latter has a clinical interpretation for the detection of monoclonal light chains, and both were used in the analysis of [Dispenzieri et al. \(2012\)](#). After this transformation, the correlation between these two variables is reduced to 0.01. We rerun the samplers on this new set of 6 variables, following the same MCMC sampling strategy and prior setup. The top model under all three prior settings is  $\{\text{Age}, \text{kap+lam}, \text{Sex}\}^{GH}$ , with posterior probabilities of 0.951 for fixed- $g$  LCM, 0.919 for fixed- $g$  Product, and 0.945 for hyper- $g$  LCM. Thus, after removing the strong correlation, the hyper- $g$  LCM prior identifies the single top model, consistent with the fixed- $g$  priors. In summary, this application not only demonstrates the variable selection performance of the proposed methods on a real data set, but also highlights the ability of the flexible GH structure to capture the multiple roles of each active variable.

## 7.2 Metastasis-free survival of breast cancer patients (NKI70)

We now analyse the NKI70 data set from the Netherlands Cancer Institute. This data set is publicly available in the `penalized` R package, and the variable dictionary is provided in

the Supplementary Material. It contains metastasis-free survival times for  $n = 144$  lymph node-positive patients, along with 5 clinical risk factors and gene expression measurements for 70 genes. The longest follow-up in the study is approximately 17 months. Considering both clinical risk factors and genes in the covariate matrix, we have  $p = 75$  variables, of which 4 are categorical. The overall censoring rate is 66.7%, with no missing values in the covariate matrix. All numerical variables are then centred and scaled. Due to the small sample size relative to the number of variables and the high censoring rate, this data set poses a considerable challenge for variable and hazard structure selection.

Apart from the two proposed priors, we also consider two reference variable selection methods: Zellner's fixed- $g$  prior for the AFT model (Rossell & Rubio 2023) and the non-local pMOM prior for the Cox model with partial likelihood (Nikooienejad et al. 2020) to benchmark our methodology. For the former, we use the `modelSelection` function in the `mombf` R package, with  $g$  set to the sample size (144), corresponding to a unit information prior, and the default Beta-Binomial(1,1) prior for the model space. For the latter, we use the `bvs` function in the `BVSNLP` R package, with the product moment (pMOM) prior on model coefficients and the same Beta-Binomial(1,1) prior for the model space. The detailed MCMC specifications are provided in the Supplementary Material. Table 3 presents the model selection results for the proposed and reference methods. Comparing the two proposed methods, we see that both have the same size of the 50% highest posterior probability set. However, under the LCM prior, a larger model posterior probability is concentrated on smaller models compared to the Product prior. This again confirms the observation from the simulation study that the LCM prior slightly favours more parsimonious models than the Product prior.

Examining the listed models for each method, the gene PRC1 appears in all of them, and the model containing only PRC1 has the highest posterior probability across all four methods. Moreover, the model  $PRC1^{GH}$  has approximately 0.03 posterior probability for both proposed methods,

Table 3: The rank of the top models, in terms of estimated posterior probability, for the proposed and reference methods for NKI70 data set. The superscript on the right bracket indicates the model type.

Model \ Rank (Posterior probability)	LCM ( $g_E = 1$ )	Product ( $g_{C_t}, g_{C_h} = 1$ )	AFT (Zellner- $g$ )	Partial-Cox (pMOM)
$\{\text{PRC1}\}^{\text{AFT}}$	1 (0.154)	1 (0.102)	1 (0.074)	1 (0.310): {PRC1}
$\{\text{PRC1, KNTC2}\}^{\text{AFT}}$	2 (0.082)	2 (0.076)	2 (0.058)	2 (0.088): {PRC1, IGFBP5.1}
$\{\text{PRC1, Age}\}^{\text{AFT}}$	3 (0.053)	3 (0.040)	3 (0.032)	3 (0.077): {PRC1, IGFBP5}
$\{\text{PRC1}\}^{\text{GH}}$	4 (0.040)	5 (0.025)	-	4 (0.034): {PRC1, IGFBP5.1, Contig32125-RC}
$\{\text{PRC1, IGFBP5.1}\}^{\text{AFT}}$	5 (0.032)	7 (0.023)	5 (0.020)	5 (0.028): {PRC1, IGFBP5, Contig32125-RC}
$\{\text{PRC1, KNTC2, IGFBP5.1}\}^{\text{AFT}}$	6 (0.029)	4 (0.029)	4 (0.024)	6 (0.017): {PRC1, COL4A2}

indicating that the difference in effect size of PRC1 on the time and hazard level may be identifiable under a larger sample size. The remaining models in each set are similar, consisting mostly of PRC1 combined with one or two of KNTC2, Age, IGFBP5.1. In addition, the posterior distribution over hazard structures (AH, PH, AFT, GH) is  $(0, 0.057, 0.900, 0.044)$  for the LCM prior and  $(0, 0.114, 0.857, 0.028)$  for the Product prior. Thus, both proposed methods agree that the AFT model is the most probable hazard structure, suggesting that a PH model could be potentially misspecified. This explains the difference between the highest-probability models under Cox-pMOM and the other three methods, highlighting the importance of conducting hazard structure selection. As expected, Cox-pMOM has the smallest 50% HPM set, reflecting the faster effect discovery of non-local priors compared to local priors (Rossell & Rubio 2023). Finally, the results from the AFT-Zellner- $g$  method in the `mombf` package are very similar to those from the Product prior: the four highest-probability models are identical, with comparable estimated posterior probabilities. This similarity arises because the former uses very similar prior and likelihood as the latter, conditional on the AFT model, and the posterior probability of the AFT structure under the Product prior is relatively high.

## 8 Discussion

We have developed a Bayesian methodology for simultaneously performing variable selection and hazard-structure selection for time-to-event data within the GH modelling framework. This model encompasses hazard structures of practical interest, including the PH and AFT models, enabling users not only to identify relevant variables but also to determine the level at which each covariate acts. We provide a principled approach for specifying covariate effects based on  $g$ -prior and propose a new model-space prior that extends the Beta-Binomial prior.

Through the simulation study, we found that the proposed priors behave similarly across scenarios in terms of variable-selection sensitivity and specificity, as well as the accuracy of hazard-structure selection. The LCM prior tends to encourage slightly greater sparsity and performs better when the true model is GH. While the number of spurious variables has little impact on performance, sample size plays a crucial role in determining true positive rates. Misspecification of the baseline hazard substantially reduces the true positive rates for both variable and hazard selection in the AH and AFT models, as time-level effects are more difficult to detect under monotonic baseline hazards. A similar pattern is observed for censoring: increasing the censoring rate from 25% to 50%, effectively shortening the follow-up period, markedly reduces the ability to detect time-level effects, especially when combined with baseline misspecification. Finally, we also demonstrate that allowing selection among the four hazard structures does not substantially affect variable-selection performance.

The results from the FLC dataset confirm the ability of our proposed methodology to identify important variables and correctly characterise their roles in a real-data setting. The comparison of results using fixed  $g$  priors with those obtained under the LCM prior combined with a robust prior on  $g$  indicates that the mixture- $g$  prior can be sensitive to high collinearity among active variables. The results from the NKI70 dataset, by contrast, evaluate the performance of the proposed methods relative to existing approaches in a more challenging scenario with moderately large  $p$ ,

small  $n$ , and a high censoring rate. Our methods identify the AFT structure as the most probable, and the resulting 50% credible sets closely resemble those obtained from the AFT–Zellner– $g$  model (Rossell & Rubio 2023).

There are several promising avenues for future work. The ideas used to construct the prior on  $\gamma$  can be readily extended to other models in which covariates play multiple roles, such as distributional regression, where covariates may influence more than two linear or additive predictors, as well as sample selection models, cure models, and related frameworks. Finally, based on the computing-time plots in the Supplementary Material for the simulation study, we observe that the current implementation requires approximately 5 to 20 minutes, depending on the setting, to run the sampler for 20,000 iterations in scenarios where  $n$  is on the order of 1,000s and  $p$  is on the order of 100s, which aligns with the applications of interest in most practical settings. Although the current implementation has substantial scope for efficiency improvements, for example, by rewriting the code in C++ instead of R, a more efficient MCMC scheme remains the key component for scaling to higher-dimensional problems, such as those arising in genomics (where  $p$  can be on the order of 1,000s). Recent advances in MCMC algorithms for variable selection (Liang et al. 2023) suggest several opportunities to enhance the efficiency of our extended ADS algorithm.

## 9 Disclosure statement

The authors have no conflicts of interest to declare.

## 10 Data Availability Statement

Deidentified data have been made available at the following URL: <https://github.com/Eric-YChen/GHBVS>

## References

Bayarri, M. J., Berger, J. O., Forte, A. & García-Donato, G. (2012), ‘Criteria for Bayesian model choice with application to variable selection’, *Annals of Statistics* **40**(3), 1550–1577.

Castellanos, M., Garcia-Donato, G. & Cabras, S. (2021), ‘A model selection approach for variable selection with censored data’, *Bayesian Analysis* **16**(1), 271–300.

Chen, Y. & Jewell, N. (2001), ‘On a general class of semiparametric hazards regression models’, *Biometrika* **88**(3), 687–702.

Cox, D. (1972), ‘Regression models and life-tables’, *Journal of the Royal Statistical Society. Series B* **34**(2), 187–220.

Cox, D. & Oakes, D. (2018), *Analysis of survival data*, Chapman and Hall/CRC.

Dispenzieri, A., Katzmann, J., Kyle, R., Larson, D., Therneau, T., Colby, C., Clark, R., Mead, G., Kumar, S., Melton, L. & Rajkumar, S. (2012), ‘Use of nonclonal serum immunoglobulin free light chains to predict overall survival in the general population’, *Mayo Clin Proc* **87**(6), 517–523.

Etezadi-Amoli, J. & Ciampi, A. (1987), ‘Extended hazard regression for censored survival data with covariates: A spline approximation for the baseline hazard function’, *Biometrics* **43**, 181–192.

García-Donato, G., Cabras, S. & Castellanos, M. (2023), ‘Model uncertainty quantification in Cox regression’, *Biometrics* **79**(3), 1726–1736.

Griffin, J. (2025), ‘Expressing and visualizing model uncertainty in Bayesian variable selection using Cartesian credible sets’, *Bayesian Analysis* **20**(4), 1371–1397.

Ley, E. & Steel, M. (2009), ‘On the effect of prior assumptions in Bayesian model averaging with applications to growth regression’, *Journal of Applied Econometrics* **24**(4), 651–674.

Li, Y. & Clyde, M. (2018), ‘Mixtures of g-priors in generalized linear models’, *Journal of the American Statistical Association* **113**(524), 1828–1845.

Liang, F., Paulo, R., Molina, G., Clyde, M. & Berger, J. (2008), ‘Mixtures of g priors for Bayesian variable selection’, *Journal of the American Statistical Association* **103**(481), 410–423.

Liang, X., Livingstone, S. & Griffin, J. (2023), ‘Adaptive MCMC for Bayesian variable selection in generalised linear models and survival models’, *Entropy* **25**(9), 1310.

Madigan, D., York, J. & Allard, D. (1995), ‘Bayesian Graphical Models for Discrete Data’, *International Statistical Review* **63**(2), 215–232.

Nikooienejad, A., Wang, W. & Johnson, V. (2020), ‘Bayesian variable selection for survival data using inverse moment priors’, *The Annals of Applied Statistics* **14**(2), 809.

Rossell, D. & Rubio, F. (2023), ‘Additive Bayesian variable selection under censoring and misspecification’, *Statistical Science* **38**, 13–29.

Rubio, F., Remontet, L., Jewell, N. & Belot, A. (2019), ‘On a general structure for hazard-based regression models: an application to population-based cancer research’, *Statistical Methods in Medical Research* **28**(8), 2404–2417.

Scott, J. & Berger, J. (2010), ‘Bayes and empirical-Bayes multiplicity adjustment in the variable-selection problem’, *The Annals of Statistics* **38**(5), 2587–2619.

Sha, N., Tadesse, M. & Vannucci, M. (2006), ‘Bayesian variable selection for the analysis of microarray data with censored outcomes’, *Bioinformatics* **22**(18), 2262–2268.

Tadesse, M. & Vannucci, M. (2021), *Handbook of Bayesian variable selection*, CRC Press.

Tong, X., Zhu, L., Leng, C., Leisenring, W. & Robison, L. (2013), ‘A general semiparametric hazards regression model: efficient estimation and structure selection’, *Statistics in Medicine* **32**(28), 4980–4994.

Vallejos, C. & Steel, M. (2015), ‘Objective Bayesian survival analysis using shape mixtures of log-normal distributions’, *Journal of the American Statistical Association* **110**(510), 697–710.

Wang, X. & George, E. I. (2007), ‘Adaptive Bayesian criteria in variable selection for generalized linear models’, *Statistica Sinica* **17**(2):, 667–690.

Zellner, A. (1986), ‘On assessing prior distributions and Bayesian regression analysis with g-prior distributions.’, *Bayesian Inference and Decision techniques: Essays in Honor of Bruno de Finetti* p. 389–399.

Zhang, J., Hanson, T. & Zhou, H. (2018), ‘Bayes factors for choosing among six common survival models’, *Lifetime Data Analysis* pp. 1–19.

Zhou, H. & Hanson, T. (2018), ‘A unified framework for fitting Bayesian semiparametric models to arbitrarily censored survival data, including spatially referenced data’, *Journal of the American Statistical Association* **113**(522), 571–581.

**Supplementary material  
for  
Bayesian variable and hazard structure selection in  
the General Hazard model**

Yulong Chen

Department of Statistical Science, University College London  
and

Jim Griffin

Department of Statistical Science, University College London  
and

Francisco Javier Rubio

Department of Statistical Science, University College London

February 4, 2026

# 1 Log-Likelihood, Gradient and Hessian functions

## 1.1 Log-likelihood function

Recall that the hazard and cumulative hazard functions can be written as

$$h(t \mid \mu, \sigma) = \frac{\frac{1}{\sigma t} f\left(\frac{\log(t) - \mu}{\sigma}\right)}{1 - F\left(\frac{\log(t) - \mu}{\sigma}\right)}, \quad H(t \mid \mu, \sigma) = -\log\left[1 - F\left(\frac{\log(t) - \mu}{\sigma}\right)\right].$$

The likelihood function of  $(\boldsymbol{\alpha}^\top, \boldsymbol{\beta}^\top, \mu, \sigma)$  is

$$L(\boldsymbol{\alpha}^\top, \boldsymbol{\beta}^\top, \mu, \sigma) = \prod_{i=1}^n h(t_i \mid \boldsymbol{\alpha}, \boldsymbol{\beta}, \mu, \sigma)^{\delta_i} \exp[-H(t_i \mid \boldsymbol{\alpha}, \boldsymbol{\beta}, \mu, \sigma)].$$

Thus, the log likelihood function can be rewritten as

$$\begin{aligned} \ell(\boldsymbol{\alpha}^\top, \boldsymbol{\beta}^\top, \mu, \sigma) &= \sum_{i=1}^n \delta_i \log h(t_i \mid \boldsymbol{\alpha}, \boldsymbol{\beta}, \mu, \sigma) - \sum_{i=1}^n H(t_i \mid \boldsymbol{\alpha}, \boldsymbol{\beta}, \mu, \sigma) \\ &= -n_o \log(\sigma) - \sum_{i=1}^n \delta_i \log(t_i) - \sum_{i=1}^n \delta_i \tilde{\mathbf{x}}_i^\top \boldsymbol{\alpha} + \sum_{i=1}^n \delta_i \mathbf{x}_i^\top \boldsymbol{\beta} \\ &\quad + \sum_{i=1}^n \delta_i \log f\left(\frac{\log(t_i) + \tilde{\mathbf{x}}_i^\top \boldsymbol{\alpha} - \mu}{\sigma}\right) - \sum_{i=1}^n \delta_i \log\left[1 - F\left(\frac{\log(t_i) + \tilde{\mathbf{x}}_i^\top \boldsymbol{\alpha} - \mu}{\sigma}\right)\right] \\ &\quad + \sum_{i=1}^n \log\left[1 - F\left(\frac{\log(t_i) + \tilde{\mathbf{x}}_i^\top \boldsymbol{\alpha} - \mu}{\sigma}\right)\right] \exp(\mathbf{x}_i^\top \boldsymbol{\beta} - \tilde{\mathbf{x}}_i^\top \boldsymbol{\alpha}), \end{aligned}$$

where  $n_o = \sum_{i=1}^n \delta_i$ . Consider the reparameterisation  $\tau = 1/\sigma$ ,  $\theta_0 = \mu/\sigma$ ,  $\boldsymbol{\theta} = -\boldsymbol{\alpha}/\sigma$ , and

$\boldsymbol{\eta} = -\boldsymbol{\beta}$ . After some algebra we can write down the log likelihood function as follows

$$\begin{aligned} \ell_n(\boldsymbol{\Psi}) &= n_o \nu - \sum_{i=1}^n \delta_i \log(t_i) + \sum_{i=1}^n \delta_i (\tilde{\mathbf{x}}_i^\top \boldsymbol{\theta} e^{-\nu} - \mathbf{x}_i^\top \boldsymbol{\eta}) \\ &\quad + \sum_{i=1}^n \delta_i \log f(e^\nu \log(t_i) - \tilde{\mathbf{x}}_i^\top \boldsymbol{\theta} - \theta_0) \\ &\quad + \sum_{i=1}^n \log F(-e^\nu \log(t_i) + \tilde{\mathbf{x}}_i^\top \boldsymbol{\theta} + \theta_0) [\exp(\tilde{\mathbf{x}}_i^\top \boldsymbol{\theta} e^{-\nu} - \mathbf{x}_i^\top \boldsymbol{\eta}) - \delta_i], \end{aligned}$$

where  $\tau = \exp(\nu)$ ,  $\boldsymbol{\Psi} = (\nu, \theta_0, \boldsymbol{\theta}^\top, \boldsymbol{\eta}^\top)^\top$ .

## 1.2 The Gradient function

The gradient function is:

$$g(\Psi) = \begin{pmatrix} \frac{\partial}{\partial \nu} \ell(\Psi) \\ \frac{\partial}{\partial \theta_0} \ell(\Psi) \\ \nabla_{\theta} \ell(\Psi) \\ \nabla_{\eta} \ell(\Psi) \end{pmatrix},$$

where,

$$\begin{aligned} \frac{\partial}{\partial \nu} \ell(\Psi) &= n_o - \sum_{i=1}^n \delta_i \tilde{\mathbf{x}}_i^\top \boldsymbol{\theta} e^{-\nu} + \sum_{i=1}^n \delta_i \frac{f'(u_i)}{f(u_i)} \log(t_i) e^\nu - \sum_{i=1}^n \frac{f(u_i)}{F(-u_i)} \log(t_i) [v_i - \delta_i] e^\nu \\ &\quad - \sum_{i=1}^n \log F(-u_i) v_i \tilde{\mathbf{x}}_i^\top \boldsymbol{\theta} e^{-\nu}, \\ \frac{\partial}{\partial \theta_0} \ell(\Psi) &= - \sum_{i=1}^n \delta_i \frac{f'(u_i)}{f(u_i)} + \sum_{i=1}^n \frac{f(u_i)}{F(-u_i)} [v_i - \delta_i], \\ \nabla_{\theta} \ell(\Psi) &= \sum_{i=1}^n \delta_i \tilde{\mathbf{x}}_i e^{-\nu} - \sum_{i=1}^n \delta_i \tilde{\mathbf{x}}_i \frac{f'(u_i)}{f(u_i)} + \sum_{i=1}^n \frac{f(u_i)}{F(-u_i)} \tilde{\mathbf{x}}_i [v_i - \delta_i] + \sum_{i=1}^n \log F(-u_i) v_i \tilde{\mathbf{x}}_i e^{-\nu}, \\ \nabla_{\eta} \ell(\Psi) &= - \sum_{i=1}^n \delta_i \mathbf{x}_i - \sum_{i=1}^n \log F(-u_i) v_i \mathbf{x}_i, \end{aligned}$$

with  $u_i = e^\nu \log(t_i) - \tilde{\mathbf{x}}_i^\top \boldsymbol{\theta} - \theta_0$  and  $v_i = \exp(e^{-\nu} \tilde{\mathbf{x}}_i^\top \boldsymbol{\theta} - \mathbf{x}_i^\top \boldsymbol{\eta})$ .

## 1.3 The Hessian matrix

The Hessian matrix is

$$H(\Psi) = \begin{pmatrix} \frac{\partial^2}{\partial \nu^2} \ell(\Psi) & \nabla_{\nu, \theta_0}^2 \ell(\Psi) & \nabla_{\nu, \theta}^2 \ell(\Psi) & \nabla_{\nu, \eta}^2 \ell(\Psi) \\ \nabla_{\nu, \theta_0}^2 \ell(\Psi) & \frac{\partial^2}{\partial \theta_0^2} \ell(\Psi) & \nabla_{\theta, \theta_0}^2 \ell(\Psi) & \nabla_{\eta, \theta_0}^2 \ell(\Psi) \\ \nabla_{\nu, \theta}^2 \ell(\Psi) & \nabla_{\theta, \theta_0}^2 \ell(\Psi) & \nabla_{\theta}^2 \ell(\Psi) & \nabla_{\eta, \theta}^2 \ell(\Psi) \\ \nabla_{\nu, \eta}^2 \ell(\Psi) & \nabla_{\eta, \theta_0}^2 \ell(\Psi) & \nabla_{\eta, \theta}^2 \ell(\Psi) & \nabla_{\eta}^2 \ell(\Psi) \end{pmatrix}.$$

The entries of the hessian matrix are:

$$\begin{aligned}
\frac{\partial^2}{\partial \nu^2} \ell(\Psi) &= \sum_{i=1}^n \delta_i \tilde{\mathbf{x}}_i^\top \boldsymbol{\theta} e^{-\nu} + \sum_{i=1}^n \delta_i \left[ \frac{f''(u_i)}{f(u_i)} - \left( \frac{f'(u_i)}{f(u_i)} \right)^2 \right] \log(t_i)^2 e^{2\nu} + \sum_{i=1}^n \delta_i \frac{f'(u_i)}{f(u_i)} \log(t_i) e^\nu \\
&\quad - \sum_{i=1}^n \left[ \frac{f'(u_i)}{F(-u_i)} + \left( \frac{f(u_i)}{F(-u_i)} \right)^2 \right] \log(t_i)^2 [v_i - \delta_i] e^{2\nu} - \sum_{i=1}^n \frac{f(u_i)}{F(-u_i)} \log(t_i) [v_i - \delta_i] e^\nu \\
&\quad + \sum_{i=1}^n \log F(-u_i) \tilde{\mathbf{x}}_i^\top \boldsymbol{\theta} e^{-\nu} v_i [1 + \tilde{\mathbf{x}}_i^\top \boldsymbol{\theta} e^{-\nu}] + 2 \sum_{i=1}^n \frac{f(u_i)}{F(-u_i)} \log(t_i) v_i \tilde{\mathbf{x}}_i^\top \boldsymbol{\theta}, \\
\frac{\partial^2}{\partial \theta_0^2} \ell(\Psi) &= \sum_{i=1}^n \delta_i \left[ \frac{f''(u_i)}{f(u_i)} - \left( \frac{f'(u_i)}{f(u_i)} \right)^2 \right] - \sum_{i=1}^n \left[ \frac{f'(u_i)}{F(-u_i)} + \left( \frac{f(u_i)}{F(-u_i)} \right)^2 \right] [v_i - \delta_i], \\
\nabla_{\boldsymbol{\theta}}^2 \ell(\Psi) &= \sum_{i=1}^n \delta_i \left[ \frac{f''(u_i)}{f(u_i)} - \left( \frac{f'(u_i)}{f(u_i)} \right)^2 \right] \tilde{\mathbf{x}}_i \tilde{\mathbf{x}}_i^\top - \sum_{i=1}^n \left[ \frac{f'(u_i)}{F(-u_i)} + \left( \frac{f(u_i)}{F(-u_i)} \right)^2 \right] \tilde{\mathbf{x}}_i \tilde{\mathbf{x}}_i^\top [v_i - \delta_i] \\
&\quad + 2 \sum_{i=1}^n \frac{f(u_i)}{F(-u_i)} v_i \tilde{\mathbf{x}}_i \tilde{\mathbf{x}}_i^\top e^{-\nu} + \sum_{i=1}^n \log F(-u_i) v_i \tilde{\mathbf{x}}_i \tilde{\mathbf{x}}_i^\top e^{-2\nu}, \\
\nabla_{\boldsymbol{\eta}}^2 \ell(\Psi) &= \sum_{i=1}^n \log F(-u_i) v_i \mathbf{x}_i \mathbf{x}_i^\top, \\
\nabla_{\boldsymbol{\theta}, \theta_0}^2 \ell(\Psi) &= \sum_{i=1}^n \delta_i \left[ \frac{f''(u_i)}{f(u_i)} - \left( \frac{f'(u_i)}{f(u_i)} \right)^2 \right] \tilde{\mathbf{x}}_i^\top + \sum_{i=1}^n \frac{f(u_i)}{F(-u_i)} v_i \tilde{\mathbf{x}}_i^\top e^{-\nu} \\
&\quad - \sum_{i=1}^n \left[ \frac{f'(u_i)}{F(-u_i)} + \left( \frac{f(u_i)}{F(-u_i)} \right)^2 \right] [v_i - \delta_i] \tilde{\mathbf{x}}_i^\top \\
\nabla_{\boldsymbol{\eta}, \theta_0}^2 \ell(\Psi) &= - \sum_{i=1}^n \frac{f(u_i)}{F(-u_i)} v_i \mathbf{x}_i, \\
\nabla_{\nu, \theta_0}^2 \ell(\Psi) &= - \sum_{i=1}^n \delta_i \left[ \frac{f''(u_i)}{f(u_i)} - \left( \frac{f'(u_i)}{f(u_i)} \right)^2 \right] \log(t_i) e^\nu - \sum_{i=1}^n \frac{f(u_i)}{F(-u_i)} v_i \tilde{\mathbf{x}}_i^\top \boldsymbol{\theta} e^{-\nu} \\
&\quad + \sum_{i=1}^n \left[ \frac{f'(u_i)}{F(-u_i)} + \left( \frac{f(u_i)}{F(-u_i)} \right)^2 \right] \log(t_i) e^\nu [v_i - \delta_i], \\
\nabla_{\boldsymbol{\eta}, \theta}^2 \ell(\Psi) &= - \sum_{i=1}^n \frac{f(u_i)}{F(-u_i)} v_i \tilde{\mathbf{x}}_i \mathbf{x}_i^\top - \sum_{i=1}^n \log F(-u_i) v_i \tilde{\mathbf{x}}_i \mathbf{x}_i^\top e^{-\nu}, \\
\nabla_{\nu, \boldsymbol{\theta}}^2 \ell(\Psi) &= - \sum_{i=1}^n \delta_i \tilde{\mathbf{x}}_i e^{-\nu} - \sum_{i=1}^n \delta_i \left[ \frac{f''(u_i)}{f(u_i)} - \left( \frac{f'(u_i)}{f(u_i)} \right)^2 \right] \log(t_i) \tilde{\mathbf{x}}_i e^\nu - \sum_{i=1}^n \frac{f(u_i)}{F(-u_i)} v_i \tilde{\mathbf{x}}_i \tilde{\mathbf{x}}_i^\top \boldsymbol{\theta} e^{-\nu} \\
&\quad + \sum_{i=1}^n \left[ \frac{f'(u_i)}{F(-u_i)} + \left( \frac{f(u_i)}{F(-u_i)} \right)^2 \right] \log(t_i) [v_i - \delta_i] \tilde{\mathbf{x}}_i e^\nu - \sum_{i=1}^n \log F(-u_i) v_i \tilde{\mathbf{x}}_i e^{-\nu} [\tilde{\mathbf{x}}_i^\top \boldsymbol{\theta} e^{-\nu} + 1] \\
&\quad - \sum_{i=1}^n \frac{f(u_i)}{F(-u_i)} \log(t_i) v_i \tilde{\mathbf{x}}_i, \\
\nabla_{\nu, \boldsymbol{\eta}}^2 \ell(\Psi) &= \sum_{i=1}^n \frac{f(u_i)}{F(-u_i)} \log(t_i) v_i \mathbf{x}_i e^\nu + \sum_{i=1}^n \log F(-u_i) v_i \mathbf{x}_i \tilde{\mathbf{x}}_i^\top \boldsymbol{\theta} e^{-\nu}
\end{aligned}$$

## 1.4 Special tractable cases

- For the case  $f = \phi$  is the Normal pdf, we have that

$$\begin{aligned}\frac{f(u_i)}{F(-u_i)} &= r(u_i), \\ \frac{f'(u_i)}{f(u_i)} &= -u_i, \\ \frac{f'(u_i)}{F(-u_i)} &= -u_i r(u_i), \\ \frac{f''(u_i)}{f(u_i)} &= -1 + u_i^2,\end{aligned}$$

where  $r(x) = \text{IMR}(-x)$  is the complementary Normal Inverse Mills ratio.

- For the case where  $f(u_i) = \frac{e^{-u_i}}{(e^{-u_i}+1)^2}$  is the Logistic pdf, we have that

$$\begin{aligned}\frac{f(u_i)}{F(-u_i)} &= F(u_i), \\ \frac{f'(u_i)}{f(u_i)} &= -\tanh\left(\frac{u_i}{2}\right), \\ \frac{f'(u_i)}{F(-u_i)} &= -f(u_i)(e^{u_i} - 1), \\ \frac{f''(u_i)}{f(u_i)} &= 1 - \frac{3}{\cosh(u_i) + 1}.\end{aligned}$$

- For the case where  $f(u_i) = \frac{1}{2} \operatorname{sech}\left(\frac{\pi}{2}u_i\right)$  is the hyperbolic secant pdf, we have that

$$\begin{aligned}F(u_i) &= \frac{2 \arctan\left(e^{\frac{\pi u_i}{2}}\right)}{\pi}, \\ \frac{f(u_i)}{F(-u_i)} &= \frac{\pi \operatorname{sech}\left(\frac{\pi u_i}{2}\right)}{4 \arctan\left(e^{-\frac{\pi u_i}{2}}\right)}, \\ \frac{f'(u_i)}{f(u_i)} &= -\frac{1}{2}\pi \tanh\left(\frac{\pi u_i}{2}\right), \\ \frac{f'(u_i)}{F(-u_i)} &= -\frac{\pi^2 \tanh\left(\frac{\pi u_i}{2}\right) \operatorname{sech}\left(\frac{\pi u_i}{2}\right)}{8 \arctan\left(e^{-\frac{\pi u_i}{2}}\right)}, \\ \frac{f''(u_i)}{f(u_i)} &= \frac{1}{8}\pi^2(\cosh(\pi u_i) - 3)\operatorname{sech}^2\left(\frac{\pi u_i}{2}\right).\end{aligned}$$

- For the case where  $f(u_i) = \left(\frac{1}{u_i^2+2}\right)^{3/2}$  is the Student- $t$  with 2 degrees of freedom pdf, we

have that

$$\begin{aligned}
F(u_i) &= \frac{u_i}{2\sqrt{2}\sqrt{\frac{u_i^2}{2} + 1}} + \frac{1}{2}, \\
\frac{f(u_i)}{F(-u_i)} &= \frac{\sqrt{\frac{1}{u_i^2+2}} \left( \sqrt{u_i^2+2} + u_i \right)}{\sqrt{u_i^2+2}}, \\
\frac{f'(u_i)}{f(u_i)} &= -\frac{3u_i}{u_i^2+2}, \\
\frac{f'(u_i)}{F(-u_i)} &= -3u_i \left( \frac{1}{u_i^2+2} \right)^{3/2} \left( \frac{u_i}{\sqrt{u_i^2+2}} + 1 \right), \\
\frac{f''(u_i)}{f(u_i)} &= \frac{6(2u_i^2-1)}{(u_i^2+2)^2}.
\end{aligned}$$

## 2 Log-Prior, Gradient and Hessian functions

### 2.1 Local Prior

The prior on  $(\boldsymbol{\theta}_\gamma, \boldsymbol{\eta}_\gamma, \nu)$  has the form of

$$\pi_L(\boldsymbol{\theta}_\gamma, \boldsymbol{\eta}_\gamma, \nu) = \left[ N\left(\boldsymbol{\theta}_j; 0, g_{C_t} n \left( \tilde{\mathbf{X}}_\gamma^\top \tilde{\mathbf{X}}_\gamma \right)^{-1} \right) N\left(\boldsymbol{\eta}_j; 0, g_{C_h} n \left( \mathbf{X}_\gamma^\top \mathbf{X}_\gamma \right)^{-1} \right) \right] \pi(\nu),$$

where

$$\pi(\nu) = \frac{\beta^\alpha e^{-\beta e^\nu}}{\Gamma(\alpha)} e^{\alpha \nu}.$$

The logarithm of this prior is

$$\begin{aligned}
\ell_L(\boldsymbol{\theta}_\gamma, \boldsymbol{\eta}_\gamma, \nu) &= -\frac{1}{2n} \left[ \boldsymbol{\theta}_\gamma^\top \left( \tilde{\mathbf{X}}_\gamma^\top \tilde{\mathbf{X}}_\gamma \right) \boldsymbol{\theta}_\gamma / g_{C_t} + \boldsymbol{\eta}_\gamma^\top \left( \mathbf{X}_\gamma^\top \mathbf{X}_\gamma \right) \boldsymbol{\eta}_\gamma / g_{C_h} \right] - \beta e^\nu + \alpha \nu \\
&\quad - \frac{p_\theta + p_\eta}{2} \log(2\pi) - \frac{1}{2} \left( \log \left| g_{C_t} n \left( \tilde{\mathbf{X}}_\gamma^\top \tilde{\mathbf{X}}_\gamma \right)^{-1} \right| + \log \left| g_{C_h} n \left( \mathbf{X}_\gamma^\top \mathbf{X}_\gamma \right)^{-1} \right| \right) \\
&\quad - \log \Gamma(\alpha) + \alpha \log \beta,
\end{aligned}$$

where  $|\cdot|$  denotes the determinant. The gradient function of log g-prior is:

$$g(\boldsymbol{\theta}_\gamma, \boldsymbol{\eta}_\gamma, \nu) = \begin{pmatrix} -\frac{1}{g_{C_t} n} \left( \tilde{\mathbf{X}}_\gamma^\top \tilde{\mathbf{X}}_\gamma \right) \boldsymbol{\theta}_\gamma \\ -\frac{1}{g_{C_h} n} \left( \mathbf{X}_\gamma^\top \mathbf{X}_\gamma \right) \boldsymbol{\eta}_\gamma \\ \alpha - \beta e^\nu \end{pmatrix},$$

and the Hessian matrix is :

$$H(\boldsymbol{\theta}_\gamma, \boldsymbol{\eta}_\gamma, \nu) = \begin{pmatrix} -\frac{1}{g_{C_t} n} (\tilde{\mathbf{X}}_\gamma^\top \tilde{\mathbf{X}}_\gamma) & \mathbf{0} & \mathbf{0} \\ \mathbf{0} & -\frac{1}{g_{C_h} n} (\mathbf{X}_\gamma^\top \mathbf{X}_\gamma) & \mathbf{0} \\ \mathbf{0} & \mathbf{0} & -\beta e^\nu \end{pmatrix}.$$

### 3 Derivation of Proposition 1: Expected Fisher information

#### Matrix for GH model

Let  $\boldsymbol{\kappa} = (\boldsymbol{\theta}_\gamma, \boldsymbol{\eta}_\gamma)^\top$ . Following the decomposition of the expected Fisher information in [Santis et al. \(2001\)](#), we could write it as

$$\begin{aligned} I(\boldsymbol{\kappa}) &= -\mathbb{E} [\nabla_{\boldsymbol{\kappa}}^2 \ell(\boldsymbol{\kappa})] \\ &= \sum_{k=1}^n \mathbb{E} \left[ -\nabla_{\boldsymbol{\kappa}}^2 \ell^{cen}(\boldsymbol{\kappa}) \mid \boldsymbol{\kappa} \right]_k \cdot P(o_k > c_k) + \sum_{k=1}^n \mathbb{E} \left[ -\nabla_{\boldsymbol{\kappa}}^2 \ell^{unc}(\boldsymbol{\kappa}) \mid \boldsymbol{\kappa} \right]_k \cdot P(o_k \leq c_k), \end{aligned}$$

where  $v_k = \exp(-\nu \tilde{\mathbf{x}}_k^\top \boldsymbol{\theta} - \mathbf{x}_k^\top \boldsymbol{\eta})$ ,  $P(o_k \leq c_k) = 1 - S(c_k) = 1 - \exp[-H_0(c_k)v_k]$ , and  $P(o_k > c_k) = S(c_k) = \exp[-H_0(c_k)v_k]$ . From Section 1.3 we know the Hessians are in the form of

$$\begin{aligned} \nabla_{\boldsymbol{\theta}}^2 \ell(\boldsymbol{\Psi}) &= \sum_{i=1}^n \delta_i \left[ \frac{f''(u_i)}{f(u_i)} - \left( \frac{f'(u_i)}{f(u_i)} \right)^2 \right] \tilde{\mathbf{x}}_i \tilde{\mathbf{x}}_i^\top - \sum_{i=1}^n \left[ \frac{f'(u_i)}{F(-u_i)} + \left( \frac{f(u_i)}{F(-u_i)} \right)^2 \right] \tilde{\mathbf{x}}_i \tilde{\mathbf{x}}_i^\top [v_i - \delta_i] \\ &\quad + 2 \sum_{i=1}^n \frac{f(u_i)}{F(-u_i)} v_i \tilde{\mathbf{x}}_i \tilde{\mathbf{x}}_i^\top e^{-\nu} + \sum_{i=1}^n \log F(-u_i) v_i \tilde{\mathbf{x}}_i \tilde{\mathbf{x}}_i^\top e^{-2\nu}, \\ \nabla_{\boldsymbol{\eta}}^2 \ell(\boldsymbol{\Psi}) &= \sum_{i=1}^n \log F(-u_i) v_i \mathbf{x}_i \mathbf{x}_i^\top. \end{aligned}$$

with  $u_i = e^\nu \log(t_i) - \tilde{\mathbf{x}}_i^\top \boldsymbol{\theta} - \theta_0$  and  $v_i = \exp(e^{-\nu} \tilde{\mathbf{x}}_i^\top \boldsymbol{\theta} - \mathbf{x}_i^\top \boldsymbol{\eta})$ . If we rearrange the above expressions, we have the following expression

$$\nabla_{\boldsymbol{\theta}}^2 \ell(\boldsymbol{\Psi}) = -\tilde{\mathbf{X}}^\top \mathbf{W}_{\boldsymbol{\theta}} \tilde{\mathbf{X}},$$

$$\nabla_{\boldsymbol{\eta}}^2 \ell(\boldsymbol{\Psi}) = -\mathbf{X}^\top \mathbf{W}_{\boldsymbol{\eta}} \mathbf{X},$$

where  $\mathbf{W}_\theta$  and  $\mathbf{W}_\eta$  are diagonal matrices with the following elements on the diagonals:

$$w_{\theta,i} = -\delta_i \left[ \frac{f''(u_i)}{f(u_i)} - \left( \frac{f'(u_i)}{f(u_i)} \right)^2 + \frac{f'(u_i)}{F(-u_i)} + \left( \frac{f(u_i)}{F(-u_i)} \right)^2 \right],$$

$$- v_i \left[ -\frac{f'(u_i)}{F(-u_i)} - \left( \frac{f(u_i)}{F(-u_i)} \right)^2 + 2 \frac{f(u_i)}{F(-u_i)} e^{-\nu} + \log F(-u_i) e^{-2\nu} \right]$$

$$w_{\eta,i} = -v_i \log F(-u_i).$$

If we write the above equations in terms of hazard functions, and consider the censored and uncensored part separately, these diagonal elements become

$$w_{\theta,i}^{cen} = -v_i \left[ h'_0(c_i) - 2\sigma h_0(c_i) + \sigma^2 H_0(c_i) \right],$$

$$w_{\eta,i}^{cen} = v_i H_0(c_i),$$

for the censored part, and

$$w_{\theta,i}^{unc} = \frac{f''(u_i)}{f(u_i)} - \left( \frac{f'(u_i)}{f(u_i)} \right)^2 + h'_0(o_i) - v_i \left[ h'_0(o_i) - 2\sigma h_0(o_i) + \sigma^2 H_0(o_i) \right],$$

$$= v_i \sigma [2h_0(o_i) - \sigma H_0(o_i)] + h'_0(o_i) [1 - v_i] - 1,$$

$$w_{\eta,i}^{unc} = v_i H_0(o_i),$$

for the uncensored part. Note that the simplification in the second line of  $w_{\theta,i}^{unc}$  requires  $f$  to be standard Gaussian.

Having the expressions for the negative Hessians, we could integrate  $o_i$  and  $c_i$  out. The integral of cumulative hazard have closed form solution, i.e.  $\int v_i H_0(o_i) dF_t(o_i) = 1$ , where  $F_t$  is the lifetime distribution derivable from the baseline  $F_0$ . A similar derivation could be found in the supplementary material of [Castellanos et al. \(2021\)](#) and will not be expanded here. However, the integrals of the baseline hazard and derivative of baseline hazard have no closed-form solution even under the assumption of  $f$  being Gaussian. For example, the term  $\int h_0(o_i) dF_t(o_i)$  could be written in the following form:

$$\int h_0(o_i) dF_t(o_i) = (v_i e^\nu)^2 \int_0^\infty o_i^{-2} \frac{\phi(e^\nu \log(o_i) - \theta_0) \cdot \phi(e^\nu \log(o_i) - \mathbf{x}_i^\top \boldsymbol{\theta} - \theta_0)}{1 - \Phi(e^\nu \log(o_i) - \theta_0)} do_i,$$

where  $\phi$  is the normal PDF and  $\Phi$  is the normal CDF. This integral obviously does not have closed form solution, and the same issue exists for  $\int h'_0(o_i) dF_t(o_i)$ .

Table S1: Expressions of diagonal elements of  $\mathbf{M}^{\delta_k}$  in Proposition 1 assuming  $f$  is standard normal, where  $i = 1, 2, \dots, n$  denotes the  $n$ -th diagonal element,  $r_i = \exp(e^{-\nu} \tilde{\mathbf{x}}_{\gamma,i}^\top \boldsymbol{\theta}_\gamma)$ , and  $v_i = \exp(e^{-\nu} \tilde{\mathbf{x}}_{\gamma,i}^\top \boldsymbol{\theta}_\gamma - \mathbf{x}_{\gamma,i}^\top \boldsymbol{\eta}_\gamma)$ . In addition,  $\mathbf{M}_{\boldsymbol{\theta}_\gamma \boldsymbol{\eta}_\gamma}^{\delta_k=1} = \mathbf{M}_{\boldsymbol{\eta}_\gamma \boldsymbol{\theta}_\gamma}^{\delta_k=1} = -\sigma + \int v_i h_0(o_k) dF_t(o_k)$  and  $\mathbf{M}_{\boldsymbol{\theta}_\gamma \boldsymbol{\eta}_\gamma}^{\delta_k=0} = \mathbf{M}_{\boldsymbol{\eta}_\gamma \boldsymbol{\theta}_\gamma}^{\delta_k=0} = -\sigma + \int v_i h_0(c_k) dF_t(c_k)$ .

$(\mathbf{M}^{\delta_k})_{i,i}$		<b>Uncensored</b>		<b>Censored</b>	
<b>Model</b>		$\mathbf{M}_{\boldsymbol{\theta}_\gamma}^{\delta_k=1}$	$\mathbf{M}_{\boldsymbol{\eta}_\gamma}^{\delta_k=1}$	$\mathbf{M}_{\boldsymbol{\theta}_\gamma}^{\delta_k=0}$	$\mathbf{M}_{\boldsymbol{\eta}_\gamma}^{\delta_k=0}$
PH	—	1	—	—	1
AH	$\sigma^2 + 1 + \int 2\sigma r_i h_0(o_k) dF_t(o_k)$ $+ \int (r_i - 1) h'_0(o_k) dF_t(o_k)$	—	$\sigma^2 + \int 2\sigma r_i h_0(c_k) dF_t(c_k)$ $+ \int r_i h'_0(c_k) dF_t(c_k)$	—	—
AFT	1	—	$\int h'_0(c_k) dF_t(c_k)$	—	—
GH	$\sigma^2 + 1 + \int 2\sigma v_i h_0(o_k) dF_t(o_k)$ $+ \int (v_i - 1) h'_0(o_k) dF_t(o_k)$	1	$\sigma^2 + \int 2\sigma v_i h_0(c_k) dF_t(c_k)$ $+ \int v_i h'_0(c_k) dF_t(c_k)$	—	1

## 4 Full expression for prior on model space

Multiplying the Beta-Binomial prior with equation (9) and (10) in the main text, we derive the following full expression of  $\pi(\gamma)$ :

$$\pi(\gamma) \propto B(a_\Lambda + |\Lambda|, b_\Lambda + p_0) \cdot \begin{cases} h_{AH}, & \text{Hz}(\gamma) = \text{AH} \\ h_{PH}, & \text{Hz}(\gamma) = \text{PH} \\ h_{AFT}, & \text{Hz}(\gamma) = \text{AFT} \\ \frac{h_{GH}}{3^{|\Lambda|-2}} \cdot \left( \frac{\left[ P_{Bin}((\omega - |\Lambda|) || \Lambda, q) \cdot (1 - 2^{(1-|\Lambda|) \cdot \mathbf{1}_{\omega=|\Lambda|} + \mathbf{1}_{\omega \neq |\Lambda|}} \right]^{-1}}{\sum_{i=0}^{|\Lambda|} \left[ P_{Bin}(i || \Lambda, q) \cdot (1 - 2^{(1-|\Lambda|) \cdot \mathbf{1}_{i=0} + \mathbf{1}_{i \neq 0}}) \right]^{-1}} \right)^{\mathbf{1}_{|\Lambda| > 1}}, & \text{Hz}(\gamma) = \text{GH.} \end{cases} \quad (1)$$

## 5 Derivation of marginal likelihood under LCM prior under integrated Laplace approximation

The marginal likelihood is given by

$$p(\mathbf{t} | \gamma) = \int \exp[\ell(\Psi_\gamma)] \pi(\Psi_\gamma) d\Psi_\gamma, \quad (2)$$

where  $\pi(\Psi_\gamma) = \pi(\boldsymbol{\theta}_\gamma, \boldsymbol{\eta}_\gamma) \pi(\nu) \pi(\theta_0)$  is the prior of the parameters. The following Gaussian priors are assigned to the parameters:

$$\begin{bmatrix} \boldsymbol{\theta}_\gamma \\ \boldsymbol{\eta}_\gamma \end{bmatrix} \mid g_E \sim N(0, n g_E \mathcal{J}_{\boldsymbol{\theta}, \boldsymbol{\eta}}(\widehat{\Psi}_\gamma)^{-1}), \quad \theta_0 \sim N(0, K), \quad \nu \sim N(\mu_\nu, \sigma_\nu^2), \quad (3)$$

where  $\mathcal{J}_{\boldsymbol{\theta}, \boldsymbol{\eta}}(\widehat{\Psi}_\gamma) = -\nabla_{\boldsymbol{\theta}, \boldsymbol{\eta}}^2(\widehat{\Psi}_\gamma)$  is the  $(\boldsymbol{\theta}_\gamma, \boldsymbol{\eta}_\gamma)^\top$  block of observed Fisher information evaluated at  $\widehat{\Psi}_\gamma$ , the MLE of  $\Psi_\gamma$ .  $K$  is a large constant,  $n$  is the sample size, and  $\mu_\nu$ ,  $g_E$ , and  $\sigma_\nu^2$  are hyperparameters.

Following the idea of integrated Laplace approximation in [Wang & George \(2007\)](#), we start by

expanding the integrated log-likelihood  $\ell(\Psi_\gamma)$  at  $\widehat{\Psi}_\gamma$ , the MLE of  $\Psi_\gamma$ :

$$\ell(\Psi_\gamma) \approx \ell(\widehat{\Psi}_\gamma) - \frac{1}{2} (\Psi_\gamma - \widehat{\Psi}_\gamma)^\top \mathcal{J}(\widehat{\Psi}_\gamma) (\Psi_\gamma - \widehat{\Psi}_\gamma), \quad (4)$$

where  $\mathcal{J}(\widehat{\Psi}_\gamma) = -\nabla^2 \ell(\widehat{\Psi}_\gamma)$  is the observed Fisher information evaluated at  $\widehat{\Psi}_\gamma$ . Plugging this approximation back to the integral in (2) and substituting in the prior, we have

$$\begin{aligned} p(\mathbf{t} \mid \boldsymbol{\gamma}) &\approx \exp[\ell(\widehat{\Psi}_\gamma)] \int \exp \left\{ -\frac{1}{2} (\Psi_\gamma - \widehat{\Psi}_\gamma)^\top \mathcal{J}(\widehat{\Psi}_\gamma) (\Psi_\gamma - \widehat{\Psi}_\gamma) \right\} \pi(\Psi_\gamma) d\Psi_\gamma \\ &\propto \exp[\ell(\widehat{\Psi}_\gamma)] (2\pi)^{-\frac{d_\gamma+2}{2}} \left| g_E \mathcal{J}_{\theta,\eta}(\widehat{\Psi}_\gamma)^{-1} \right|^{-\frac{1}{2}} \\ &\quad \times \int \exp \left\{ -\frac{1}{2} (\Psi_\gamma - \widehat{\Psi}_\gamma)^\top \mathcal{J}(\widehat{\Psi}_\gamma) (\Psi_\gamma - \widehat{\Psi}_\gamma) - \frac{1}{2ng_E} \begin{bmatrix} \boldsymbol{\theta}_\gamma \\ \boldsymbol{\eta}_\gamma \end{bmatrix}^\top \mathcal{J}_{\theta,\eta}(\widehat{\Psi}_\gamma) \begin{bmatrix} \boldsymbol{\theta}_\gamma \\ \boldsymbol{\eta}_\gamma \end{bmatrix} \right. \\ &\quad \left. - \frac{1}{2\sigma_\nu^2} (\nu - \mu_\nu)^2 - \frac{1}{2K} \theta_0^2 \right\} d\Psi_\gamma. \end{aligned}$$

For cleaner presentation, we omit the  $(\widehat{\Psi}_\gamma)$  in  $\mathcal{J}_{..}$ , as the Fisher information will all be evaluated at  $\widehat{\Psi}_\gamma$ . For the rest of this section only, denote  $\boldsymbol{\kappa}_\gamma = [\boldsymbol{\theta}_\gamma, \boldsymbol{\eta}_\gamma]^\top$ , then the exponent in the integral could be written as

$$\begin{aligned} & -\frac{1}{2} (\Psi_\gamma - \widehat{\Psi}_\gamma)^\top \mathcal{J}(\widehat{\Psi}_\gamma) (\Psi_\gamma - \widehat{\Psi}_\gamma) - \frac{1}{2ng_E} \begin{bmatrix} \boldsymbol{\theta}_\gamma \\ \boldsymbol{\eta}_\gamma \end{bmatrix}^\top \mathcal{J}_{\boldsymbol{\kappa}}(\widehat{\Psi}_\gamma) \begin{bmatrix} \boldsymbol{\theta}_\gamma \\ \boldsymbol{\eta}_\gamma \end{bmatrix} - \frac{1}{2\sigma_\nu^2} (\nu - \mu_\nu)^2 - \frac{1}{2K} \theta_0^2 \\ &= -\frac{1}{2} [(\boldsymbol{\beta}_\gamma - \widehat{\boldsymbol{\kappa}}_\gamma)^\top \mathcal{J}_{\theta,\eta}(\boldsymbol{\beta}_\gamma - \widehat{\boldsymbol{\kappa}}_\gamma) + 2(\boldsymbol{\kappa}_\gamma - \widehat{\boldsymbol{\kappa}}_\gamma)^\top \mathcal{J}_{\theta,\eta,\nu}(\nu - \widehat{\nu}) \\ &\quad + 2(\boldsymbol{\kappa}_\gamma - \widehat{\boldsymbol{\kappa}}_\gamma)^\top \mathcal{J}_{\theta,\eta,\theta_0}(\theta_0 - \widehat{\theta}_0) + (\nu - \widehat{\nu})^2 \mathcal{J}_{\nu\nu} + 2(\nu - \widehat{\nu})(\theta_0 - \widehat{\theta}_0) \mathcal{J}_{\nu,\theta_0} + (\theta_0 - \widehat{\theta}_0)^2 \mathcal{J}_{\theta_0\theta_0}] \\ &\quad - \frac{1}{2ng_E} \boldsymbol{\beta}_\gamma^\top \mathcal{J}_{\theta,\eta} \boldsymbol{\beta}_\gamma - \frac{1}{2\sigma_\nu^2} (\nu - \mu_\nu)^2 - \frac{1}{2K} \theta_0^2. \end{aligned}$$

We will now discuss the non-null model case and null model case separately.

## 5.1 Non-null model case

**5.1.0.1  $\boldsymbol{\kappa}_\gamma = [\boldsymbol{\theta}_\gamma, \boldsymbol{\eta}_\gamma]^\top$  part.** The parts involving  $\boldsymbol{\kappa}$  in the above equation could be written as

$$\begin{aligned}
& -\frac{1}{2} \boldsymbol{\kappa}_\gamma^\top \left[ \mathcal{J}_{\boldsymbol{\theta}, \eta} + \frac{1}{ng_E} \mathcal{J}_{\boldsymbol{\theta}, \eta} \right] \boldsymbol{\kappa}_\gamma + \boldsymbol{\kappa}_\gamma^\top \left[ \mathcal{J}_{\boldsymbol{\theta}, \eta} \hat{\boldsymbol{\kappa}}_\gamma - \mathcal{J}_{\boldsymbol{\theta}, \eta, \nu} (\nu - \hat{\nu}) - \mathcal{J}_{\boldsymbol{\theta}, \eta, \theta_0} (\theta_0 - \hat{\theta}_0) \right] \\
& = -\frac{1}{2} \boldsymbol{\kappa}_\gamma^\top \mathcal{J}_{\boldsymbol{\theta}, \eta} \left( 1 + \frac{1}{ng_E} \right) \boldsymbol{\kappa}_\gamma + \boldsymbol{\kappa}_\gamma^\top \mathcal{J}_{\boldsymbol{\theta}, \eta} \hat{\boldsymbol{\kappa}}_\gamma - \boldsymbol{\kappa}_\gamma^\top \mathcal{J}_{\boldsymbol{\theta}, \eta, \nu} (\nu - \hat{\nu}) - \boldsymbol{\kappa}_\gamma^\top \mathcal{J}_{\boldsymbol{\theta}, \eta, \theta_0} (\theta_0 - \hat{\theta}_0) \\
& = -\frac{1+ng_E}{2ng_E} \boldsymbol{\kappa}_\gamma^\top \mathcal{J}_{\boldsymbol{\theta}, \eta} \boldsymbol{\kappa}_\gamma + \boldsymbol{\kappa}_\gamma^\top \mathbf{b} \\
& = -\frac{1+ng_E}{2ng_E} \left( \boldsymbol{\kappa}_\gamma - \frac{ng_E}{1+ng_E} \mathcal{J}_{\boldsymbol{\theta}, \eta}^{-1} \mathbf{b} \right)^\top \mathcal{J}_{\boldsymbol{\theta}, \eta} \left( \boldsymbol{\kappa}_\gamma - \frac{ng_E}{1+ng_E} \mathcal{J}_{\boldsymbol{\theta}, \eta}^{-1} \mathbf{b} \right) + \frac{ng_E}{2(1+ng_E)} \mathbf{b}^\top \mathcal{J}_{\boldsymbol{\theta}, \eta}^{-1} \mathbf{b},
\end{aligned}$$

where  $\mathbf{b} = \mathcal{J}_{\boldsymbol{\theta}, \eta} \hat{\boldsymbol{\kappa}}_\gamma - \mathcal{J}_{\boldsymbol{\theta}, \eta, \nu} (\nu - \hat{\nu}) - \mathcal{J}_{\boldsymbol{\theta}, \eta, \theta_0} (\theta_0 - \hat{\theta}_0)$ . After the completion of square, the integral with respect to  $\boldsymbol{\kappa}_\gamma$  becomes

$$\int \exp \left\{ -\frac{1+ng_E}{2ng_E} \left( \boldsymbol{\kappa}_\gamma - \frac{ng_E}{1+ng_E} \mathcal{J}_{\boldsymbol{\theta}, \eta}^{-1} \mathbf{b} \right)^\top \mathcal{J}_{\boldsymbol{\theta}, \eta} \left( \boldsymbol{\kappa}_\gamma - \frac{ng_E}{1+ng_E} \mathcal{J}_{\boldsymbol{\theta}, \eta}^{-1} \mathbf{b} \right) \right\} d\boldsymbol{\kappa}_\gamma = \left( \frac{2\pi ng_E}{1+ng_E} \right)^{\frac{p+g}{2}} |\mathcal{J}_{\boldsymbol{\theta}, \eta}|^{-\frac{1}{2}}. \quad (5)$$

**5.1.0.2  $\nu, \theta_0$  part** The remaining part is given by

$$\begin{aligned}
& -\frac{1}{2\sigma_\nu^2} (\nu - \mu_\nu)^2 - \frac{1}{2K} \theta_0^2 + \frac{ng_E}{2(1+ng_E)} \mathbf{b}^\top \mathcal{J}_{\boldsymbol{\theta}, \eta}^{-1} \mathbf{b} \\
& = -\frac{1}{2\sigma_\nu^2} (\nu - \mu_\nu)^2 - \frac{1}{2K} \theta_0^2 - \frac{1}{2} (\nu - \hat{\nu})^2 \mathcal{J}_{\nu\nu} - (\nu - \hat{\nu}) (\theta_0 - \hat{\theta}_0) \mathcal{J}_{\nu, \theta_0} - \frac{1}{2} (\theta_0 - \hat{\theta}_0)^2 \mathcal{J}_{\theta_0 \theta_0} \\
& + \frac{ng_E}{2(1+ng_E)} \left[ (\nu - \hat{\nu})^2 \mathcal{J}_{\boldsymbol{\theta}, \eta, \nu}^\top \mathcal{J}_{\boldsymbol{\theta}, \eta}^{-1} \mathcal{J}_{\boldsymbol{\theta}, \eta, \nu} + 2(\nu - \hat{\nu}) (\theta_0 - \hat{\theta}_0) \mathcal{J}_{\boldsymbol{\theta}, \eta, \nu}^\top \mathcal{J}_{\boldsymbol{\theta}, \eta}^{-1} \mathcal{J}_{\boldsymbol{\theta}, \eta, \theta_0} + (\theta_0 - \hat{\theta}_0)^2 \mathcal{J}_{\boldsymbol{\theta}, \eta, \theta_0}^\top \mathcal{J}_{\boldsymbol{\theta}, \eta}^{-1} \mathcal{J}_{\boldsymbol{\theta}, \eta, \theta_0} \right]
\end{aligned}$$

Define the partial information matrix for  $(\nu, \theta_0)$  as

$$\tilde{\mathcal{J}} = \begin{bmatrix} \tilde{\mathcal{J}}_{\nu\nu} & \tilde{\mathcal{J}}_{\nu, \theta_0} \\ \tilde{\mathcal{J}}_{\theta_0, \nu} & \tilde{\mathcal{J}}_{\theta_0 \theta_0} \end{bmatrix},$$

where each entry is an adjusted Schur complement given by

$$\begin{aligned}
\tilde{\mathcal{J}}_{\nu\nu} &= \mathcal{J}_{\nu\nu} - \frac{ng_E}{1+ng_E} \mathcal{J}_{\boldsymbol{\theta}, \eta, \nu}^\top \mathcal{J}_{\boldsymbol{\theta}, \eta}^{-1} \mathcal{J}_{\boldsymbol{\theta}, \eta, \nu} \\
\tilde{\mathcal{J}}_{\nu, \theta_0} &= \mathcal{J}_{\nu, \theta_0} - \frac{ng_E}{1+ng_E} \mathcal{J}_{\boldsymbol{\theta}, \eta, \nu}^\top \mathcal{J}_{\boldsymbol{\theta}, \eta}^{-1} \mathcal{J}_{\boldsymbol{\theta}, \eta, \theta_0} \\
\tilde{\mathcal{J}}_{\theta_0, \nu} &= \mathcal{J}_{\theta_0, \nu} - \frac{ng_E}{1+ng_E} \mathcal{J}_{\boldsymbol{\theta}, \eta, \theta_0}^\top \mathcal{J}_{\boldsymbol{\theta}, \eta}^{-1} \mathcal{J}_{\boldsymbol{\theta}, \eta, \nu}.
\end{aligned}$$

Then we could rewrite the remaining part as

$$-\frac{1}{2} \begin{bmatrix} \nu - \hat{\nu} \\ \theta_0 - \hat{\theta}_0 \end{bmatrix}^\top \tilde{\mathcal{J}} \begin{bmatrix} \nu - \hat{\nu} \\ \theta_0 - \hat{\theta}_0 \end{bmatrix} - \frac{1}{2\sigma_\nu^2} (\nu - \mu_\nu)^2 - \frac{1}{2K} \theta_0^2 = -\frac{1}{2} \mathbf{z}^\top \mathbf{P}_\gamma \mathbf{z} + \mathbf{h}_\gamma^\top \mathbf{z} + C_\gamma,$$

where

$$\mathbf{z} = (\nu, \theta_0)^\top, \quad \mathbf{P}_\gamma = \begin{bmatrix} \tilde{\mathcal{J}}_{\nu\nu} + \frac{1}{\sigma_\nu^2} & \tilde{\mathcal{J}}_{\nu,\theta_0} \\ \tilde{\mathcal{J}}_{\nu,\theta_0} & \tilde{\mathcal{J}}_{\theta_0\theta_0} + \frac{1}{K} \end{bmatrix}, \quad \mathbf{h}_\gamma = \begin{bmatrix} \tilde{\mathcal{J}}_{\nu\nu}\hat{\nu} + \tilde{\mathcal{J}}_{\nu,\theta_0}\hat{\theta}_0 + \frac{\mu_\nu}{\sigma_\nu^2} \\ \tilde{\mathcal{J}}_{\nu,\theta_0}\hat{\nu} + \tilde{\mathcal{J}}_{\theta_0\theta_0}\hat{\theta}_0 \end{bmatrix},$$

and

$$\begin{aligned} C_\gamma = & -\frac{\mu_\nu^2}{2\sigma_\nu^2} - \frac{1}{2}\hat{\nu}^2\mathcal{J}_{\nu\nu} - \hat{\nu}\hat{\theta}_0\mathcal{J}_{\nu,\theta_0} - \frac{1}{2}\hat{\theta}_0^2\mathcal{J}_{\theta_0\theta_0} + \frac{ng_E}{2(1+ng_E)}\hat{\nu}^2\mathcal{J}_{\theta,\eta,\nu}^\top\mathcal{J}_{\theta,\eta,\nu}^{-1}\mathcal{J}_{\theta,\eta,\nu} \\ & + \frac{ng_E}{(1+ng_E)}\hat{\nu}\hat{\theta}_0\mathcal{J}_{\theta,\eta,\nu}^\top\mathcal{J}_{\theta,\eta,\theta_0}^{-1}\mathcal{J}_{\theta,\eta,\theta_0} + \frac{ng_E}{2(1+ng_E)}\hat{\theta}_0^2\mathcal{J}_{\theta,\eta,\theta_0}^\top\mathcal{J}_{\theta,\eta,\theta_0}^{-1}\mathcal{J}_{\theta,\eta,\theta_0}. \end{aligned}$$

Therefore, after completing the square, the integral with respect to  $\nu$  and  $\theta_0$  becomes

$$\int \exp \left\{ -\frac{1}{2} \mathbf{z}^\top \mathbf{P}_\gamma \mathbf{z} + \mathbf{h}_\gamma^\top \mathbf{z} + C_\gamma \right\} d\mathbf{z} = (2\pi)^{|\mathbf{P}_\gamma|^{-\frac{1}{2}}} \exp \left\{ \frac{1}{2} \mathbf{h}_\gamma^\top \mathbf{P}_\gamma^{-1} \mathbf{h}_\gamma + C_\gamma \right\}. \quad (6)$$

Finally, combining (5) and (6) and plugging back into (4), the marginal likelihood is approximately proportional to

$$p(\mathbf{t} \mid \boldsymbol{\gamma}) \approx \hat{p}(\mathbf{t} \mid \boldsymbol{\gamma}) \propto \exp[\ell(\widehat{\boldsymbol{\Psi}}_\gamma)](1+ng_E)^{-\frac{d_\gamma}{2}} |\mathbf{P}_\gamma|^{-\frac{1}{2}} \exp \left\{ \frac{1}{2} \mathbf{h}_\gamma^\top \mathbf{P}_\gamma^{-1} \mathbf{h}_\gamma + C_\gamma \right\}. \quad (7)$$

## 5.2 Null model case

When  $\boldsymbol{\gamma} \neq \mathbf{0}$ , we only have the  $(\nu, \theta_0)$  part, and the exponent in the integral becomes

$$\begin{aligned} & -\frac{1}{2}[(\nu - \hat{\nu})^2\mathcal{J}_{\nu\nu} + 2(\nu - \hat{\nu})(\theta_0 - \hat{\theta}_0)\mathcal{J}_{\nu,\theta_0} + (\theta_0 - \hat{\theta}_0)^2\mathcal{J}_{\theta_0\theta_0}] - \frac{1}{2\sigma_\nu^2}(\nu - \mu_\nu)^2 - \frac{1}{2K}\theta_0^2 \\ & = -\frac{1}{2} \mathbf{z}^\top \mathbf{P}_0 \mathbf{z} + \mathbf{h}_0^\top \mathbf{z} + C_0, \end{aligned}$$

where

$$\mathbf{z} = (\nu, \theta_0)^\top, \quad \mathbf{P}_0 = \begin{bmatrix} \mathcal{J}_{\nu\nu} + \frac{1}{\sigma_\nu^2} & \mathcal{J}_{\nu,\theta_0} \\ \mathcal{J}_{\nu,\theta_0} & \mathcal{J}_{\theta_0\theta_0} + \frac{1}{K} \end{bmatrix}, \quad \mathbf{h}_0 = \begin{bmatrix} \mathcal{J}_{\nu\nu}\hat{\nu} + \mathcal{J}_{\nu,\theta_0}\hat{\theta}_0 + \frac{\mu_\nu}{\sigma_\nu^2} \\ \mathcal{J}_{\nu,\theta_0}\hat{\nu} + \mathcal{J}_{\theta_0\theta_0}\hat{\theta}_0 \end{bmatrix},$$

and

$$C_0 = -\frac{\mu_\nu^2}{2\sigma_\nu^2} - \frac{1}{2}(\hat{\nu}_0)^2 \mathcal{J}_{\nu\nu} - \hat{\nu}\hat{\theta}_0 \mathcal{J}_{\nu,\theta_0} - \frac{1}{2}(\hat{\theta}_0)^2 \mathcal{J}_{\theta_0\theta_0}.$$

After completing the square, we have the following approximation for the marginal likelihood:

$$\hat{p}(\mathbf{t} \mid \boldsymbol{\gamma} = \mathbf{0}) \propto \exp[\ell(\hat{\Psi}_0)] |\mathbf{P}_0|^{-\frac{1}{2}} \exp\left\{\frac{1}{2}\mathbf{h}_0^\top \mathbf{P}_0^{-1} \mathbf{h}_0 + C_0\right\}.$$

## 6 Proof of Theoretical Results

Let us define the following limit function. By the weak law of large numbers, we have that

$$M_n(\boldsymbol{\Psi}_\gamma) = \frac{\ell_n(\boldsymbol{\Psi}_\gamma)}{n} \xrightarrow{\text{Pr}} M(\boldsymbol{\Psi}_\gamma),$$

where

$$M(\boldsymbol{\Psi}_\gamma) = P(\delta_1 = 1) E_{\varphi_0} [\log(h(o_1 \mid \boldsymbol{\Psi}_\gamma)) \mid \delta_1 = 1] - E_{\varphi_0} [H(t_1 \mid \boldsymbol{\Psi}_\gamma)],$$

and  $\varphi_0$  is the true generating model. Define also  $\mathbf{v} = (t_1, o_1, c_1, \delta_1)^\top$ , and the function

$$m(\boldsymbol{\Psi}_\gamma, \mathbf{v}) = \delta_1 \log(h(o_1 \mid \boldsymbol{\Psi}_\gamma)) - H(t_1 \mid \boldsymbol{\Psi}_\gamma),$$

which is assumed to be finite for each  $\boldsymbol{\Psi}_\gamma \in \Gamma_\gamma$ .

Let us also denote by  $\mathbf{X}_\gamma$  and  $\tilde{\mathbf{X}}_\gamma$ , the design matrices associated with model  $\gamma$ , and  $\mathbf{X}_{\gamma,O}$  and  $\tilde{\mathbf{X}}_{\gamma,O}$ , the design matrices associated with model  $\gamma$  and the uncensored observations. Consider the following technical conditions.

- C1. The parameter space is a compact subset  $\Gamma_\gamma \subset \mathbb{R}^{p+q+2}$ .
- C2. There exists  $\tilde{n} > 0$  such that, for  $n > \tilde{n}$ , the matrices  $\mathbf{X}_\gamma^\top \mathbf{X}_\gamma$ ,  $\tilde{\mathbf{X}}_\gamma^\top \tilde{\mathbf{X}}_\gamma$ ,  $\mathbf{X}_{\gamma,O}^\top \mathbf{X}_{\gamma,O}$  and  $\tilde{\mathbf{X}}_{\gamma,O}^\top \tilde{\mathbf{X}}_{\gamma,O}$  are positive definite.
- C3. Conditionally independent censoring.  $O_i \perp C_i \mid \mathbf{x}_i$ .
- C4. The maximum  $\boldsymbol{\Psi}_\gamma^* = \text{argmax}_{\Gamma_\gamma} M(\boldsymbol{\Psi}_\gamma)$  is a unique interior point of  $\Gamma_\gamma$ .

C5. The baseline hazard  $h(t | \mu, \sigma)$  is continuous in  $t > 0$ . Moreover,  $M(\Psi_\gamma) < \infty$  for all  $\Psi_\gamma$ , and  $|m(\Psi_\gamma; \mathbf{v})| \leq \psi_0(\mathbf{v})$  for all  $\Psi_\gamma \in \Gamma_\gamma$ , where

$$\int \psi_0(\mathbf{v}) d\varphi(\mathbf{v}) < \infty.$$

C6.  $\frac{\partial^2 m(\Psi_\gamma; \mathbf{v})}{\partial \Psi_{\gamma_i} \partial \Psi_{\gamma_j}}$  is continuous in  $\mathbf{v}$ , and there exist functions  $\psi_1(\mathbf{v})$  and  $\psi_2(\mathbf{v})$  such that

$$\begin{aligned} \left| \frac{\partial m(\Psi_\gamma; \mathbf{v})}{\partial \Psi_{\gamma_i}} \cdot \frac{\partial m(\Psi_\gamma; \mathbf{v})}{\partial \Psi_{\gamma_j}} \right| &\leq \psi_1(\mathbf{v}), \\ \left| \frac{\partial^2 m(\Psi_\gamma; \mathbf{v})}{\partial \Psi_{\gamma_i} \partial \Psi_{\gamma_j}} \right| &\leq \psi_2(\mathbf{v}), \end{aligned}$$

where

$$\begin{aligned} \int \psi_1(\mathbf{v}) d\varphi(\mathbf{v}) &< \infty, \\ \int \psi_2(\mathbf{v}) d\varphi(\mathbf{v}) &< \infty. \end{aligned}$$

C7. The matrix  $E_\varphi [\nabla m(\Psi_\gamma^*; \mathbf{v}) \nabla m(\Psi_\gamma^*; \mathbf{v})^\top]$  is non-singular and the Hessian matrix  $\nabla^2 M(\Psi_\gamma)$  has constant rank in a neighbourhood of  $\Psi_\gamma^*$ .

Condition C1 is imposed mainly for convenience, but the results extend to locally compact sets. The set  $\Gamma_\gamma$  may be taken to be any sufficiently large compact set. Condition C2 ensures the absence of collinearity in the design matrices for both the time-level and hazard-level effects for sufficiently large samples. Condition C3 restricts the censoring mechanism to be non-informative, since informative censoring would require modifications to the likelihood function. Conditions C4–C7 are standard regularity assumptions used in asymptotic theory (White 1981, 1982, van der Vaart 2000).

**Lemma 1** *Suppose that conditions C1–C5 are satisfied. Then,  $\widehat{\Psi}_\gamma \xrightarrow{\text{Pr}} \Psi_\gamma^*$ , as  $n \rightarrow \infty$ .*

**Lemma 2** *Suppose that conditions C1–C7 are satisfied. Then,  $\sqrt{n} (\widehat{\Psi}_\gamma - \Psi_\gamma^*) \xrightarrow{D} N \left( 0, V(\Psi_\gamma^*)^{-1} \mathbb{E}_{F_0} [\nabla m(\Psi_\gamma^*) \nabla m(\Psi_\gamma^*)^\top] V(\Psi_\gamma^*)^{-1} \right)$ , where  $V(\Psi_\gamma^*)$  is the Hessian matrix of  $M(\Psi_\gamma)$  evaluated at  $\Psi_\gamma^*$ .*

**Lemma 3** Suppose that conditions C1-C7 are satisfied. Let  $\mathcal{J}(\widehat{\Psi})$  denote the observed Fisher information evaluated at the MLE  $\widehat{\Psi}$ , then

$$\mathcal{J}(\widehat{\Psi}_\gamma)/n \xrightarrow{\text{Pr}} -\nabla^2 M(\Psi_\gamma^*), \quad n \rightarrow \infty.$$

For each entry of the observed Fisher information  $\mathcal{J}_{a,b}(\widehat{\Psi}_\gamma)$ ,  $a, b \in (\nu, \theta_0, \theta_1, \dots, \theta_{p_\gamma}, \eta_1, \dots, \eta_{q_\gamma})$ , we have

$$\mathcal{J}_{a,b}(\widehat{\Psi}_\gamma)/n \xrightarrow{\text{Pr}} -\nabla^2 M_{a,b}(\Psi_\gamma^*) = c, \quad n \rightarrow \infty,$$

where  $c$  is a constant.

## Proof of Lemma 1

First, note that the GH model is identifiable as we are using baseline hazards associated with distributions from the log-location scale family, and the GH model is identifiable provided that the baseline hazard is not a member of the Weibull family of distributions (Chen & Jewell 2001). Moreover, conditions C1-C5 are equivalent to Assumptions A1-A3 in White (1982). Similar to A1 in White (1982), the compactness assumption of C1 is made for theoretical convenience, but it could be relaxed with a locally compact assumption White (1981). C2 indicates that for sufficiently large sample size, the design matrices have full rank, and C3 implies the censoring mechanism is independent of the survival time given the set of observed variables (non-informative censoring). C4 and C5 corresponds to A3 of White (1982). C4 is the fundamental identification condition (White 1982), which assumes the existence and uniqueness of the maximum of the expected log-likelihood. C5 ensures that the model discrimination measure, the Kullback-Leibler Information Criterion, is well defined. Consequently, the conditions of Theorem 2.2 in White (1982) are satisfied, which implies that  $\widehat{\Psi}_\gamma \xrightarrow{\text{Pr}} \Psi_\gamma^*$ , as  $n \rightarrow \infty$ . That is, the MLE is consistent under model misspecification.

## Proof of Lemma 2

The result follows by noticing that conditions C1-C7 are equivalent to Assumptions A1-A6 in [White \(1982\)](#). C6 corresponds to A4 and A5, and it ensures that the first two derivatives of  $m(\Psi_\gamma; \mathbf{v})$  with respect to  $\Psi_\gamma$  exists and dominated by functions integrable with respect to  $\varphi$  for all  $\mathbf{v}$ . These assumptions justifies the use of mean value theorem and law of large numbers for proving the asymptotic normality of Theorem 3.2 in [White \(1982\)](#). Lastly, C7, corresponding to A6, is essential for deriving locally identifiable property of  $\Psi_\gamma$  ([White 1982](#)), and guarantees the entries of the Fisher information matrix are well-defined. Moreover, it ensures that  $\nabla^2 M(\Psi_\gamma)$  is invertible and the covariance matrix of the asymptotic normal distribution in [Lemma 2](#) is well-defined. The result then follows from Theorem 3.2 in [White \(1982\)](#), which establishes the asymptotic normality of the MLE under misspecification of the GH model.

### 6.1 Proof of Lemma 3

Appealing to [Lemma 1](#), we have  $\widehat{\Psi}_\gamma \xrightarrow{\text{Pr}} \Psi_\gamma^*$  as  $n \rightarrow \infty$ . Applying continuous mapping theorem and have  $n^{-1}H(\widehat{\Psi}_\gamma) \xrightarrow{\text{Pr}} \nabla^2 M(\Psi_\gamma^*)$  as  $n \rightarrow \infty$ , where  $\nabla^2 M(\Psi_\gamma^*)$  is a negative definite matrix according to C4. And since  $\mathcal{J}(\widehat{\Psi}_\gamma) = -H(\widehat{\Psi}_\gamma)$ , we have  $n^{-1}\mathcal{J}(\widehat{\Psi}_\gamma) \xrightarrow{\text{Pr}} -\nabla^2 M(\Psi_\gamma^*)$  as  $n \rightarrow \infty$ .

For each entry of  $\nabla^2 M(\Psi_\gamma^*)$ , we could refer to the expressions in [section 1.3](#) after taking their expectations. By C4 we have  $\Psi_\gamma^*$  is a unique interior maximum, therefore all elements in  $\Psi_\gamma^* = (\nu^*, \theta_0^*, \theta_1^*, \dots, \theta_{p_\gamma}^*, \eta_1^*, \dots, \eta_{q_\gamma}^*)$  are constants, which implies  $v_i^*$  is constant. Assuming the observed times  $t_1, \dots, t_n$  are finite, combining with the fact that  $X$  and  $\tilde{X}$  are assumed fixed, then  $u_i^*$  is also constant. Since  $f$  and  $F$  are valid PDF and valid CDF and therefore continuous,  $f(u_i^*)$  and  $F(u_i^*)$  are also constants greater than 0. Moreover, by C6, we have that  $f''$  and  $f'$  are continuous. Therefore, the ratios  $\frac{f(u_i^*)}{F(u_i^*)}$ ,  $\frac{f''(u_i^*)}{f(u_i^*)} - \left(\frac{f'(u_i^*)}{f(u_i^*)}\right)^2$ , and  $\frac{f'(u_i^*)}{F(-u_i^*)} + \left(\frac{f(u_i^*)}{F(-u_i^*)}\right)^2$  are also constants. For example, when  $f$  is the PDF of a normal or a logistic distribution, we could refer to [section 1.4](#) and have those ratios in nice forms. After characterizing all terms involved in  $\nabla^2 M(\Psi_\gamma^*)$ , we

have that for each element of  $\nabla^2 M_{a^*, b^*}(\Psi_\gamma^*)$ ,  $a^*, b^* \in (\nu^*, \theta_0^*, \theta_1^*, \dots, \theta_{p_\gamma}^*, \eta_1^*, \dots, \eta_{q_\gamma}^*)$ ,

$$\nabla^2 M_{a^*, b^*}(\Psi_\gamma^*) = \mathcal{O}_p(1).$$

Combining with the previous result of  $n^{-1} \mathcal{J}(\widehat{\Psi}_\gamma) \xrightarrow{\text{Pr}} -\nabla^2 M(\Psi_\gamma^*)$  as  $n \rightarrow \infty$  entry by entry, we conclude the proof.

## 6.2 Proof of Proposition 2

We characterise the asymptotic rates of:

$$\widehat{B}_{\gamma, \gamma^*} = \frac{\widehat{p}(\mathbf{t} \mid \gamma)}{\widehat{p}(\mathbf{t} \mid \gamma^*)},$$

where  $\widehat{p}(\mathbf{t} \mid \gamma)$  is obtained via an integrated Laplace approximation:

$$\widehat{p}(\mathbf{t} \mid \gamma) \approx \exp[\ell(\widehat{\Psi}_\gamma)] (1 + n g_E)^{-\frac{d_\gamma}{2}} |\mathbf{P}_\gamma|^{-\frac{1}{2}} \exp \left\{ \frac{1}{2} \mathbf{h}_\gamma^\top \mathbf{P}_\gamma^{-1} \mathbf{h}_\gamma + C_\gamma \right\}$$

where  $\widehat{\Psi}_\gamma = \arg \max_{\Psi_\gamma} \ell(\Psi_\gamma)$  is the maximum likelihood estimator (MLE). We consider the case of  $\gamma^* = \mathbf{0}$  and  $\gamma^* \neq \mathbf{0}$  separately. For convenience, we omit the subscript of  $\gamma$  under  $\mathbf{h}_\gamma$ ,  $\mathbf{P}_\gamma$ , and  $C_\gamma$ , and we use  $*$  to denote the subscript  $\gamma^*$ .

**6.2.0.1 Case  $\gamma^* \neq \mathbf{0}$**  Let us factorise the Bayes factor as:

$$\widehat{B}_{\gamma, \gamma^*} = (1 + n g_E)^{\frac{d_\gamma - d_{\gamma^*}}{2}} \exp\{Z_1\} Z_2 \exp\{Z_3\},$$

where

$$\begin{aligned} Z_1 &= \ell(\widehat{\Psi}_\gamma) - \ell(\widehat{\Psi}_{\gamma^*}), \\ Z_2 &= \frac{|\mathbf{P}|^{-\frac{1}{2}}}{|\mathbf{P}_*|^{-\frac{1}{2}}}, \\ Z_3 &= \frac{\frac{1}{2} \mathbf{h}_\gamma^\top \mathbf{P}_\gamma^{-1} \mathbf{h}_\gamma + C}{\frac{1}{2} \mathbf{h}_*^\top \mathbf{P}_*^{-1} \mathbf{h}_* + C_*}. \end{aligned}$$

For  $Z_1$ , we again consider the case of  $\gamma^* \subset \gamma$  and  $\gamma^* \not\subset \gamma$  separately. For  $\gamma^* \subset \gamma$ , we perform a second order Taylor expansion

$$\begin{aligned}
Z_1 &= \ell(\widehat{\Psi}_\gamma) - \ell(\widehat{\Psi}_{\gamma^*}) + \mathcal{O}_p(1) \\
&= (\widehat{\Psi}_\gamma - \widehat{\Psi}_{\gamma^*})^\top \nabla^2 \ell(\widehat{\Psi}_\gamma) (\widehat{\Psi}_\gamma - \widehat{\Psi}_{\gamma^*}) + \mathcal{O}_p(1) \\
&= \sqrt{n} (\widehat{\Psi}_\gamma - \widehat{\Psi}_{\gamma^*})^\top \nabla^2 M(\Psi_\gamma^*) \sqrt{n} (\widehat{\Psi}_\gamma - \widehat{\Psi}_{\gamma^*}) + \mathcal{O}_p(1) \\
&= \phi_n^\top \nabla^2 M(\Psi_\gamma^*) \phi_n + \mathcal{O}_p(1),
\end{aligned} \tag{8}$$

where  $\phi_n = \sqrt{n} (\widehat{\Psi}_\gamma - \widehat{\Psi}_{\gamma^*})$  and the third line follows from  $\frac{1}{n} \nabla^2 \ell(\widehat{\Psi}_\gamma) \xrightarrow{\text{Pr}} \nabla^2 M(\Psi_\gamma^*)$ . In this case of  $\gamma^* \subset \gamma$ , we have that  $\Psi_\gamma^* = \Psi_{\gamma^*}$ . So we could rewrite  $\phi$  as

$$\phi_n = \sqrt{n} (\widehat{\Psi}_\gamma - \widehat{\Psi}_{\gamma^*}) = \sqrt{n} (\widehat{\Psi}_\gamma - \Psi_\gamma^*) - \sqrt{n} (\Psi_{\gamma^*}^* - \widehat{\Psi}_{\gamma^*}).$$

Applying Lemma 2 on the final terms, we have that  $\sqrt{n} (\widehat{\Psi}_\gamma - \Psi_\gamma^*) \xrightarrow{D} N(\mathbf{0}, \Sigma_\gamma)$  and  $\sqrt{n} (\Psi_{\gamma^*}^* - \widehat{\Psi}_{\gamma^*}) \xrightarrow{D} N(\mathbf{0}, \Sigma_{\gamma^*})$ . Therefore,

$$\phi_n \xrightarrow{D} N(\mathbf{0}, \Sigma), \quad n \rightarrow \infty,$$

where  $\Sigma = \Sigma_\gamma + \Sigma_{\gamma^*}$ . Since  $\Sigma$  is a positive definite covariance matrix and  $\nabla^2 M(\Psi_\gamma^*)$  is a real symmetric matrix, applying Lemma 1 and Theorem 1 in [Baldessari \(1967\)](#), the first term in (8) could be written asymptotically as a linear combination of independent Chi-squared random variables (see also [Proposition 1 in Iqbal et al. 2025](#)):

$$\phi_n^\top \nabla^2 M(\Psi_\gamma^*) \phi_n \xrightarrow{D} \sum_j \lambda_j \chi_{r_j}^2,$$

where  $\lambda_j$  is the  $j$ -th unique eigenvalue of  $\nabla^2 M(\Psi_\gamma^*) \Sigma$  and  $r_j$  is its corresponding order of multiplicity. Combining this result with (8), we have that  $Z_1$  is stochastically bounded

$$Z_1 \xrightarrow{D} \sum_j \lambda_j \chi_{r_j}^2 + \mathcal{O}_p(1) = \mathcal{O}_p(1).$$

For  $\gamma^* \not\subset \gamma$ , applying continuous mapping theory on Lemma 1, we have  $\ell(\widehat{\Psi}_\gamma) \xrightarrow{\text{Pr}} \ell(\widehat{\Psi}_\gamma^*)$  and  $\ell(\widehat{\Psi}_{\gamma^*}) \xrightarrow{\text{Pr}} \ell(\widehat{\Psi}_{\gamma^*}^*)$ . By weak law of large numbers, we have  $\frac{1}{n}\ell(\widehat{\Psi}_\gamma^*) \xrightarrow{\text{Pr}} M(\widehat{\Psi}_\gamma^*)$  and  $\frac{1}{n}\ell(\widehat{\Psi}_{\gamma^*}^*) \xrightarrow{\text{Pr}} M(\widehat{\Psi}_{\gamma^*}^*)$ . Therefore,

$$\frac{1}{n}Z_1 = \frac{1}{n}(\ell(\widehat{\Psi}_\gamma) - \ell(\widehat{\Psi}_{\gamma^*})) \xrightarrow{\text{Pr}} M(\widehat{\Psi}_\gamma^*) - M(\widehat{\Psi}_{\gamma^*}^*) < 0. \quad (9)$$

Although  $M(\widehat{\Psi}_\gamma^*) - M(\widehat{\Psi}_{\gamma^*}^*)$  could not be further bounded, it is driven by the KL-optimal errors of  $\gamma$  and  $\gamma^*$  (Rossell & Rubio 2023).

For  $Z_2$ , recall the expression for the  $2 \times 2$  matrix  $\mathbf{P}$  is

$$\mathbf{P} = \begin{bmatrix} \mathcal{J}_{\nu\nu} - \frac{ng_E}{1+ng_E} \mathcal{J}_{\theta,\eta,\nu}^\top \mathcal{J}_{\theta,\eta}^{-1} \mathcal{J}_{\theta,\eta,\nu} + \frac{1}{\sigma_\nu^2} & \mathcal{J}_{\nu,\theta_0} - \frac{ng_E}{1+ng_E} \mathcal{J}_{\theta,\eta,\nu}^\top \mathcal{J}_{\theta,\eta}^{-1} \mathcal{J}_{\theta,\eta,\theta_0} \\ \mathcal{J}_{\nu,\theta_0} - \frac{ng_E}{1+ng_E} \mathcal{J}_{\theta,\eta,\nu}^\top \mathcal{J}_{\theta,\eta}^{-1} \mathcal{J}_{\theta,\eta,\theta_0} & \mathcal{J}_{\theta_0\theta_0} - \frac{ng_E}{1+ng_E} \mathcal{J}_{\theta,\eta,\theta_0}^\top \mathcal{J}_{\theta,\eta}^{-1} \mathcal{J}_{\theta,\eta,\theta_0} + \frac{1}{K} \end{bmatrix}.$$

Note that all entries in  $\mathbf{P}$  is composed of entries in the observed Fisher information matrix. Therefore, by Lemma 3, all of the four entries are of order  $\mathcal{O}_p(n)$ , and the determinant ratio is given by

$$Z_2 = \frac{|\mathbf{P}|^{-\frac{1}{2}}}{|\mathbf{P}_*|^{-\frac{1}{2}}} = \frac{\mathcal{O}_p(n^{-1})}{\mathcal{O}_p(n^{-1})} = \mathcal{O}_p(1), \quad (10)$$

where the orders of the numerator and denominator follow from the eigen decomposition of  $\mathbf{P}$  and  $\mathbf{P}^*$ .

For  $Z_3$ , recall the expression for  $\mathbf{h}$  is

$$\mathbf{h} = \begin{bmatrix} (\mathcal{J}_{\nu\nu} - \frac{ng_E}{1+ng_E} \mathcal{J}_{\theta,\eta,\nu}^\top \mathcal{J}_{\theta,\eta}^{-1} \mathcal{J}_{\theta,\eta,\nu})\widehat{\nu} + (\mathcal{J}_{\nu,\theta_0} - \frac{ng_E}{1+ng_E} \mathcal{J}_{\theta,\eta,\nu}^\top \mathcal{J}_{\theta,\eta}^{-1} \mathcal{J}_{\theta,\eta,\theta_0})\widehat{\theta}_0 + \frac{\mu_\nu}{\sigma_\nu^2} \\ (\mathcal{J}_{\nu,\theta_0} - \frac{ng_E}{1+ng_E} \mathcal{J}_{\theta,\eta,\nu}^\top \mathcal{J}_{\theta,\eta}^{-1} \mathcal{J}_{\theta,\eta,\theta_0})\widehat{\nu} + (\mathcal{J}_{\theta_0\theta_0} - \frac{ng_E}{1+ng_E} \mathcal{J}_{\theta,\eta,\theta_0}^\top \mathcal{J}_{\theta,\eta}^{-1} \mathcal{J}_{\theta,\eta,\theta_0})\widehat{\theta}_0 \end{bmatrix}.$$

Following the same logic for  $Z_2$ , we have the two elements in  $\mathbf{h}$  are of  $\mathcal{O}_p(n)$ . For the inverse  $\mathbf{P}^{-1}$ , since each element of  $\mathbf{P}$  is of  $\mathcal{O}_p(n)$ , each element of  $\mathbf{P}^{-1}$  is of  $\mathcal{O}_p(n^{-1})$ . Therefore, each element in the sum of the quadratic term,  $\frac{1}{2}\mathbf{h}^\top \mathbf{P}^{-1} \mathbf{h} = \frac{1}{2} \sum_{i=1}^2 \sum_{j=1}^2 h_i (\mathbf{P}^{-1})_{ij} h_j$ , is of order  $h_i (\mathbf{P}^{-1})_{ij} h_j = \mathcal{O}_p(n) \cdot \mathcal{O}_p(n^{-1}) \cdot \mathcal{O}_p(n) = \mathcal{O}_p(n)$ . Therefore the overall order of the quadratic

term is  $\frac{1}{2} \sum_{i=1}^2 \sum_{j=1}^2 \mathcal{O}_p(n) = \mathcal{O}_p(n)$ . Recall the expression for  $C$  is

$$\begin{aligned} C = & -\frac{\mu_\nu^2}{2\sigma_\nu^2} - \frac{1}{2}\hat{\nu}^2\mathcal{J}_{\nu\nu} - \hat{\nu}\hat{\theta}_0\mathcal{J}_{\nu,\theta_0} - \frac{1}{2}\hat{\theta}_0^2\mathcal{J}_{\theta_0\theta_0} + \frac{ng_E}{2(1+ng_E)}\hat{\nu}^2\mathcal{J}_{\theta,\eta,\nu}^\top\mathcal{J}_{\theta,\eta,\nu}^{-1}\mathcal{J}_{\theta,\eta,\nu} \\ & + \frac{ng_E}{(1+ng_E)}\hat{\nu}\hat{\theta}_0\mathcal{J}_{\theta,\eta,\nu}^\top\mathcal{J}_{\theta,\eta,\theta_0}^{-1}\mathcal{J}_{\theta,\eta,\theta_0} + \frac{ng_E}{2(1+ng_E)}\hat{\theta}_0^2\mathcal{J}_{\theta,\eta,\theta_0}^\top\mathcal{J}_{\theta,\eta,\theta_0}^{-1}\mathcal{J}_{\theta,\eta,\theta_0}. \end{aligned}$$

From the expression, we could see that  $C$  is composed of quadratic and linear terms of components of the observed Fisher information, therefore according to Lemma 3,  $C$  is of  $\mathcal{O}_p(n)$ . Then the numerator for  $Z_3$ ,  $\frac{1}{2}\mathbf{h}^\top \mathbf{P}^{-1} \mathbf{h} + C$ , is of order  $\mathcal{O}_p(n)$ . For the denominator, we could obtain the same asymptotic rate for  $\mathbf{h}_*$ ,  $\mathbf{P}_*^{-1}$ , and  $C_*$ . Therefore, the order of  $Z_3$  is

$$Z_3 = \frac{\frac{1}{2}\mathbf{h}^\top \mathbf{P}^{-1} \mathbf{h} + C}{\frac{1}{2}\mathbf{h}_*^\top \mathbf{P}_*^{-1} \mathbf{h}_* + C_*} = \frac{\mathcal{O}_p(n)}{\mathcal{O}_p(n)} = \mathcal{O}_p(1). \quad (11)$$

Combining the three exponents together, for  $\gamma^* \subset \gamma$  we have

$$\hat{B}_{\gamma,\gamma^*} = (1+ng_E)^{\frac{d_\gamma - d_{\gamma^*}}{2}} \exp\{\mathcal{O}_p(1)\} \mathcal{O}_p(1) \exp\{\mathcal{O}_p(1)\} = (1+ng_E)^{\frac{d_\gamma - d_{\gamma^*}}{2}} \exp\{\mathcal{O}_p(1)\},$$

and for  $\gamma^* \not\subset \gamma$  we have

$$\hat{B}_{\gamma,\gamma^*} = (1+ng_E)^{\frac{d_\gamma - d_{\gamma^*}}{2}} \exp\left\{n\left(M(\widehat{\Psi}_\gamma^*) - M(\widehat{\Psi}_{\gamma^*}^*)\right) + \mathcal{O}_p(1)\right\}.$$

**6.2.0.2 Case  $\gamma^* = 0$**  When the true model is null, the Bayes factor becomes:

$$\hat{B}_{\gamma,\gamma^*} = (1+ng_E)^{\frac{d_\gamma}{2}} \exp\{Z_1\} Z_2 \exp\{Z_3\},$$

where

$$\begin{aligned} Z_1 &= \ell(\widehat{\Psi}_\gamma) - \ell(\widehat{\Psi}_0), \\ Z_2 &= \frac{|\mathbf{P}|^{-\frac{1}{2}}}{|\mathbf{P}_0|^{-\frac{1}{2}}}, \\ Z_3 &= \frac{\frac{1}{2}\mathbf{h}^\top \mathbf{P}^{-1} \mathbf{h} + C}{\frac{1}{2}\mathbf{h}_0^\top \mathbf{P}_0^{-1} \mathbf{h}_0 + C_0}. \end{aligned}$$

Recall the expression for  $\mathbf{h}_0, \mathbf{P}_0, C_0$  is

$$\mathbf{P}_0 = \begin{bmatrix} \mathcal{J}_{\nu\nu} + \frac{1}{\sigma_\nu^2} & \mathcal{J}_{\nu,\theta_0} \\ \mathcal{J}_{\nu,\theta_0} & \mathcal{J}_{\theta_0\theta_0} + \frac{1}{K} \end{bmatrix}, \quad \mathbf{h}_0 = \begin{bmatrix} \mathcal{J}_{\nu\nu}\hat{\nu} + \mathcal{J}_{\nu,\theta_0}\hat{\theta}_0 + \frac{\mu_\nu}{\sigma_\nu^2} \\ \mathcal{J}_{\nu,\theta_0}\hat{\nu} + \mathcal{J}_{\theta_0\theta_0}\hat{\theta}_0 \end{bmatrix},$$

and

$$C_0 = -\frac{\mu_\nu^2}{2\sigma_\nu^2} - \frac{1}{2}(\hat{\nu}_0)^2 \mathcal{J}_{\nu\nu} - \hat{\nu}\hat{\theta}_0 \mathcal{J}_{\nu,\theta_0} - \frac{1}{2}(\hat{\theta}_0)^2 \mathcal{J}_{\theta_0\theta_0}.$$

We could observe that each of the entries in  $\mathbf{h}_0, \mathbf{P}_0$  are of  $\mathcal{O}_p(n)$ , and  $C_0$  is also of  $\mathcal{O}_p(n)$ .

Therefore,  $\mathbf{h}_0, \mathbf{P}_0, C_0$  have the same rate as  $\mathbf{h}, \mathbf{P}, C$ , and  $Z_2$  and  $Z_3$  are then of  $\mathcal{O}_p(1)$ . For  $Z_1$ , the proof is identical to the previous case, which leads to  $Z_1 = \mathcal{O}_p(1), n \rightarrow \infty$  for  $\gamma^* \subset \gamma$ , and  $Z_1 = n(M(\widehat{\Psi}_\gamma^*) - M(\widehat{\Psi}_0^*)), n \rightarrow \infty$  for  $\gamma^* \not\subset \gamma$ . Combining these together, we have that for  $\gamma^* \not\subset \gamma$

$$\widehat{B}_{\gamma, \gamma^*} = (1 + ng_E)^{\frac{d\gamma}{2}} \exp\{\mathcal{O}_p(1)\} \mathcal{O}_p(1) \exp\{\mathcal{O}_p(1)\} = (1 + ng_E)^{\frac{d\gamma}{2}} \exp\{\mathcal{O}_p(1)\},$$

and for  $\gamma^* \not\subset \gamma$  we have

$$\widehat{B}_{\gamma, \gamma^*} = (1 + ng_E)^{\frac{d\gamma}{2}} \exp\left\{n(M(\widehat{\Psi}_\gamma^*) - M(\widehat{\Psi}_{\gamma^*}^*)) + \mathcal{O}_p(1)\right\}.$$

Note that the Bayes factor rates are the same for both  $\gamma^* \neq \mathbf{0}$  and  $\gamma^* = \mathbf{0}$ , and conclude the proof.

### 6.3 Proof of Corollary 1

We could write the statement as

$$\widehat{\pi}(\gamma^* | \mathbf{t}, \boldsymbol{\delta}) = \left(1 + \sum_{\gamma \neq \gamma^*} \widehat{B}_{\gamma, \gamma^*} \frac{\pi(\gamma)}{\pi(\gamma^*)}\right)^{-1} \xrightarrow{\text{Pr}} 1.$$

By Proposition 2, for case  $\gamma \subset \gamma^*$ , we have  $\widehat{B}_{\gamma, \gamma^*} = \mathcal{O}_p(1)$  immediately; for case  $\gamma \not\subset \gamma^*$ ,  $M(\widehat{\Psi}_{\gamma^*}^*) - M(\widehat{\Psi}_\gamma^*) > 0$ , so we still have  $\widehat{B}_{\gamma, \gamma^*} = \mathcal{O}_p(1)$ . Therefore,  $\widehat{B}_{\gamma, \gamma^*} \xrightarrow{\text{Pr}} 0$  for either of the cases. And hence, we have

$$\sum_{\gamma \neq \gamma^*} \widehat{B}_{\gamma, \gamma^*} \frac{\pi(\gamma)}{\pi(\gamma^*)} \xrightarrow{\text{Pr}} 0,$$

and we conclude that

$$\left(1 + \sum_{\gamma \neq \gamma^*} \widehat{B}_{\gamma, \gamma^*} \frac{\pi(\gamma)}{\pi(\gamma^*)}\right)^{-1} \xrightarrow{\text{Pr}} 1.$$

## 6.4 Proof of Proposition 3

The proof of this result represents an extension of the Bayes factor rates characterisation in [Rossell & Rubio \(2023\)](#) to the context where a variable plays more than one role in the model. We emphasise that this proof presents a characterisation of the asymptotic behaviour of Bayes factors obtained with the Laplace approximation. That is, we characterise the asymptotic rates of:

$$\tilde{B}_{\gamma, \gamma^*} = \frac{\tilde{p}(\mathbf{t} \mid \boldsymbol{\gamma})}{\tilde{p}(\mathbf{t} \mid \boldsymbol{\gamma}^*)},$$

where  $\tilde{p}(\mathbf{t} \mid \boldsymbol{\gamma})$  is obtained via a Laplace approximation:

$$\tilde{p}(\mathbf{t} \mid \boldsymbol{\gamma}) = \exp\{\ell(\tilde{\Psi}_\gamma) + \log \pi(\tilde{\Psi}_\gamma)\} (2\pi)^{d_\gamma/2} \left| H(\tilde{\Psi}_\gamma) + \nabla^2 \log \pi(\tilde{\Psi}_\gamma) \right|^{-1/2},$$

where  $\tilde{\Psi}_\gamma = \arg \max_{\Psi_\gamma} \{\ell(\Psi_\gamma) + \log \pi(\Psi_\gamma)\}$  is the maximum a posteriori (MAP) under prior  $\pi(\Psi_\gamma)$ .

First, let us factorise the Bayes factor as:

$$\tilde{B}_{\gamma, \gamma^*} = (2\pi)^{\frac{d_\gamma - d_{\gamma^*}}{2}} \exp\{Z_1\} Z_2 Z_3,$$

where

$$\begin{aligned} Z_1 &= \ell(\tilde{\Psi}_\gamma) - \ell(\tilde{\Psi}_{\gamma^*}), \\ Z_2 &= \frac{\pi(\tilde{\Psi}_\gamma \mid \boldsymbol{\gamma})}{\pi(\tilde{\Psi}_{\gamma^*} \mid \boldsymbol{\gamma})}, \\ Z_3 &= \frac{\left| H(\tilde{\Psi}_{\gamma^*}) + \nabla^2 \log \pi(\tilde{\Psi}_{\gamma^*}) \right|^{-1/2}}{\left| H(\tilde{\Psi}_\gamma) + \nabla^2 \log \pi(\tilde{\Psi}_\gamma) \right|^{-1/2}}. \end{aligned}$$

We start with  $Z_3$  by rewriting it as

$$Z_3 = n^{\frac{d_{\gamma^*} - d_\gamma}{2}} \frac{\left| n^{-1} \left[ H(\tilde{\Psi}_{\gamma^*}) + \nabla^2 \log \pi(\tilde{\Psi}_{\gamma^*}) \right] \right|^{\frac{1}{2}}}{\left| n^{-1} \left[ H(\tilde{\Psi}_\gamma) + \nabla^2 \log \pi(\tilde{\Psi}_\gamma) \right] \right|^{\frac{1}{2}}}.$$

From Lemma 1, the MAP estimators  $\tilde{\Psi}_{\gamma^*} \xrightarrow{\text{Pr}} \Psi_{\gamma^*}^*$  and  $\tilde{\Psi}_\gamma \xrightarrow{\text{Pr}} \Psi_\gamma^*$  as  $n \rightarrow \infty$ . Therefore, applying the continuous mapping theorem, we have  $n^{-1} H(\tilde{\Psi}_\gamma^*) \xrightarrow{\text{Pr}} \nabla^2 M(\Psi_\gamma^*)$ , as  $n \rightarrow \infty$ .

The same result follows for  $\gamma^*$ :  $n^{-1}H(\tilde{\Psi}_{\gamma^*}^*) \xrightarrow{\text{Pr}} \nabla^2 M(\Psi_{\gamma^*}^*)$ , as  $n \rightarrow \infty$ . According to C4,  $\Psi_{\gamma}^*$  and  $\tilde{\Psi}_{\gamma^*}^*$  are unique interior maximums, which implies the negative definiteness of  $\nabla^2 M(\Psi_{\gamma}^*)$  and  $\nabla^2 M(\tilde{\Psi}_{\gamma^*}^*)$ . We also have  $n^{-1}\mathbf{X}_{\gamma}^{\top}\mathbf{X}_{\gamma}$  and  $n^{-1}\tilde{\mathbf{X}}_{\gamma}^{\top}\tilde{\mathbf{X}}_{\gamma}$  converges in probability to positive definite matrices. Therefore, the matrices  $n^{-1}\nabla^2 \log \pi(\tilde{\Psi}_{\gamma}) = \mathcal{O}_p(1)$  and  $n^{-1}\nabla^2 \log \pi(\tilde{\Psi}_{\gamma^*}) = \mathcal{O}_p(1)$ . Combining these together, we have

$$\frac{\left|n^{-1}[H(\tilde{\Psi}_{\gamma^*}) + \nabla^2 \log \pi(\tilde{\Psi}_{\gamma^*})]\right|^{\frac{1}{2}}}{\left|n^{-1}[H(\tilde{\Psi}_{\gamma}) + \nabla^2 \log \pi(\tilde{\Psi}_{\gamma})]\right|^{\frac{1}{2}}} \xrightarrow{\text{Pr}} \frac{\left|\nabla^2 M(\Psi_{\gamma^*}^*)\right|^{\frac{1}{2}}}{\left|\nabla^2 M(\Psi_{\gamma}^*)\right|^{\frac{1}{2}}}, \quad n \rightarrow \infty.$$

And since  $\Psi_{\gamma}^*$  and  $\Psi_{\gamma^*}^*$  are fixed by assumption, then  $\left|\nabla^2 M(\Psi_{\gamma^*}^*)\right|^{\frac{1}{2}}$  and  $\left|\nabla^2 M(\Psi_{\gamma}^*)\right|^{\frac{1}{2}}$  would be constants, so we have

$$Z_3 n^{\frac{d_{\gamma} - d_{\gamma^*}}{2}} \xrightarrow{\text{Pr}} \frac{\left|\nabla^2 M(\Psi_{\gamma^*}^*)\right|^{\frac{1}{2}}}{\left|\nabla^2 M(\Psi_{\gamma}^*)\right|^{\frac{1}{2}}} \in (0, \infty).$$

Therefore, since  $Z_3 n^{\frac{d_{\gamma} - d_{\gamma^*}}{2}}$  converges in probability into a constant, we have

$$Z_3 = \mathcal{O}_p\left(n^{\frac{d_{\gamma^*} - d_{\gamma}}{2}}\right). \quad (12)$$

Another pair of results that follows from applying continuous mapping theorem on Lemma 1 is  $\pi(\tilde{\Psi}_{\gamma} | \gamma) \xrightarrow{\text{Pr}} \pi(\tilde{\Psi}_{\gamma}^* | \gamma)$  and  $\pi(\tilde{\Psi}_{\gamma^*} | \gamma) \xrightarrow{\text{Pr}} \pi(\tilde{\Psi}_{\gamma^*}^* | \gamma)$ . Then we can construct the following asymptotic equation for  $Z_2$

$$Z_2 \frac{\pi(\tilde{\Psi}_{\gamma^*}^* | \gamma)}{\pi(\tilde{\Psi}_{\gamma}^* | \gamma)} \xrightarrow{\text{Pr}} 1, \quad n \rightarrow \infty, \quad (13)$$

with any continuous non-vanishing prior  $\pi$ . We start by characterizing  $\tilde{\nu}$  and  $\tilde{\theta}_0$ . Recall that  $\nu \sim Ga(a_{\nu}, b_{\nu})$  and  $\pi(\theta_0) \propto 1$ , we have

$$\begin{aligned} \frac{\pi(\tilde{\nu}_{\gamma})\pi(\tilde{\theta}_{0\gamma})}{\pi(\tilde{\nu}_{\gamma^*})\pi(\tilde{\theta}_{0\gamma^*})} &\propto \left(\frac{\tilde{\nu}_{\gamma}}{\tilde{\nu}_{\gamma^*}}\right)^{a_{\nu}} e^{b_{\nu}(\tilde{\nu}_{\gamma^*} - \tilde{\nu}_{\gamma})} \\ &= \mathcal{O}_p(1), \end{aligned}$$

as the domains of  $\tilde{\nu}_{\gamma^*}$  and  $\tilde{\nu}_\gamma$  are compact subset of  $(0, \infty)$ , the ratio and the exponential term are bounded from below and above.

Therefore, the ratio in the left-hand side of (13) could be expanded as

$$\begin{aligned} \frac{\pi(\tilde{\Psi}_{\gamma^*}^* | \gamma)}{\pi(\tilde{\Psi}_\gamma^* | \gamma)} &\propto \frac{\pi(\tilde{\theta}_{\gamma^*}^* | \gamma) \pi(\tilde{\eta}_{\gamma^*}^* | \gamma)}{\pi(\tilde{\theta}_\gamma^* | \gamma) \pi(\tilde{\eta}_\gamma^* | \gamma)} \\ &= g_{C_t}^{\frac{q_\gamma - q_{\gamma^*}}{2}} g_{C_h}^{\frac{p_\gamma - p_{\gamma^*}}{2}} \frac{\left| n^{-1} \tilde{\mathbf{X}}_{\gamma^*}^\top \tilde{\mathbf{X}}_{\gamma^*} \right|^{\frac{1}{2}} \left| n^{-1} \mathbf{X}_{\gamma^*}^\top \mathbf{X}_{\gamma^*} \right|^{\frac{1}{2}}}{\left| n^{-1} \tilde{\mathbf{X}}_\gamma^\top \tilde{\mathbf{X}}_\gamma \right|^{\frac{1}{2}} \left| n^{-1} \mathbf{X}_\gamma^\top \mathbf{X}_\gamma \right|^{\frac{1}{2}}} \\ &\times \exp \left( -\frac{1}{2ng_{C_t}} \left[ \tilde{\theta}_\gamma^{*T} \tilde{\mathbf{X}}_\gamma^\top \tilde{\mathbf{X}}_\gamma \tilde{\theta}_\gamma^* - \tilde{\theta}_{\gamma^*}^{*T} \tilde{\mathbf{X}}_{\gamma^*}^\top \tilde{\mathbf{X}}_{\gamma^*} \tilde{\theta}_{\gamma^*}^* \right] \right) \\ &\times \exp \left( -\frac{1}{2ng_{C_h}} \left[ \tilde{\eta}_\gamma^{*T} \mathbf{X}_\gamma^\top \mathbf{X}_\gamma \tilde{\eta}_\gamma^* - \tilde{\eta}_{\gamma^*}^{*T} \mathbf{X}_{\gamma^*}^\top \mathbf{X}_{\gamma^*} \tilde{\eta}_{\gamma^*}^* \right] \right) \end{aligned}$$

And since  $n^{-1} \tilde{\mathbf{X}}_{\gamma^*}^\top \tilde{\mathbf{X}}_{\gamma^*}$ ,  $n^{-1} \tilde{\mathbf{X}}_\gamma^\top \tilde{\mathbf{X}}_\gamma$ ,  $n^{-1} \mathbf{X}_{\gamma^*}^\top \mathbf{X}_{\gamma^*}$ , and  $n^{-1} \mathbf{X}_\gamma^\top \mathbf{X}_\gamma$  converges in probability to positive definite matrices, and  $\tilde{\eta}_\gamma^*$ ,  $\tilde{\eta}_{\gamma^*}^*$ ,  $\tilde{\theta}_\gamma^*$ , and  $\tilde{\theta}_{\gamma^*}^*$  are fixed by assumption, the product of the determinants and exponential terms converges into a constant  $k \in (0, \infty)$ . So we have

$$\frac{\pi(\tilde{\Psi}_{\gamma^*}^* | \gamma)}{\pi(\tilde{\Psi}_\gamma^* | \gamma)} \xrightarrow{\text{Pr}} k \cdot g_{C_t}^{\frac{q_\gamma - q_{\gamma^*}}{2}} g_{C_h}^{\frac{p_\gamma - p_{\gamma^*}}{2}}.$$

Now, appealing to Slutsky's theorem, we have

$$Z_2 \frac{\pi(\tilde{\Psi}_{\gamma^*}^* | \gamma)}{\pi(\tilde{\Psi}_\gamma^* | \gamma)} \xrightarrow{\text{Pr}} 1 \implies Z_2 \cdot k g_{C_t}^{\frac{q_\gamma - q_{\gamma^*}}{2}} g_{C_h}^{\frac{p_\gamma - p_{\gamma^*}}{2}} \xrightarrow{\text{Pr}} 1, \quad n \rightarrow \infty.$$

And since  $k$  is a constant, we have

$$Z_2 = \mathcal{O}_p \left( g_{C_t}^{\frac{q_{\gamma^*} - q_\gamma}{2}} g_{C_h}^{\frac{p_{\gamma^*} - p_\gamma}{2}} \right). \quad (14)$$

For the characterization of  $Z_1$ , we need to consider the case of  $\gamma^* \not\subset \gamma$  and  $\gamma^* \subset \gamma$  separately.

**6.4.0.1 Case  $\gamma^* \subset \gamma$**  This represents the situation where the optimal model is within the specified model family. We start by establishing the relationship between the MAP  $\tilde{\Psi}_\gamma$  and MLE  $\widehat{\Psi}_\gamma$ . Performing a second order Taylor expansion with remainder around the MLE estimate  $\widehat{\Psi}_\gamma$

(Chapter 16, [van der Vaart \(2000\)](#)), we have that there exists  $\bar{\Psi}_\gamma$  in the line joining the MAP  $\tilde{\Psi}_\gamma$  and MLE  $\widehat{\Psi}_\gamma$  such that,

$$\begin{aligned}\ell(\tilde{\Psi}_\gamma) - \ell(\widehat{\Psi}_\gamma) &= (\tilde{\Psi}_\gamma - \widehat{\Psi}_\gamma) \nabla \ell(\widehat{\Psi}_\gamma) + (\tilde{\Psi}_\gamma - \widehat{\Psi}_\gamma)^\top \nabla^2 \ell(\bar{\Psi}_\gamma) (\tilde{\Psi}_\gamma - \widehat{\Psi}_\gamma) \\ &= 0 + \sqrt{n} (\tilde{\Psi}_\gamma - \widehat{\Psi}_\gamma)^\top \frac{\nabla^2 \ell(\bar{\Psi}_\gamma)}{n} \sqrt{n} (\tilde{\Psi}_\gamma - \widehat{\Psi}_\gamma) \\ &= \sqrt{n} (\tilde{\Psi}_\gamma - \widehat{\Psi}_\gamma)^\top \nabla^2 M(\bar{\Psi}_\gamma) \sqrt{n} (\tilde{\Psi}_\gamma - \widehat{\Psi}_\gamma) + \mathcal{O}_p(1) \\ &= \mathcal{O}_p(1),\end{aligned}$$

where the last line follows from the fact  $\frac{\nabla^2 \ell(\bar{\Psi}_\gamma)}{n} \xrightarrow{\text{Pr}} \nabla^2 M(\bar{\Psi}_\gamma)$ ,  $\nabla^2 M(\bar{\Psi}_\gamma)$  is a symmetric negative-definite matrix (C7), and appealing to Proposition 2 in [Rossell & Telesca \(2017\)](#). The same results follows for  $\tilde{\Psi}_{\gamma^*}$ . Therefore, we would have

$$Z_1 = \ell(\tilde{\Psi}_\gamma) - \ell(\tilde{\Psi}_{\gamma^*}) = \ell(\widehat{\Psi}_\gamma) - \ell(\widehat{\Psi}_{\gamma^*}) + \mathcal{O}_p(1).$$

We now perform a second order Taylor expansion on  $Z_1$

$$\begin{aligned}Z_1 &= \ell(\widehat{\Psi}_\gamma) - \ell(\widehat{\Psi}_{\gamma^*}) + \mathcal{O}_p(1) \\ &= (\widehat{\Psi}_\gamma - \widehat{\Psi}_{\gamma^*})^\top \nabla^2 \ell(\widehat{\Psi}_\gamma) (\widehat{\Psi}_\gamma - \widehat{\Psi}_{\gamma^*}) + \mathcal{O}_p(1) \\ &= \sqrt{n} (\widehat{\Psi}_\gamma - \widehat{\Psi}_{\gamma^*})^\top \nabla^2 M(\widehat{\Psi}_{\gamma^*}) \sqrt{n} (\widehat{\Psi}_\gamma - \widehat{\Psi}_{\gamma^*}) + \mathcal{O}_p(1) \\ &= \boldsymbol{\phi}_n^\top \nabla^2 M(\widehat{\Psi}_{\gamma^*}) \boldsymbol{\phi}_n + \mathcal{O}_p(1),\end{aligned}\tag{15}$$

where  $\boldsymbol{\phi}_n = \sqrt{n} (\widehat{\Psi}_\gamma - \widehat{\Psi}_{\gamma^*})$  and the third line follows from  $\frac{1}{n} \nabla^2 \ell(\widehat{\Psi}_\gamma) \xrightarrow{\text{Pr}} \nabla^2 M(\widehat{\Psi}_{\gamma^*})$ . In this case of  $\gamma^* \subset \gamma$ , we have that  $\Psi_\gamma^* = \Psi_{\gamma^*}$ . So we could rewrite  $\boldsymbol{\phi}$  as

$$\boldsymbol{\phi}_n = \sqrt{n} (\widehat{\Psi}_\gamma - \widehat{\Psi}_{\gamma^*}) = \sqrt{n} (\widehat{\Psi}_\gamma - \Psi_\gamma^*) - \sqrt{n} (\Psi_{\gamma^*} - \widehat{\Psi}_{\gamma^*}).$$

Applying Lemma 2 on the final terms, we have that  $\sqrt{n} (\widehat{\Psi}_\gamma - \Psi_\gamma^*) \xrightarrow{D} N(\mathbf{0}, \Sigma_\gamma)$  and  $\sqrt{n} (\Psi_{\gamma^*} - \widehat{\Psi}_{\gamma^*}) \xrightarrow{D} N(\mathbf{0}, \Sigma_{\gamma^*})$ . Therefore,

$$\boldsymbol{\phi}_n \xrightarrow{D} N(\mathbf{0}, \Sigma), \quad n \rightarrow \infty,$$

where  $\Sigma = \Sigma_\gamma + \Sigma_{\gamma^*}$ . Since  $\Sigma$  is a positive definite covariance matrix and  $\nabla^2 M(\Psi_\gamma^*)$  is a real symmetric matrix, applying Lemma 1 and Theorem 1 in [Baldessari \(1967\)](#), the first term in (15) could be written asymptotically as a linear combination of independent Chi-squared random variables ([Rossell & Rubio 2018, Iqbal et al. 2025](#)):

$$\phi_n^\top \nabla^2 M(\Psi_\gamma^*) \phi_n \xrightarrow{D} \sum_j \lambda_j \chi_{r_j}^2,$$

where  $\lambda_j$  is the  $j$ -th unique eigenvalue of  $\nabla^2 M(\Psi_\gamma^*) \Sigma$  and  $r_j$  is its corresponding order of multiplicity. Combining this result with (15), we have that  $Z_1$  is stochastically bounded

$$Z_1 \xrightarrow{D} \sum_j \lambda_j \chi_{r_j}^2 + \mathcal{O}_p(1) = \mathcal{O}_p(1). \quad (16)$$

Lastly, combining (12), (14), and (16), we obtain the desired result for case  $\gamma^* \subset \gamma$

$$\tilde{B}_{\gamma, \gamma^*} = (2\pi)^{\frac{d_\gamma - d_{\gamma^*}}{2}} \exp(Z_1) Z_2 Z_3 = \mathcal{O}_p \left( 1 \cdot n^{\frac{d_{\gamma^*} - d_\gamma}{2}} \cdot g_{C_t}^{\frac{q_{\gamma^*} - q_\gamma}{2}} g_{C_h}^{\frac{p_{\gamma^*} - p_\gamma}{2}} \right).$$

**6.4.0.2 Case  $\gamma^* \not\subset \gamma$**  Applying continuous mapping theory on Lemma 1, we have  $\ell(\tilde{\Psi}_\gamma) \xrightarrow{\text{Pr}} \ell(\tilde{\Psi}_{\gamma^*})$  and  $\ell(\tilde{\Psi}_{\gamma^*}) \xrightarrow{\text{Pr}} \ell(\tilde{\Psi}_{\gamma^*}^*)$ . By weak law of large numbers, we have  $\frac{1}{n} \ell(\tilde{\Psi}_\gamma^*) \xrightarrow{\text{Pr}} M(\tilde{\Psi}_\gamma^*)$  and  $\frac{1}{n} \ell(\tilde{\Psi}_{\gamma^*}^*) \xrightarrow{\text{Pr}} M(\tilde{\Psi}_{\gamma^*}^*)$ . Therefore,

$$\frac{1}{n} Z_1 = \frac{1}{n} (\ell(\tilde{\Psi}_\gamma) - \ell(\tilde{\Psi}_{\gamma^*})) \xrightarrow{\text{Pr}} M(\tilde{\Psi}_\gamma^*) - M(\tilde{\Psi}_{\gamma^*}^*) < 0. \quad (17)$$

Although  $M(\tilde{\Psi}_\gamma^*) - M(\tilde{\Psi}_{\gamma^*}^*)$  could not be further bounded, it is driven by the KL-optimal errors of  $\gamma$  and  $\gamma^*$  ([Rossell & Rubio 2023](#)). Combining (17) with (12) and (14), we derive the desired result for case  $\gamma^* \not\subset \gamma$ :

$$\tilde{B}_{\gamma, \gamma^*} = \mathcal{O}_p \left( 1 \cdot n (M(\tilde{\Psi}_\gamma^*) - M(\tilde{\Psi}_{\gamma^*}^*)) \cdot n^{\frac{d_{\gamma^*} - d_\gamma}{2}} \cdot g_{C_t}^{\frac{q_{\gamma^*} - q_\gamma}{2}} g_{C_h}^{\frac{p_{\gamma^*} - p_\gamma}{2}} \right),$$

and conclude the proof of Proposition 3.

## 6.5 Proof of Corollary 2

We could write the statement as

$$\tilde{\pi}(\boldsymbol{\gamma}^* \mid \mathbf{t}, \boldsymbol{\delta}) = \left( 1 + \sum_{\gamma \neq \gamma^*} \tilde{B}_{\gamma, \gamma^*} \frac{\pi(\boldsymbol{\gamma})}{\pi(\boldsymbol{\gamma}^*)} \right)^{-1} \xrightarrow{\text{Pr}} 1.$$

By Proposition 3, for case  $\boldsymbol{\gamma} \subset \boldsymbol{\gamma}^*$ , we have  $\tilde{B}_{\boldsymbol{\gamma}, \boldsymbol{\gamma}^*} = \mathcal{O}_p(1)$  immediately; for case  $\boldsymbol{\gamma} \not\subset \boldsymbol{\gamma}^*$ ,  $M(\tilde{\Psi}_{\boldsymbol{\gamma}^*}^*) - M(\tilde{\Psi}_{\boldsymbol{\gamma}}^*) > 0$ , so we still have  $\tilde{B}_{\boldsymbol{\gamma}, \boldsymbol{\gamma}^*} = \mathcal{O}_p(1)$ . Therefore,  $\tilde{B}_{\boldsymbol{\gamma}, \boldsymbol{\gamma}^*} \xrightarrow{\text{Pr}} 0$  for either of the cases. And hence, we have

$$\sum_{\gamma \neq \gamma^*} \tilde{B}_{\boldsymbol{\gamma}, \boldsymbol{\gamma}^*} \frac{\pi(\boldsymbol{\gamma})}{\pi(\boldsymbol{\gamma}^*)} \xrightarrow{\text{Pr}} 0,$$

and we conclude that

$$\left( 1 + \sum_{\gamma \neq \gamma^*} \tilde{B}_{\boldsymbol{\gamma}, \boldsymbol{\gamma}^*} \frac{\pi(\boldsymbol{\gamma})}{\pi(\boldsymbol{\gamma}^*)} \right)^{-1} \xrightarrow{\text{Pr}} 1.$$

## 7 Detail of the extended ADS sampler

Table S2: Move selection probabilities by hazard class and state pattern

Class	Condition	A/D	A/D_GH	S	C	$C^A$
Null	—	—	—	—	—	—
AH/PH	All equal	0.50	—	—	0.25	0.25
AH/PH	Mixed	0.50	—	0.10	0.20	0.20
AFT	All 4s	0.60	—	—	—	0.40
AFT	Mixed	0.60	—	0.20	—	0.20
GH	All in $\{0, 3\}$ , all 3s	—	0.50	—	0.25	0.25
GH	All in $\{0, 3\}$ , mixed	—	0.50	0.15	0.15	0.20
GH	Not all in $\{0, 3\}$	—	0.50	0.25	0.25	—

---

**Algorithm 1** GetValidIdx: Filter out valid indices for A/D\_GH

---

**Require:**  $\gamma$  with  $\text{Haz}(\gamma) = \text{GH}$

- 1:  $p_k \leftarrow |\{j : \gamma_j = k\}|$  for  $k = 0, 1, 2, 3$
- 2: **if**  $p_3 = 1$  and remaining forms AH/PH **then return**  $\{j : \gamma_j \neq 3\}$
- 3: **else if**  $p_3 = 0, p_1 > 1, p_2 = 1$  **then return**  $\{j : \gamma_j \neq 2\}$
- 4: **else if**  $p_3 = 0, p_2 > 1, p_1 = 1$  **then return**  $\{j : \gamma_j \neq 1\}$
- 5: **else if**  $p_3 = 0, p_1 = 1, p_2 = 1$  **then return**  $\{j : \gamma_j = 0\}$
- 6: **else return**  $\{1, \dots, p\}$
- 7: **end if**

---

---

**Algorithm 2** Extended ADS sampler — Part 1: A\_null, A/D, A/D\_GH

---

**Require:** Current state  $\gamma$

**Ensure:** Proposed state  $\gamma'$  and  $\log q = \log q_{\text{rev}} - \log q_{\text{fwd}}$

```

1:  $\gamma' \leftarrow \gamma$ ;  $H \leftarrow \text{Haz}(\gamma)$ ; select move  $M$  per Table S2

2: if  $M = \text{A\_null}$  then

3:    $j \sim \text{Unif}\{1, \dots, p\}$ ;  $v \sim \text{Unif}\{1, 2, 3, 4\}$ ;  $\gamma'_j \leftarrow v$ 

4:    $q_{\text{fwd}} \leftarrow 1/p/4$ 

5:    $q_{\text{rev}} \leftarrow \begin{cases} P(\text{A/D\_GH}|\gamma')/|\text{GetValidIdx}(\gamma')| & \text{if GH} \\ P(\text{A/D}|\gamma')/p & \text{o.w.} \end{cases}$ 

6: else if  $M = \text{A/D}$  then

7:    $j \sim \text{Unif}\{1, \dots, p\}$ 

8:   if  $\gamma_j > 0$  then  $\gamma'_j \leftarrow 0$  ▷ Delete

9:   else  $\gamma'_j \leftarrow \mathbf{1}[H=\text{AH}] + 2 \cdot \mathbf{1}[H=\text{PH}] + 4 \cdot \mathbf{1}[H=\text{AFT}]$  ▷ Add

10:  end if

11:   $q_{\text{fwd}} \leftarrow P(\text{A/D}|\gamma)/p$ 

12:   $q_{\text{rev}} \leftarrow \begin{cases} 1/p/4 & \text{if } \gamma' = 0 \\ P(\text{A/D}|\gamma')/p & \text{o.w.} \end{cases}$ 

13: else if  $M = \text{A/D\_GH}$  then

14:    $\mathcal{V} \leftarrow \text{GetValidIdx}(\gamma)$ ;  $j \sim \text{Unif}(\mathcal{V})$ 

15:   if  $\gamma_j > 0$  then  $\gamma'_j \leftarrow 0$ ;  $q_{\text{fwd}} \leftarrow P(\text{A/D\_GH}|\gamma)/|\mathcal{V}|$  ▷ Delete

16:    $q_{\text{rev}} \leftarrow \begin{cases} 1/p/4 & \text{if } \gamma' = 0 \\ P(\text{A/D\_GH}|\gamma')/|\mathcal{V}'|/3 & \text{o.w.} \end{cases}$ 

17:   else  $\gamma'_j \sim \text{Unif}\{1, 2, 3\}$ ;  $q_{\text{fwd}} \leftarrow P(\text{A/D\_GH}|\gamma)/|\mathcal{V}'|/3$  ▷ Add

18:    $q_{\text{rev}} \leftarrow P(\text{A/D\_GH}|\gamma')/|\mathcal{V}'|$  where  $\mathcal{V}' = \text{GetValidIdx}(\gamma')$ 

19: end if

20: end if

```

---

---

**Algorithm 3** Extended ADS sampler — Part 2:  $C, S, C^A$ 


---

```

1: if  $M = \mathbf{C}$  then
2:    $\mathcal{N} \leftarrow \{j : \gamma_j \neq 0\}; j \sim \text{Unif}(\mathcal{N}); \gamma'_j \sim \text{Unif}(\{1, 2, 3\} \setminus \{\gamma_j\})$ 
3:    $q_{\text{fwd}} \leftarrow P(\mathbf{C}|\boldsymbol{\gamma})/|\mathcal{N}|/2; q_{\text{rev}} \leftarrow P(\mathbf{C}|\boldsymbol{\gamma}')/|\mathcal{N}|/2$ 
4: else if  $M = \mathbf{S}$  then
5:    $j_1 \sim \text{Unif}\{1, \dots, p\}; v_1 \leftarrow \gamma_{j_1}; \mathcal{O} \leftarrow \{j : \gamma_j \neq v_1\}; j_2 \sim \text{Unif}(\mathcal{O}); v_2 \leftarrow \gamma_{j_2}$ 
6:   if  $v_1 + v_2 \neq 3$  then  $(\gamma'_{j_1}, \gamma'_{j_2}) \leftarrow (v_2, v_1)$  ▷ Standard swap
7:   else if  $v_1 \in \{1, 2\}$  then  $(\gamma'_{j_1}, \gamma'_{j_2}) \sim \text{Unif}\{(0, 3), (3, 0)\}$  ▷  $(1, 2) \rightarrow (0, 3)/(3, 0)$ 
8:   else  $(\gamma'_{j_1}, \gamma'_{j_2}) \sim \text{Unif}\{(1, 2), (2, 1)\}$  ▷  $(0, 3) \rightarrow (1, 2)/(2, 1)$ 
9:   end if
10:   $p'_{\mathcal{O}} \leftarrow |\{j : \gamma'_j \neq \gamma'_{j_1}\}|$ 
11:   $q_{\text{fwd}} \leftarrow P(\mathbf{S}|\boldsymbol{\gamma})/p/|\mathcal{O}|; \text{if } v_1 + v_2 = 3: q_{\text{fwd}} \leftarrow q_{\text{fwd}}/2$ 
12:   $q_{\text{rev}} \leftarrow P(\mathbf{S}|\boldsymbol{\gamma}')/p/p'_{\mathcal{O}}; \text{if } \gamma'_{j_1} + \gamma'_{j_2} = 3: q_{\text{rev}} \leftarrow q_{\text{rev}}/2$ 
13: else if  $M = C^A$  then
14:   if  $H = \text{AFT}$  then
15:      $v \sim \text{Unif}\{1, 2, 3\}; \text{replace all 4s with } v$ 
16:      $q_{\text{fwd}} \leftarrow P(C^A|\boldsymbol{\gamma})/3; q_{\text{rev}} \leftarrow \begin{cases} P(C^A|\boldsymbol{\gamma}') & \text{if GH} \\ P(C^A|\boldsymbol{\gamma}')/2 & \text{if AH/PH} \end{cases}$ 
17:   else if  $H = \text{GH}$  then
18:     Replace all 3s with 4
19:      $q_{\text{fwd}} \leftarrow P(C^A|\boldsymbol{\gamma}); q_{\text{rev}} \leftarrow P(C^A|\boldsymbol{\gamma}')/3$ 
20:   else ▷ AH or PH
21:      $v \sim \text{Unif}(\{1, 2, 4\} \setminus \{v_{\text{old}}\}); \text{replace all nonzeros with } v$ 
22:      $q_{\text{fwd}} \leftarrow P(C^A|\boldsymbol{\gamma})/2; q_{\text{rev}} \leftarrow \begin{cases} P(C^A|\boldsymbol{\gamma}')/3 & \text{if AFT} \\ P(C^A|\boldsymbol{\gamma}')/2 & \text{o.w.} \end{cases}$ 
23:   end if
24: end if
25: return  $\boldsymbol{\gamma}', \log q \leftarrow \log q_{\text{rev}} - \log q_{\text{fwd}}$ 

```

---

Once the MCMC sample has been obtained, two standard approaches can be used to estimate the posterior model probabilities. The first, and most common, is to calculate the proportion of times each model appears in the MCMC sample. This provides an asymptotically unbiased estimate of the model posterior probabilities, but it may require a large number of iterations to stabilise. Let  $M_{mc}$  be the subset of model space being visited by the MCMC chain(s) and  $\pi(\mathbf{t}, \boldsymbol{\gamma})$  be the un-normalised posterior distribution of models under either ILA or LA. The second method estimates the model posterior probabilities by normalising upon all the visited models from the chain:

$$\hat{p}(\boldsymbol{\gamma}_m \mid \mathbf{t}) = \frac{\pi(\mathbf{t}, \boldsymbol{\gamma}_m)}{\sum_{m \in M_{mc}} \pi(\mathbf{t}, \boldsymbol{\gamma}_m)}.$$

Although the second method depends on accurate approximation of the marginal likelihood and MCMC convergence, it offers greater stability and lower variance. Note that this approach is not asymptotically unbiased with respect to the number of samples, since it requires visiting all models, a condition that can only be met with a sufficiently large number of MCMC iterations. Both estimates are available in our implementation, but in this paper we adopt the second method and evaluate its performance. Similarly, the posterior distribution of the hazard structures could be computed in the same manner:

$$\hat{p}(\text{Hz}(\boldsymbol{\gamma}) = l \mid \mathbf{t}) = \frac{\sum_{\boldsymbol{\gamma}_k} \pi(\mathbf{t}, \boldsymbol{\gamma}_k, \text{Hz}(\boldsymbol{\gamma}_k) = l)}{\sum_{m \in M_{mc}} \pi(\mathbf{t}, \boldsymbol{\gamma}_m)}.$$

## 8 Additional information for the simulation study

In addition to the simulation setting mentioned in Section 6 of the main text, for the underlying baseline hazard, we consider using either a  $\text{Lognormal}(1.55, 0.7)$  distribution or a  $\text{PGW}(1, 1, 2)$  distribution. The parameters for the baseline hazards are chosen such that the corresponding survival functions are around 0.05 at  $t = 15$ . The coefficients of the active variables for the true models are:  $(1, -1, 0.25, -0.25)$  for PH/AH/AFT models and  $\alpha_{active} = (1, 0.25, -1, -0.25)$  and  $\beta_{active} = (0.25, -1, -0.25, 1)$  for GH model. The survival times are generated using the `simGH` function from `HazReg` R package, followed by administrative censoring to create corresponding level of right-censoring on average. The setting for MCMC across all runs is as follows: 1 chain with 20,000 total iterations, 10,000 burn-in, and thinning period of 2, which results in 5,000 posterior samples of models. The initial model is chosen by the following procedure: we fit a Cox-LASSO model (using `cv.glmnet` from `glmnet` package, 10-fold cross-validation), followed by a step-wise selection on the selected PH model on the time-dependent part, based on BIC. This initialisation is very cheap to compute and would yield a GH model that is better than a random initialisation. In case where  $p$  is larger than the values considered here, the initialisation process could be simplified to only using the variables selected by Cox-LASSO model and start with the GH model containing them with all  $\gamma = 3$ .

The model sensitivity and specificity results in Figure 2 of the main text are the true positive rate and true negative rate, respectively. The number of true positives of a model  $\gamma$  given the true model  $\gamma^*$  is calculated by  $\sum_{j=1}^p \mathbf{1}(\gamma_j \neq 0 \text{ and } \gamma_j^* \neq 0)$ , and the number of true negatives is  $\gamma$  given the true model  $\gamma^*$  is calculated by  $\sum_{j=1}^p \mathbf{1}(\gamma_j = 0 \text{ and } \gamma_j^* = 0)$ .

### 8.1 Figures for large-scale simulation

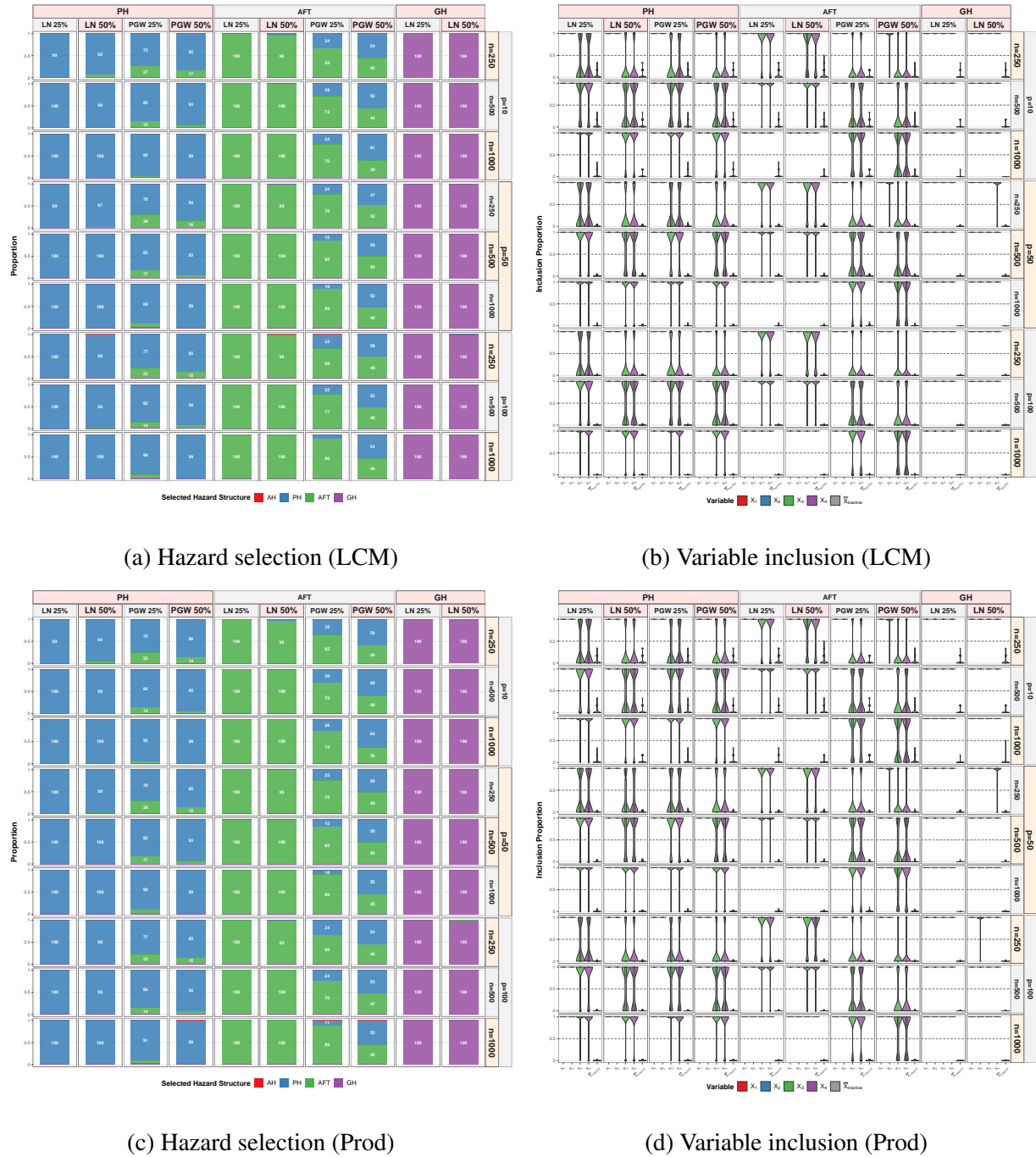


Figure S1: Detailed hazard structure selection and variable inclusion results across the 250 MC simulations for all scenarios and prior settings.

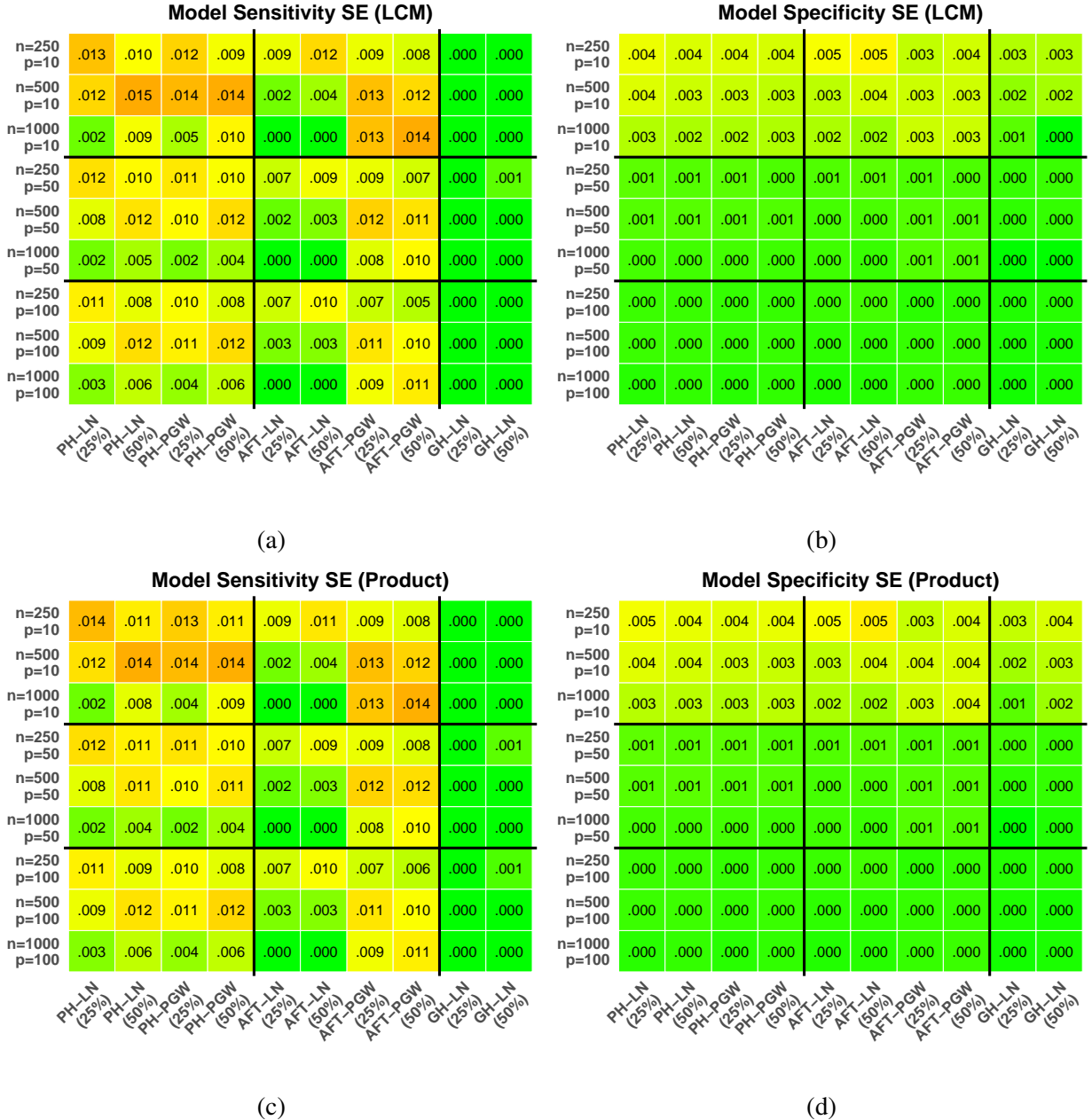
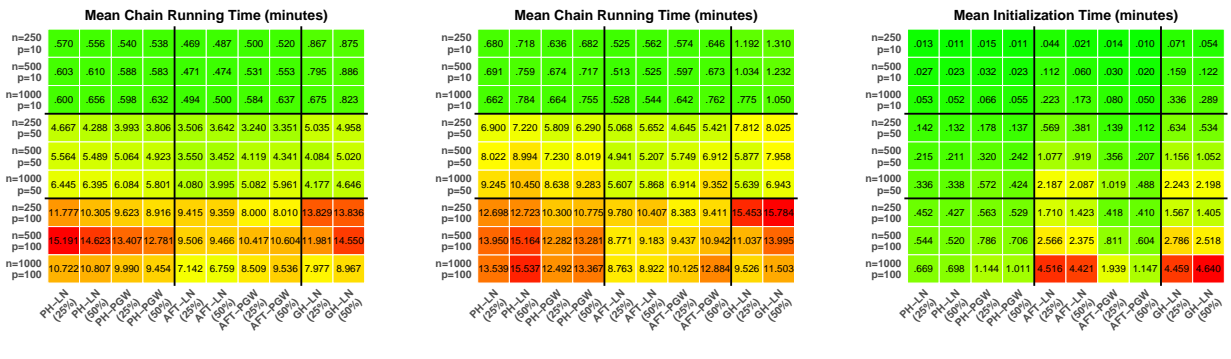


Figure S2: Standard error of sensitivity and specificity of variable selection across the 250 MC simulations for all scenarios and prior settings, based on the highest estimated posterior probability models. (a) SE of sensitivity for all simulation scenarios under LCM prior; (b) SE of specificity under LCM prior; (c) SE of sensitivity under Product prior; (d) SE of specificity under Product prior.

Figure S3: Mean time (in minutes) of initialisation and running the chains across the 250 MC simulations for all scenarios and prior settings. The result is based on a single core of Intel(R) Xeon(R) Gold 6240 CPU @2.60GHz. (a) Mean running time for 20,000 iterations of MCMC under LCM prior; (b) Mean running time for 20,000 iterations of MCMC under Product prior; (c) Initialisation time using the method discussed in Section 6 of main text.



## 8.2 Results for additional study on influence of hazard selection on variable selection

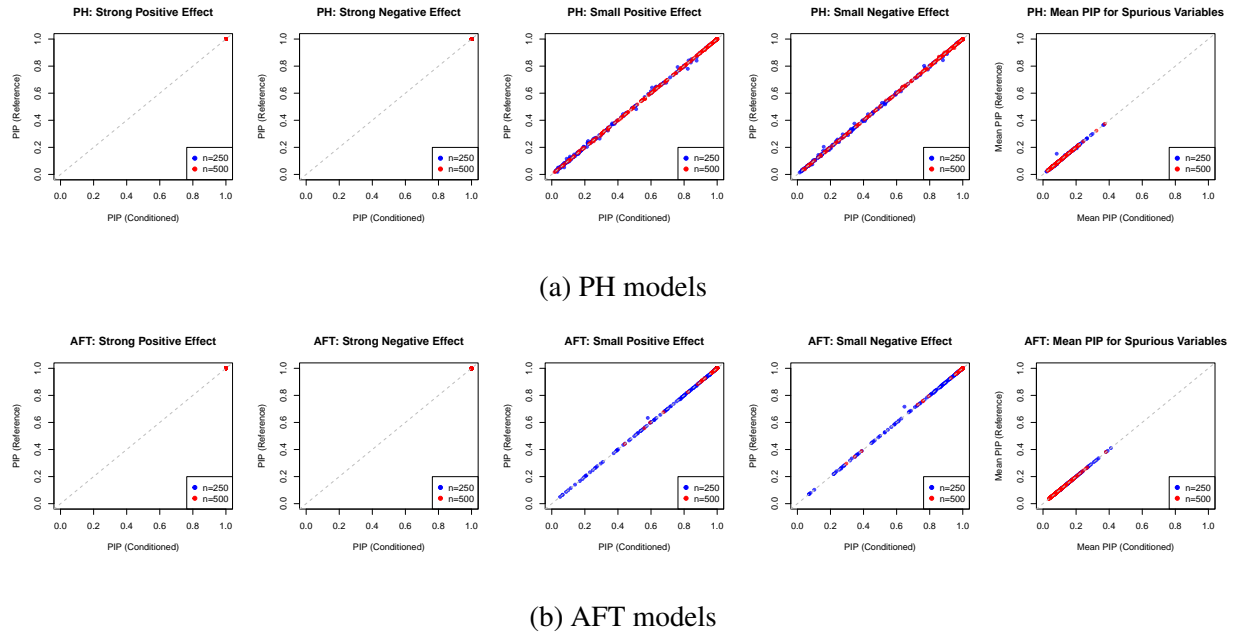
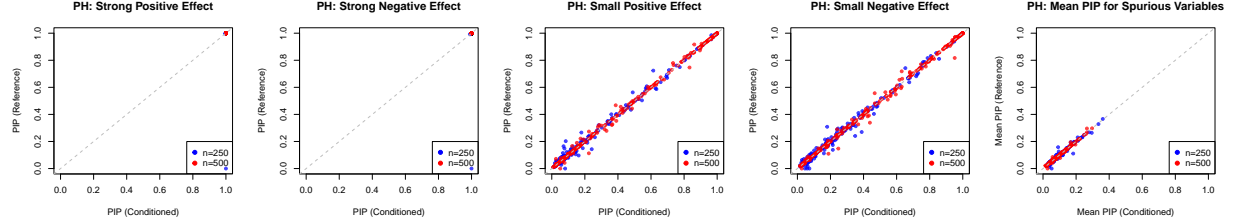
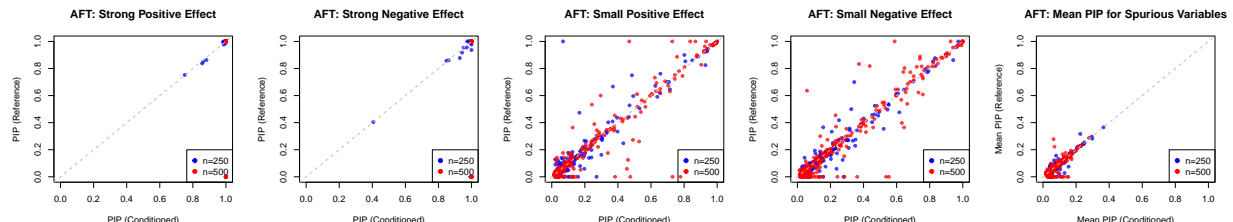


Figure S4: Demonstration of the influence of conducting variable selection with the more complex GH model under different simpler true hazard structures, for  $n = 250, 500$  with LCM prior. The censoring rate is 25% with log-normal baseline hazard. The  $x$ -axis is the PIP, conditioned on the given hazard structure, from the large-scale simulation, and  $y$ -axis is the reference PIP from direct fitting of the simpler structures. The first four columns correspond to the four active variables, and the last column is the average PIP of all the spurious variables.

Here we assess the interplay of performing simultaneous variable and hazard-structure selection. For each configuration with  $p = 10$ ,  $n \in 250, 500$ , a censoring rate of 25%, a log-normal baseline hazard, and true hazard structures of PH and AFT, we conduct an additional 250 Monte Carlo simulations. In each simulation, we modify the prior on the model space so that only models corresponding to the true hazard structure receive positive prior probability, effectively preventing all other structures from being visited. We then compare the resulting PIPs with those obtained in the earlier large-scale simulation under the full model space. This allows us to determine whether



(a) PH models



(b) AFT models

Figure S5: Demonstration of the influence of conducting variable selection with the more complex GH model under different simpler true hazard structures, for  $n = 250, 500$  with LCM prior. The censoring rate is 50% with PGW baseline hazard. The  $x$ -axis is the PIP, conditioned on the given hazard structure, from the large-scale simulation, and  $y$ -axis is the reference PIP from direct fitting of the simpler structures. The first four columns correspond to the four active variables, and the last column is the average PIP of all the spurious variables.

variable-selection performance changes when using a more complex hazard structure than the true one. Figure S4 displays the relationship between the PIPs for each of the four active variables and the mean PIP of the spurious variables under the LCM prior. The points lie closely along the diagonal reference line in all panels, indicating that variable-selection performance is hardly affected by adopting a richer hazard structure when the true hazard structure receives a high posterior probability.

We additionally conducted a similar set of simulations with a censoring rate of 50% and a PGW baseline hazard to investigate whether poor hazard-structure selection could influence variable selection. The corresponding results are provided in Figure S5. For PH models, the variable-

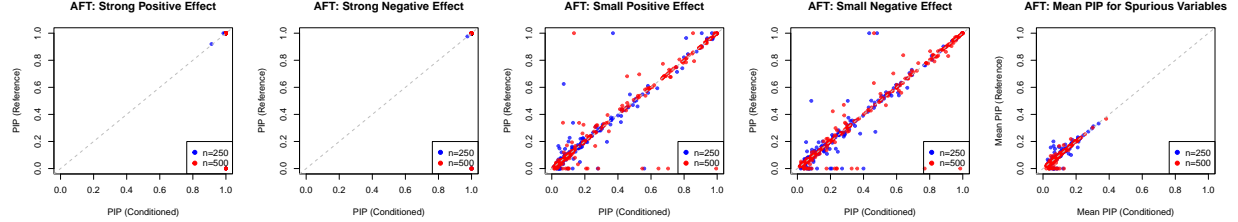


Figure S6: Demonstration of the influence of conducting variable selection with the more complex GH model under true hazard structure being AFT, for  $n = 250, 500$  with LCM prior. The censoring rate is 20% with PGW baseline hazard.

selection performance again appears stable, with most points remaining tightly clustered around the diagonal. This is because the hazard selection accuracy under this scenario is still very high, around 86% for  $n = 250$ . However, for the AFT model, the true positive rates for the active variables are affected by the substantially poorer hazard-structure selection accuracy, as we could observe from Figure 2 of main text a decrease of hazard selection accuracy from 0.996 for AFT-LN (25%) to 0.448 for AFT-PGW (50%) under  $n = 250, p = 10$ . Moreover, as suggested by Figure S1, the PH model is instead often being selected, as time-level effects are harder to be detected for monotonic baseline with high censoring rate. However, the variable selection performance seems not to be largely affected: in the plots for small effects, despite a larger spread, the points are evenly spread around the diagonal line. The specificity is also hardly affected. In addition, as implied by Figure S6, the difference is a synergy of both higher censoring rate and misspecified baseline hazard. These findings suggest that hazard-structure selection would usually not affect variable selection, but under poor hazard selection due to misspecified baseline hazard and higher censoring (shorter follow-ups), the difference in selection of smaller time-level effects, comparing to the true hazard, may have larger variability.

## 9 Variable dictionary for real application

Table S3: Variables from the flchain (FLC) data set in R package `survival`, adopted from Therneau (2024).

Variable	Description
age	Age in years
sex	Sex of the subject (F = female, M = male)
kappa	Serum free light chain, kappa portion
lambda	Serum free light chain, lambda portion
creatinine	Serum creatinine level
mgus	Indicator for monoclonal gammopathy diagnosis (1 = diagnosed with MGUS, 0 = not diagnosed)
futime	Days from enrollment until death (note: 3 subjects had sample obtained on death date)
death	Vital status (0 = alive at last contact, 1 = dead)

Table S4: Variables from the nki70 data set in R package `penalized`, adopted from [Goeman et al. \(2022\)](#). The details of the 70 genes are omitted.

---

Variable	Description
Diam	Diameter of the tumor (two levels)
N	Number of affected lymph nodes (two levels)
ER	Estrogen receptor status (two levels)
Grade	Grade of the tumor (three ordered levels)
Age	Patient age at diagnosis (years)
TSPYL5–DKFZP586A0522	Gene expression measurements of 70 prognostic genes (70 gene columns)

---

## 10 MCMC detail for study of (NKI70)

To obtain stable posterior samples under this challenging dataset, we run all four settings sufficiently long such that the differences in estimated model posterior probabilities across the chains are less than 0.01. For each of the two proposed priors (LCM and Product), we run the MCMC sampler for 110,000 iterations, with 10,000 burn-in steps, 10 chains, and a thinning period of 100. Running multiple long chains ensures adequate exploration of high-probability models and reduces the variability of the estimated model posterior probabilities.

For the fixed- $g$  prior AFT model, we apply the same MCMC settings as the proposed methods. For the non-local pMOM prior partial-Cox model, they implement a variant of the Shotgun Stochastic Search (SSS) algorithm called S5, initially proposed by [Shin et al. \(2018\)](#). To obtain stable estimation of posterior probabilities of the models, we perform a parallel run on 10 CPUs, with each run consisting of 1,100 iterations for each of the 10 temperature schedules.

## 11 Experiment on polarised censoring time

One particular scenario where the assumption of equal contribution of all samples to the prior covariance could be problematic is when the censoring times are concentrated at the extremes of the follow-up period, as discussed in [Castellanos et al. \(2021\)](#), where this situation is referred to as “polarised censoring time”. They considered a toy data set to demonstrate the bias induced by the regular  $g$ -prior under polarised censoring times in their Table 1. We generate the data set following the same procedure as in their Section 3, and conduct variable selection using both of LCM and Product priors. We restrict the model space within the AFT models and run the chain for 20,000 iterations with 10,000 burn-in’s. Table S5 shows the PIP for the three variables under the two priors. We could observe a big difference between PIP of the two priors. Comparing this result with Table 2 of [Castellanos et al. \(2021\)](#), we could observe that the variable selection performance

of the LCM prior is not impacted by the polarised censoring time, since the observed Fisher information matrix automatically adjust the contribution of these abnormal observations to the prior covariance matrix. On the other hand, Product prior gives equal weights to all observations, which leads to underestimation of the prior covariance and therefore a poorer variable selection performance.

Table S5: PIP for the Motivating Example.

Method	X1	X2	X3
AFT-LCM	1	1	0.503
AFT-Product	0.593	0.707	0.451

## References

Baldessari, B. (1967), ‘The distribution of a quadratic form of normal random variables’, *The Annals of Mathematical Statistics* **38**(6), 1700–1704.

Castellanos, M., Garcia-Donato, G. & Cabras, S. (2021), ‘A model selection approach for variable selection with censored data’, *Bayesian Analysis* **16**(1), 271–300.

Chen, Y. & Jewell, N. (2001), ‘On a general class of semiparametric hazards regression models’, *Biometrika* **88**(3), 687–702.

Goeman, J. J., Meijer, R. J. & Chaturvedi, N. (2022), *Penalized: L1 (lasso and fused lasso) and L2 (ridge) penalized estimation in GLMs and in the Cox model*. R package version 0.9-52.

Iqbal, A., Ogundimu, E. & Rubio, F. (2025), ‘Bayesian variable selection under sample selection and model misspecification’, *Bayesian Analysis* **NA**, 1–27.

Rossell, D. & Rubio, F. (2018), ‘Tractable Bayesian variable selection: beyond normality’, *Journal of the American Statistical Association* **113**, 1742–1758.

Rossell, D. & Rubio, F. (2023), ‘Additive Bayesian variable selection under censoring and misspecification’, *Statistical Science* **38**, 13–29.

Rossell, D. & Telesca, D. (2017), ‘Non-local priors for high-dimensional estimation’, *Journal of the American Statistical Association* **112**(517), 254–265.

Santis, F. D., Mortera, J. & Nardi, A. (2001), ‘Jeffreys priors for survival models with censored data’, *Journal of Statistical Planning and Inference* **99**(2), 193–209.

Shin, M., Bhattacharya, A. & Johnson, V. E. (2018), ‘Scalable Bayesian variable selection using nonlocal prior densities in ultrahigh-dimensional settings’, *Statistica Sinica* **28**(2), 1053–1078.

Therneau, T. M. (2024), *A Package for Survival Analysis in R*. R package version 3.8-3.

**URL:** <https://CRAN.R-project.org/package=survival>

van der Vaart, A. (2000), *Asymptotic Statistics*, Cambridge University Press, New York.

Wang, X. & George, E. I. (2007), 'Adaptive Bayesian criteria in variable selection for generalized linear models', *Statistica Sinica* **17**(2):, 667–690.

White, H. (1981), 'Consequences and detection of misspecified nonlinear regression models', *Journal of the American Statistical Association* **76**(374), 419–433.

White, H. (1982), 'Maximum likelihood estimation of misspecified models', *Econometrica: Journal of the Econometric Society* pp. 1–25.